NAVAL POSTGRADUATE SCHOOL

MONTEREY, CALIFORNIA

THESIS

PERFORMANCE ANALYSIS OF ALTERNATIVE LINK-16/JTIDS COMPATIBLE WAVEFORMS WITH COMPLEX 64-BI-ORTHOGONAL-KEYED MODULATION

by

Cheng Hoe Kee

December 2008

Thesis Advisor: Clark Robertson
Second Reader: Roberto Cristi

Approved for public release; distribution is unlimited

THIS PAGE INTENTIONALLY LEFT BLANK

REPORT DOCUMENTATION PAGE			Form Approved OMB No. 0704-0188
Public reporting burden for this collection of information is estimated to average 1 hour per response, including the time for reviewing instruction, searching existing data sources, gathering and maintaining the data needed, and completing and reviewing the collection of information. Send comments regarding this burden estimate or any other aspect of this collection of information, including suggestions for reducing this burden, to Washington headquarters Services, Directorate for Information Operations and Reports, 1215 Jefferson Davis Highway, Suite 1204, Arlington, VA 22202-4302, and to the Office of Management and Budget, Paperwork Reduction Project (0704-0188) Washington DC 20503.			
1. AGENCY USE ONLY *(Leave blank)*	**2. REPORT DATE** December 2008	**3. REPORT TYPE AND DATES COVERED** Master's Thesis	
4. TITLE AND SUBTITLE Performance Analysis of Alternative Link-16/JTIDS Compatible Waveforms with Complex 64-Bi-orthogonal-Keyed Modulation		**5. FUNDING NUMBERS**	
6. AUTHOR(S) Cheng Hoe Kee			
7. PERFORMING ORGANIZATION NAME(S) AND ADDRESS(ES) Naval Postgraduate School Monterey, CA 93943-5000		**8. PERFORMING ORGANIZATION REPORT NUMBER**	
9. SPONSORING /MONITORING AGENCY NAME(S) AND ADDRESS(ES) N/A		**10. SPONSORING/MONITORING AGENCY REPORT NUMBER**	
11. SUPPLEMENTARY NOTES The views expressed in this thesis are those of the author and do not reflect the official policy or position of the Department of Defense or the U.S. Government.			
12a. DISTRIBUTION / AVAILABILITY STATEMENT Approved for public release; distribution is unlimited		**12b. DISTRIBUTION CODE**	

13. ABSTRACT (maximum 200 words)

The Joint Tactical Information Distribution System (JTIDS)/Link-16 is a hybrid frequency-hopped, direct sequence spread spectrum system which is used for the exchange of real-time tactical data. The five-bit data symbols are encoded with a (31,15) Reed-Solomon (RS) code and transmitted over the channel with cyclical code-shift keying modulation. Although JTIDS/Link-16 has proven to be operationally useful, one of its primary drawbacks is its limited data rate. This thesis focuses on performance analyses of alternative waveforms that achieve better data rates and better performance in terms of required signal power. Two alternative waveforms were considered in this thesis. The first alternative JTIDS/Link-16 waveform uses (31,15) RS encoding just as the original JTIDS/Link-16 waveform, but the five-bit symbol stream generated at the output of the RS encoder undergoes serial-to-parallel conversion to two five-bit symbol streams. Each five-bit symbol stream is then mapped into a six-bit symbol stream before being independently transmitted on the in-phase (I) and quadrature (Q) components of the carrier using complex 64-ary bi-orthogonal keying modulation (64-BOK). The second alternative JTIDS/Link-16 waveform uses (63, 47) RS encoding, where the six-bit symbol stream generated at the output of the RS encoder undergoes serial-to-parallel conversion to six-bit symbol streams which are then each independently transmitted on the I and Q components of the carrier using complex 64-BOK modulation. The performance results obtained for the two alternative JTIDS/Link-16 waveforms are compared to those obtained for the existing JTIDS/Link-16 waveform for additive white Gaussian noise (AWGN) as well as when both AWGN and pulse-noise interference (PNI) are present. Errors-and-erasures decoding (EED) as well as errors-only decoding are also considered for the two alternative waveforms. From the analyses, we see that the two proposed alternative JTIDS/Link-16 waveforms perform better in the presence of AWGN as well as both AWGN and PNI. There is no significant advantage when EED is used for either of the two alternative waveforms considered. When perfect-side information demodulation is used, the results show significant improvements in performance for the two alternative waveforms when both AWGN and PNI are present.

14. SUBJECT TERMS JTIDS/Link-16, *M*-ary Bi-Orthogonal Keying, Reed-Solomon coding, Pulse-Noise Interference, Additive White Gaussian Noise, Error-and-Erasure decoding, Perfect-Side Information.			**15. NUMBER OF PAGES** 139
			16. PRICE CODE
17. SECURITY CLASSIFICATION OF REPORT Unclassified	**18. SECURITY CLASSIFICATION OF THIS PAGE** Unclassified	**19. SECURITY CLASSIFICATION OF ABSTRACT** Unclassified	**20. LIMITATION OF ABSTRACT** UU

NSN 7540-01-280-5500

Standard Form 298 (Rev. 2-89)
Prescribed by ANSI Std. 239-18

THIS PAGE INTENTIONALLY LEFT BLANK

Approved for public release; distribution is unlimited

PERFORMANCE ANALYSIS OF ALTERNATIVE LINK-16/JTIDS COMPATIBLE WAVEFORMS WITH COMPLEX 64-BI-ORTHOGONAL-KEYED MODULATION

Cheng Hoe Kee
Civilian, Defence Science & Technology Agency (DSTA), Singapore
B.S., Engineering.(EE), University of Glasgow, 1996

Submitted in partial fulfillment of the
requirements for the degree of

MASTER OF SCIENCE IN ELECTRICAL ENGINEERING

from the

NAVAL POSTGRADUATE SCHOOL
December 2008

Author: Cheng Hoe Kee

Approved by: R. Clark Robertson
Thesis Advisor

Roberto Cristi
Second Reader

Jeffrey B. Knorr
Chairman, Department of Electrical and Computer Engineering

THIS PAGE INTENTIONALLY LEFT BLANK

ABSTRACT

The Joint Tactical Information Distribution System (JTIDS)/Link-16 is a hybrid frequency-hopped, direct sequence spread spectrum system which is used for the exchange of real-time tactical data. The five-bit data symbols are encoded with a (31,15) Reed-Solomon (RS) code and transmitted over the channel with cyclical code-shift keying modulation. Although JTIDS/Link-16 has proven to be operationally useful, one of its primary drawbacks is its limited data rate. This thesis focuses on performance analyses of alternative waveforms that achieve better data rates and better performance in terms of required signal power. Two alternative waveforms were considered in this thesis. The first alternative JTIDS/Link-16 waveform uses (31,15) RS encoding just as the original JTIDS/Link-16 waveform, but the five-bit symbol stream generated at the output of the RS encoder undergoes serial-to-parallel conversion to two five-bit symbol streams. Each five-bit symbol stream is then mapped into a six-bit symbol stream before being independently transmitted on the in-phase (I) and quadrature (Q) components of the carrier using complex 64-ary bi-orthogonal keying modulation (64-BOK). The second alternative JTIDS/Link-16 waveform uses (63,47) RS encoding, where the six-bit symbol stream generated at the output of the RS encoder undergoes serial-to-parallel conversion to six-bit symbol streams which are then each independently transmitted on the I and Q components of the carrier using complex 64-BOK modulation. The performance results obtained for the two alternative JTIDS/Link-16 waveforms are compared to those obtained for the existing JTIDS/Link-16 waveform for additive white Gaussian noise (AWGN) as well as when both AWGN and pulse-noise interference (PNI) are present. Errors-and-erasures decoding (EED) as well as errors-only decoding are also considered for the two alternative waveforms. From the analyses, we see that the two proposed alternative JTIDS/Link-16 waveforms perform better in the presence of AWGN as well as both AWGN and PNI. There is no significant advantage when EED is used for either of the two alternative waveforms considered. When perfect-side information demodulation is used, the results show significant improvements in performance for the two alternative waveforms when both AWGN and PNI are present.

THIS PAGE INTENTIONALLY LEFT BLANK

TABLE OF CONTENTS

THIS PAGE INTENTIONALLY LEFT BLANK

LIST OF FIGURES

LIST OF TABLES

THIS PAGE INTENTIONALLY LEFT BLANK

EXECUTIVE SUMMARY

The Joint Tactical Information Distribution System (JTIDS)/Link-16 is one of the tactical communication links that is used by the U.S. and NATO countries. Its capability to provide both voice and data communications makes it effective for joint service operations since it has the ability to connect air, land and sea assets.

JTIDS is a hybrid frequency-hopped, direct sequence spread spectrum system which is used for the exchange of real-time tactical data. The data symbols are encoded with a (31,15) Reed-Solomon (RS) code, and the resulting code symbols are modulated with cyclical code-shift keying modulation (CCSK), where there are five bits for each symbol. JTIDS primary drawback is its limited data rate. This thesis focuses on performance analyses of two alternative JTIDS/Link-16 waveforms that achieve both a better data rate and superior performance to that of the original JTIDS/Link-16 waveform.

The first alternative JTIDS/Link-16 waveform utilizes complex 64-ary bi-orthogonal keying modulation (64-BOK) instead of CCSK used in the original JTIDS/Link-16 waveform. The (31,15) RS code is the same as used for the original JTIDS/Link-16 waveform where blocks of 15 data symbols are encoded into blocks of 31 coded symbols and undergo a serial-to-parallel conversion into two streams of five-bit symbols. The five-bit symbols are converted into six-bit symbols and transmitted independently on the in-phase (I) and quadrature (Q) components of the carrier utilizing complex 64-BOK modulation with a diversity of two.

The second alternative JTIDS/Link-16 waveform utilizes complex 64-BOK modulation like the first alternative waveform. For the second alternative waveform, a (63,47) RS code is used instead of the (31,15) RS code used for the original JTIDS/Link-16 waveform. Using complex 64-BOK and a (63,47) RS code, we see that a change in the JTIDS/Link-16 data structure is required, where blocks of 47 six-bit data symbols are encoded into blocks of 63 six-bit code symbols and undergo serial-to-parallel conversion

into two streams of six-bit symbols. The six-bit symbols are then transmitted independently on the I and Q components of the carrier utilizing complex 64-BOK modulation with a diversity of two.

The performances of the first and second alternative JTIDS/Link-16 waveforms were analyzed for both AWGN (additive white Gaussian noise) as well as AWGN plus PNI (pulse-noise interference). The performance with EED (errors-and-erasures) decoding was also examined. The analyses of the two waveforms take into consideration the single-pulse (no diversity) structure and the double-pulse (a diversity of two) structure. Perfect-side information (PSI) was also considered for the double-pulse structure.

The analyses show that there is no significant advantage when EED is used. When PSI is considered, there is significant improvement in performance, where the two proposed alternative waveforms perform well when PNI is present.

The results obtained were compared to those for the existing JTIDS/Link-16 waveform for AWGN as well as when PNI is also present. Both proposed waveforms perform better than the existing JTIDS/Link-16 waveform for both AWGN only as well as AWGN plus PNI for both the single-pulse and the double-pulse structures.

The primary advantage of the two proposed alternative waveforms is the improvement in data rate and the reduction in required signal power as compared to the existing JTIDS/Link-16 waveform for the same probability of information bit error. The first and second alternative JTIDS/Link-16 waveforms support a data rate that is greater than the original JTIDS waveform by a factor of 2.4 and 4.44, respectively, while requiring less signal power to achieve the same probability of information bit error. When only AWGN is present and for the same probability of information bit error, the E_b / N_0 required for the first and second alternative JTIDS/Link-16 waveforms is less than that required by the original JTIDS/Link-16 waveform by 2.7 dB and 3.8 dB, respectively. Neither of the proposed alternative waveforms requires a change in bandwidth or chip rate, but the basic data structure of JTIDS will have to be modified if either of the alternative waveforms are to be implemented.

ACKNOWLEDGMENTS

I would like to thank Professor Clark Robertson of the Naval Postgraduate School with my utmost gratitude for his guidance, teaching and contribution to the successful completion of this thesis work.

I would also like to thank Professor Roberto Cristi of the Naval Postgraduate School for reviewing this thesis and provided me with sound advice as my second reader.

I also like to thank my wife Siew Peng, Lee for her loving support and encouragement.

Lastly, I would like to thank my sponsor, Defence Science and Technology Agency (DSTA) for presenting me with the opportunity to pursue my academic work in the Naval Postgraduate School.

THIS PAGE INTENTIONALLY LEFT BLANK

I. INTRODUCTION

A. OVERVIEW

Today's warfare leverages on information technology to achieve information supremacy and situational awareness in a network centric warfare environment [9]. The proliferation of advanced technology on digital data-links creates the critical communication platforms to support and ensure seamless and reliable communications in network enabled operations.

The Joint Tactical Information Distribution System (JTIDS)/Link-16 is one of the tactical communication links that is used by U.S. and NATO countries. Its capability to provide both voice and data communications makes it effective for joint service operations since it has the ability to connect air, land and sea assets.

JTIDS is a hybrid frequency-hopped, direct sequence spread spectrum system which is used for the exchange of real-time tactical data. The data symbols are encoded with a (31,15) Reed-Solomon (RS) code, and the resulting code symbols are modulated with cyclical code-shift keying modulation, where there are five bits for each symbol. JTIDS primary drawback is its limited data rate. This thesis focuses on performance analyses of two alternative JTIDS/Link-16 waveforms that achieve both a better data rate and superior performance to that of JTIDS/Link-16.

B. THESIS OBJECTIVE

One of the limitations of JTIDS/Link-16 is the limited data throughput that is inherent in its basic architecture. Numerous studies have been conducted to improve on the data rate. One example is the Link-16 Enhanced Throughput (LET) developed by Viasat in the U.S, which works by replacing the spread spectrum and Reed-Solomon encoding with a different encoding scheme [2]. Although this solution improves the data throughput, it comes at the expense of a reduction in jamming resistance and transmission range and may be unsuitable for combat situations.

The objective of this thesis is to analyze two alternative physical layer channel waveforms that improve the data rate and reduce the required signal-to-noise ratio as compared to the existing JTIDS/Link-16 channel waveform. The two alternative JTIDS/Link-16 waveforms considered both utilize complex *M*-ary bi-orthogonal keying (*M*BOK) with (n,k) Reed Solomon (RS) encoding. Both alternative waveforms will require a fundamental modification to the JTIDS/Links data structure, but both alternative waveforms maintain the same chip rate as the original JTIDS/Link-16 waveform. Consequently, the waveform bandwidth is unchanged, and no change is required to the direct sequence spread spectrum structure, the frequency-hopping structure, or the radio frequency (RF) portions of the JTIDS/Link-16 transceiver.

The first alternative waveform utilizes (31,15) RS encoding identical to the original JTIDS, where the five-bit symbol stream generated at the output of the RS encoder undergoes serial-to-parallel conversion to two five-bit symbol streams. These five-bit symbol streams are then mapped into six-bit symbol streams before being independently transmitted on the in-phase (I) and quadrature (Q) components of the carrier using 64-BOK modulation. Hence, every six five-bit symbols undergo conversion to five six-bit symbols.

The second alternative waveform utilizes (63,47) RS encoding, which is different from the code used for the original JTIDS, where the six-bit symbol stream generated at the output of the RS encoder undergoes serial-to-parallel conversion to two six-bit symbol streams, which are independently transmitted on the I and Q components of the carrier using 64-BOK modulation.

This thesis follows a previous research effort investigated where the performance of an alternative waveform utilizing (31,15) RS encoding and 32-BOK modulation was investigated [9]. The alternative waveform in [9] requires a change to the transceiver of the original JTIDS/Link 16 waveform but not the data structure. For this thesis, although the two alternative waveforms investigated require a modification to the JTIDS/Link-16 data structure, both waveforms will increase the data rate, where the first alternative waveform and the second alternative waveform improve the data rate by 2.4 times and

4.44 times, respectively. To the best of the author's knowledge, neither of the two proposed waveforms have been previously considered as an alternative waveform for JTIDS/Link-16.

C. THESIS OUTLINE

The overview and objective of this thesis were introduced in this chapter, followed by Chapter II, which provides some prerequisite knowledge to facilitate in comprehension of the remainder of the thesis. The performance analysis of the first alternative waveform with (31, 15) RS encoding and 64-BOK modulation for both the single-pulse and double-pulse structures are presented in Chapter III. The performance of the second alternative waveform with (63, 47) RS encoding and 64-BOK modulation for both the single-pulse and double-pulse structures are presented in Chapter IV. Lastly, the conclusion of this thesis is presented in Chapter V with recommendations for future research areas.

THIS PAGE INTENTIONALLY LEFT BLANK

II. BACKGROUND

This chapter covers some of the required background knowledge and concepts necessary to understand the subsequent analysis performed for the alternative JTIDS/Link-16 waveforms.

A. *M*-ARY BI-ORTHOGONAL SIGNALS

M-ary bi-orthogonal keying (*M*BOK) can be viewed as a hybrid of *M*-ary orthogonal modulation and binary phase-shift keying (BPSK), where a set of *M* bi-orthogonal signals are constructed from $M/2$ orthogonal signals by including the negatives of the orthogonal signals [15]. This means that a bi-orthogonal signal set consists of two sets of orthogonal signals such that each signal in one set has its antipodal signal in the other set. The advantage of bi-orthogonal modulation is the reduction in bandwidth by almost half as compared to orthogonal modulation. When baseband orthogonal signals are used, bi-orthogonal modulation requires half as many chips per symbol as compared to orthogonal modulation for the same number of bits per symbol. Bi-orthogonal modulation also performs slightly better than orthogonal modulation since antipodal signal vectors have better distance properties than orthogonal ones [8].

The channel waveform for complex *M*BOK can be represented by

$$s(t) = \pm A_c c_i(t)\cos(2\pi f_c t + \theta) - (\pm) A_c c_j(t)\sin(2\pi f_c t + \theta) \tag{2.1}$$

where the waveform is transmitted for $T_s = 2kT_b$ seconds, $2k$ represents the number of bits per symbol, and $c_i(t)$ and $c_j(t)$ represent the baseband, orthogonal waveforms with 2^{k-1} pulses of duration T_c where $T_c = T_s / 2^{k-1}$ and i or j may be the same or different depending on the data bits. From (2.1), it can be seen that complex 2^k-BOK is equivalent to transmitting 2^k-BOK independently on both the I and Q components of the carrier. As a result, complex 2^k-BOK is actually a 2^{2k}-ary modulation technique.

The block diagram of a *M*-ary bi-orthogonal receiver is shown in Figure 1 [10].

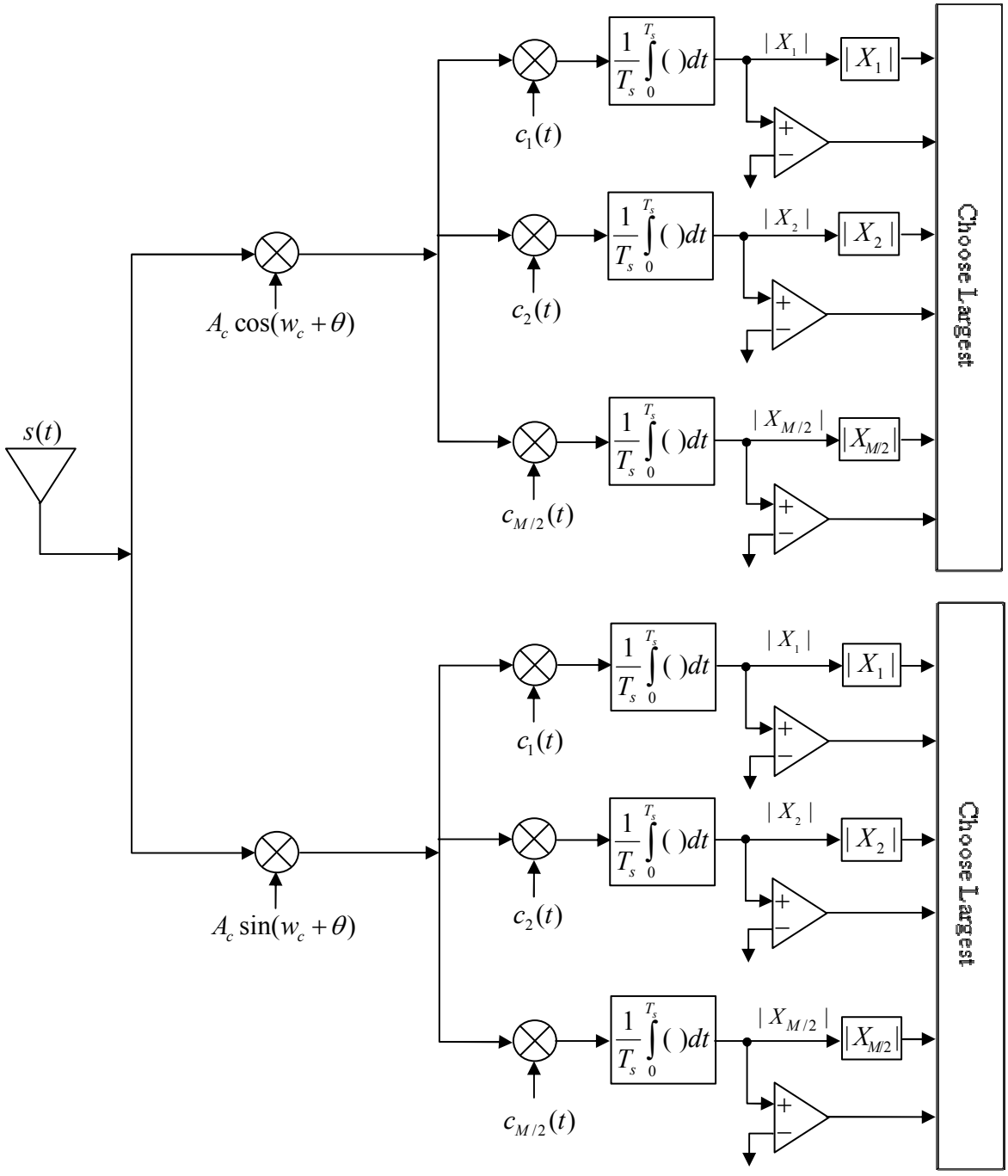

Figure 1. Block diagram of a *M*-ary bi-orthogonal receiver.

When the receiver input noise is Gaussian, then the conditional probability density functions of the random variables X_m that model the integrator outputs, where $m = 1, 2, ..., M/2$, are given by

$$f_{X_m}(x_m \mid m) = \frac{1}{\sqrt{2\pi}\sigma} e^{\frac{-(x_m - \sqrt{2}A_c)^2}{2\sigma^2}} \quad \text{for } m \le M/2, \tag{2.2}$$

$$f_{X_m}(x_m \mid m) = \frac{1}{\sqrt{2\pi}\sigma} e^{-\frac{(x_m + \sqrt{2}A_c)^2}{2\sigma^2}} \quad \text{for } (M/2)+1 \le m \le M, \tag{2.3}$$

and

$$f_{X_n}(x_n \mid n, n \ne m) = \frac{1}{\sqrt{2\pi}\sigma} e^{-\frac{x_n^2}{2\sigma^2}}, \tag{2.4}$$

where the variance is $\sigma^2 = N_0 / T_s$ and N_0 is the two-sided Gaussian noise power spectral density at the input of each integrator.

B. PERFORMANCE OF *M*-BOK IN AWGN

For additive white Gaussian noise (AWGN) with channel power spectral density of $N_0/2$, the probability of channel symbol error for *M*BOK is [10]

$$p_s = 1 - \frac{1}{\sqrt{2\pi}} \int_{-\sqrt{2E_s/N_0}}^{\infty} e^{\frac{-u^2}{2}} \left[1 - 2Q\left(u + \sqrt{\frac{2E_s}{N_0}}\right) \right]^{\frac{M}{2}-1} du, \tag{2.5}$$

where the average energy per channel symbol $E_s = A_c^2 T_s$, A_c^2 is the average received signal power and T_s is the symbol duration.

C. PERFORMANCE IN AWGN WITH PULSED-NOISE INTERFERENCE

For military applications, it is imperative to consider the performance of the system when subjected to pulsed-noise interference. In this thesis, the performances of the alternative JTIDS/Link-16 waveforms in AWGN as well as pulse-noise interference (PNI) are considered.

A channel that is affected by AWGN has a noise signal that is assumed to be uniformly spread across the spectrum and is time-independent at the receiver. This assumption may not be valid when there is PNI in the channel. If the PNI is assumed to be Gaussian, then the total noise power at the integrator outputs of the receiver when both AWGN and PNI are present is given by

$$\sigma_x^2 = \sigma_0^2 + \sigma_I^2 \tag{2.6}$$

since the AWGN and the PNI are assumed to be independent, where $\sigma_0^2 = N_0 / T_s$ and $\sigma_I^2 = N_I / \rho T_s$. The parameter ρ is the fraction of time that a narrowband Gaussian noise interferer is switched on. When the interferer is switched on continuously, then $\rho = 1$ and the PNI is equivalent to barrage noise interference.

Consequently, when a signal experiences PNI, the probability of symbol error is given by

$$\begin{aligned} P_s = {} & \Pr(\textit{Interferer is OFF})\, p_s(AWGN) \\ & + \Pr(\textit{Interferer is ON})\, p_s(AWGN + PNI) \end{aligned}. \tag{2.7}$$

Since $\Pr(\textit{Interferer is ON}) = \rho$, then (2.7) is equivalent to

$$P_s = (1-\rho)\, p_s(AWGN) + \rho\, p_s(AWGN + PNI), \tag{2.8}$$

where $p_s(x)$ represents the probability of channel symbol error for condition x. We assume that a symbol is either totally free of PNI or has both AWGN and PNI for the entire symbol duration.

D. PERFORMANCE WITH DIVERSITY

JTIDS/Link-16 employs several techniques to improve interference immunity on its communication links, and diversity is one of the techniques used. In JTIDS/Link-16, diversity is implemented as a simple repetition code using either the single-pulse (no diversity) or the standard double-pulse (STDP) structure (sequential diversity of two).

For the STDP, effective redundancy is achieved by transmitting the same symbol twice at different carrier frequencies and receiving each redundant symbol independently

at the receiver [11]. Although there are four basic JTIDS message formats used, the STDP message format is the one with the best interference resistance and also provides compensation for propagation problems or antenna coverage limitations in maneuvering platforms [2].

When there is a diversity of order L and each diversified signal is received independently, where ρ is the fraction of time when the channel is affected by PNI, the probability that i of L receptions are affected by PNI is represented as [12]

$$\Pr(i \ of \ L \ pulses \ jammed) = \binom{L}{i} \rho^i (1-\rho)^{L-i}, \tag{2.9}$$

where there are $\binom{L}{i}$ different ways that i of L receptions can be jammed. Consequently, for a system with a diversity of L, the probability of symbol error is

$$P_s = \sum_{i=0}^{L} [\Pr(i \ of \ L \ signals \ jammed) \, p_s(i)], \tag{2.10}$$

where $p_s(i)$ is the conditional probability of channel symbol error in the event that i of L diversity receptions are affected by PNI.

Substituting (2.9) into (2.10), we get

$$P_s = \sum_{i=0}^{L} \left[\binom{L}{i} \rho^i (1-\rho)^{L-i} p_s(i) \right]. \tag{2.11}$$

E. FORWARD ERROR CORRECTION CODING

Communication systems that are used by the military should perform reliably and accurately in the presence of noise and interference, and one of the most effective and economical ways of achieving this goal is to employ block forward error correction (FEC) coding. In a communication system that employs block FEC coding, k information bits from the information source are encoded by an encoder into n coded bits and

transmitted over the channel. At the receiver, the decoder extracts the original k information bits and improves the reliability by correcting up to t bits errors in every block of n coded bits received.

For JTIDS/Link-16, the FEC coding that is used is (31,15) RS coding, where RS codes are linear, non-binary Bose-Chaudhuri-Hocquenghem (BCH) codes. As an example, a (n,k) RS encoder encodes k information m-bit symbols (mk information bits) and generates n coded m-bit symbols (mn coded bits).

The probability of decoder error or block error for an (n,k) RS code is upper bounded by the sum of probabilities that a received code word differs from the correct code word by i symbols for all $i > t$ and is given by [13]

$$P_E \le \sum_{j=t+1}^{n} \binom{n}{j} p_s{}^j (1-p_s)^{n-j} \tag{2.12}$$

or

$$P_E \le 1 - \sum_{j=0}^{t} \binom{n}{j} p_s{}^j (1-p_s)^{n-j} , \tag{2.13}$$

where t is the symbol-error correcting capability of the code, and p_s is the channel symbol error probability. The inequality holds for either a perfect code or a bounded distance decoder.

Assuming that the probability of information symbol error given j coded symbol errors is approximated by j/n, we get the probability of information symbol error from (2.12) as

$$P_s \approx \frac{1}{n} \sum_{j=t+1}^{n} j \binom{n}{j} p_s{}^j (1-p_s)^{n-j} . \tag{2.14}$$

Substituting $n = 2^m - 1$ into (2.14), we get

$$P_s \approx \frac{1}{2^m - 1} \sum_{j=t+1}^{2^m-1} j \binom{2^m - 1}{j} p_s{}^j (1-p_s)^{2^m-1-j} , \tag{2.15}$$

where m represents the number of bits per symbol.

The probability of bit error is approximated by taking the average of the upper and lower bound on the probability of bit error given that a symbol error has occurred and is given by

$$P_b \approx \frac{m+1}{2m} P_s \tag{2.16}$$

In subsequent chapters, the probability of symbol error for the alternative JTIDS/Link-16 waveforms is obtained by using (2.14) or (2.15) together with (2.16).

F. ERRORS-AND-ERASURES DECODING

Error-and-erasures decoding (EED) is a simple form of soft decision decoding that is implemented at the receiver to utilize ambiguously received symbols. Thus, the number of possible outputs of the demodulator per symbol is the number of symbols plus an erasure. As an example, for binary modulation, the output of the demodulator is ternary instead of binary, and consists of three possible output states; bit 1, 0 and erasure (e).

If a received code word has a single erased bit, all valid code words are separated by a Hamming distance of at least $d_{\min} - 1$, where $d_{\min}$ is the minimum Hamming distance of the code. Similarly, for a code word with j erasures, all valid code words are separated by a Hamming distance of at least $d_{\min} - j$. Hence, the effective free distance between valid code words is

$$d_{\min_{eff}} = d_{\min} - j \,. \tag{2.17}$$

Consequently, we get

$$t_c = \frac{1}{2}\lfloor d_{\min} - j - 1 \rfloor, \tag{2.18}$$

where t_c is the number of correctable errors in the non-erased bits of the code word; the $\lfloor x \rfloor$ implies rounding x down to an integer value; and j indicates the number of

erasures. From (2.18), a combination of t_c errors and j erasures are correctable as long as

$$2t_c + j < d_{\min}, \tag{2.19}$$

from this we see that twice as many erasures as errors are correctable. Intuitively, this explanation makes sense since the locations of erasures are known, but the locations of errors are not.

For error-and-erasures decoding, the probability that there are a total of i errors and j erasures in a block of n symbols is given by

$$\Pr(i, j) = \binom{n}{i}\binom{n-i}{j} p_s{}^i p_e{}^j p_c{}^{n-i-j}, \tag{2.20}$$

where p_e is the probability of channel symbol erasure, p_c is the probability of correct channel symbol detection, and each symbol is assumed to be received independently. The probability of channel symbol error is given by

$$p_s = 1 - p_e - p_c, \tag{2.21}$$

A block error does not occur as long as $d_{\min} > 2i + j$, so from (2.20) the probability of correct block decoding is given by

$$P_C = \sum_{i=0}^{t} \binom{n}{i} p_s{}^i \sum_{j=0}^{d_{\min}-1-2i} \binom{n-i}{j} p_e{}^j p_c{}^{n-i-j}, \tag{2.22}$$

and the probability of block error is

$$P_E = 1 - P_C. \tag{2.23}$$

Substituting (2.22) into (2.23), we get the probability of block error as

$$P_E = 1 - \sum_{i=0}^{t} \binom{n}{i} p_s{}^i \sum_{j=0}^{d_{\min}-1-2i} \binom{n-i}{j} p_e{}^j p_c{}^{n-i-j} \tag{2.24}$$

Using (2.24) and approximating the probability of symbol error by taking the average of the upper and lower bound on the probability of symbol error given that a block error has occurred, we obtain

$$P_s \approx \frac{k+1}{2k} P_E \tag{2.25}$$

Similarly, the probability of bit error is approximated by taking the average of the upper and lower bound on the probability of bit error given that a symbol error has occurred and is given by (2.16).

G. PERFECT-SIDE INFORMATION

Perfect-side information (PSI) can be considered for a system with a diversity of L when the diversity receptions are received independently. For the double-pulse structure, when neither received symbol in the repetitive pulses is affected by PNI, the symbols are combined and demodulated accordingly. If either pulse suffers from PNI, the affected symbol is discarded and the decision is made based on the single-pulse structure with AWGN. If both diversity receptions are affected by PNI, the signal is recovered by the receiver in the normal fashion. To implement PSI, we require at least a diversity of two, and the performance of the system in a pulse-noise environment with $\rho < 1$ is expected to improve.

H. CHAPTER SUMMARY

This chapter covered the introduction of *M*-ary bi-orthogonal signals and addressed the concepts and background necessary to examine the performance of two alternative JTIDS/Link-16 waveforms. The concepts of diversity, errors-and-erasures decoding and perfect side information modulation were also covered. In the next chapter, the performance of the first alternative JTIDS waveform that utilizes (31,15) RS coding with complex 64-BOK modulation is examined. The analyses of the performance of the two alternative JTIDS waveforms assume transmission over a channel both with AWGN as well as AWGN plus PNI. Both the single-pulse (no diversity) and double-pulse (with diversity) structures are considered.

THIS PAGE INTENTIONALLY LEFT BLANK

III. ALTERNATIVE JTIDS/LINK-16 WAVEFORM WITH (31,15) RS ENCODING AND 64-BOK MODULATION

In this chapter, we examine the performance of the first alternative JTIDS/Link-16 waveform for both AWGN as well as AWGN plus PNI. Subsequently, we also examine the performance when EED is used. In Section B of the chapter, the analyses are for the single-pulse (no diversity) structure, while in Section C the double-pulse (with diversity) structure is considered.

A. CONVERSION BETWEEN FIVE-BIT SYMBOL AND SIX-BIT SYMBOL STREAMS USING 64-BOK WITH (31,15) RS ENCODING

In this section, the concept of conversion between five-bit symbol and six-bit symbol streams are explained.

The first alternative waveform utilizes (31,15) RS encoding identical to that used by the original JTIDS, where the five-bit symbols generated at the output of the RS encoder undergo serial-to-parallel conversion to two five-bit symbol streams. These five-bit symbols are mapped into six-bit symbols before being independently transmitted on the I and Q components of the carrier using 64-BOK.

The concept of mapping from five-bit symbols into six-bit symbols is shown in Figure 2. At the transmitter, blocks of six five-bit symbols at the RS encoder output are converted into blocks of five six-bit symbols and modulated with 64-BOK. At the receiver, the process is reversed. Blocks of six-bit symbols are demodulated and converted back into blocks of five-bit symbols before being decoded by the RS decoder. A block of six five-bit symbols has the same total probability of correct symbol detection as a block of five six-bit symbols. When each symbol is received independently, then

$$p_{c5}{}^{6} = p_{c6}{}^{5}, \tag{3.1}$$

where p_{c5} is the total probability of correct symbol detection in a block of six five-bit symbols and p_{c6} is the total probability of correct symbol detection in a block of five six-bit symbols.

From (3.1), the probability of correct five-bit symbol detection can be obtained as

$$p_{c5} = (p_{c6})^{5/6} \quad , \tag{3.2}$$

and the probability of a five-bit channel symbol error is given by

$$p_{s5} = 1 - \left(p_{c6}\right)^{\frac{5}{6}} . \tag{3.3}$$

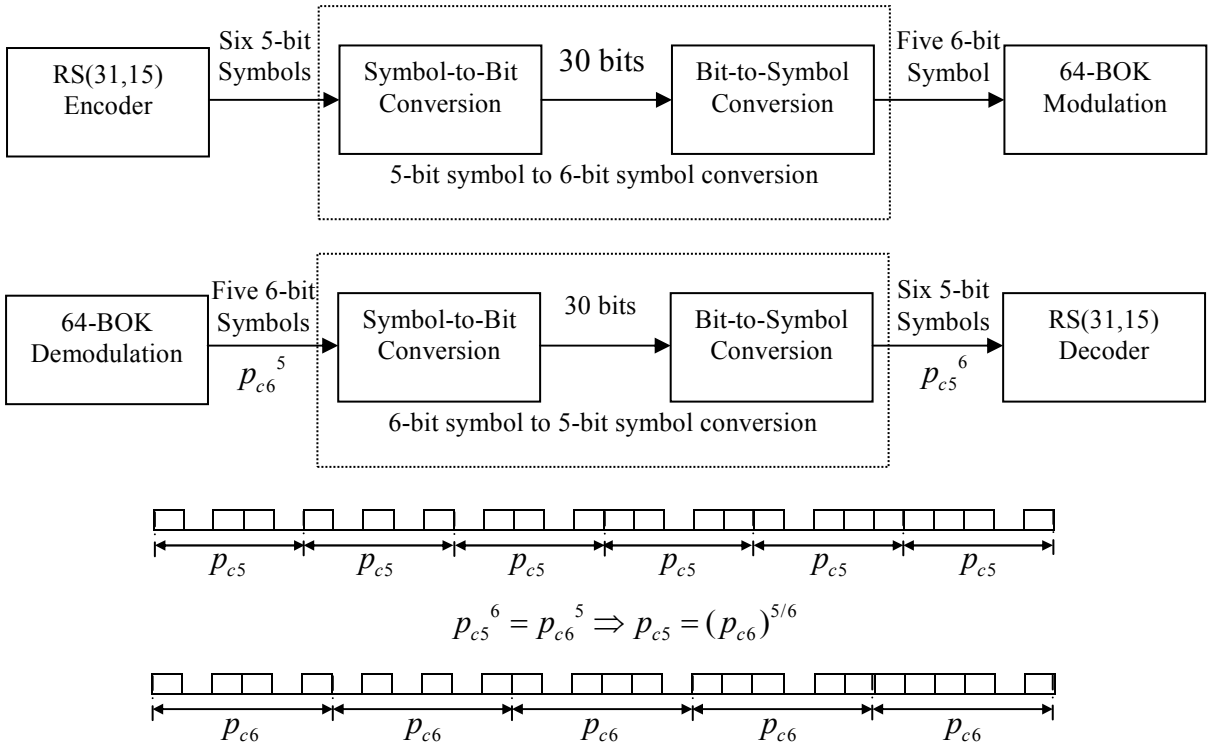

Figure 2. Conversion between five-bit symbol and six-bit symbol using 64-BOK with (31,15) RS encoding.

B. PERFORMANCE OF 64-BOK WITH (31,15) RS CODING FOR THE SINGLE-PULSE STRUCTURE

In this section, we investigate the performance of the first alternative JTIDS/Link-16 waveform for the single-pulse (no diversity) structure. The analyses cover the performance of the waveform both with and without EED and for both AWGN only as well as AWGN plus PNI. For this alternative waveform, in addition to expecting at least a slight reduction in required signal power to achieve the same P_b due to increasing the modulation order from 32 to 64, there will also be an increase in the data rate. This

occurs because we are transmitting modulated streams of six-bit symbols when using 64-BOK, which provides an increase of 1.2 as compared to streams of five-bit symbols. Since this alternative waveform utilizes both I and Q components of the carrier to transmit independent six-bit symbol streams, there is an overall increase in data rate of 2.4 as compared to the JTIDS/Link-16 waveform.

1. Performance in AWGN

The probability of correct six-bit channel symbol detection for 64-BOK demodulation in AWGN is given by [10]

$$p_{c6} = \frac{1}{\sqrt{2\pi}} \int_{-\sqrt{2rE_s/N_0}}^{\infty} e^{-\frac{u^2}{2}} \left[1 - 2Q\left(u + \sqrt{\frac{2rE_s}{N_0}} \right) \right]^{\frac{M}{2}-1} du \,. \tag{3.4}$$

Expressed in terms of average bit energy E_b, we have

$$p_{c6} = \frac{1}{\sqrt{2\pi}} \int_{-\sqrt{2rm_1E_b/N_0}}^{\infty} e^{-\frac{u^2}{2}} \left[1 - 2Q\left(u + \sqrt{\frac{2rm_1E_b}{N_0}} \right) \right]^{\frac{M}{2}-1} du \,, \tag{3.5}$$

or

$$p_{c6} = \frac{1}{\sqrt{2\pi}} \int_{-\sqrt{2rm_1\gamma_b}}^{\infty} e^{-\frac{u^2}{2}} \left[1 - 2Q\left(u + \sqrt{2rm_1\gamma_b} \right) \right]^{\frac{M}{2}-1} du \,, \tag{3.6}$$

where m_1 is the number of bits per symbol received by *M*-BOK demodulator, which is six bits per symbol for 64-BOK, $r = k/n$ is the code rate of RS encoder; and $\gamma_b = E_b / N_0$.

At the receiver, the demodulated six-bit symbols from the 64-BOK demodulator are converted to five-bit symbols before being decoded by the (31,15) RS decoder.

Substituting (3.6) into (3.2), we get

$$p_{c5} = \left\{ \frac{1}{\sqrt{2\pi}} \int_{-\sqrt{2rm_1\gamma_b}}^{\infty} e^{-\frac{u^2}{2}} \left[1 - 2Q\left(u + \sqrt{2rm_1\gamma_b} \right) \right]^{\frac{M}{2}-1} du \right\}^{\frac{5}{6}} . \tag{3.7}$$

Using (3.3) and (3.7), we obtain the probability of five-bit channel symbol error as

$$p_{s5} = 1 - \left\{ \frac{1}{\sqrt{2\pi}} \int_{-\sqrt{2rm_1\gamma_b}}^{\infty} e^{-\frac{u^2}{2}} \left[1 - 2Q\left(u + \sqrt{2rm_1\gamma_b} \right) \right]^{\frac{M}{2}-1} du \right\}^{\frac{5}{6}} . \tag{3.8}$$

Using (2.14) and (3.8), we obtain the probability of symbol error for 64-BOK with (31, 15) RS decoding in the presence of AWGN as

$$P_s \approx \frac{1}{n} \sum_{j=t+1}^{n} j \binom{n}{j} p_{s5}{}^{j} (1 - p_{s5})^{n-j} . \tag{3.9}$$

Using (3.9) in (2.16), we obtain the probability of bit error as

$$P_b \approx \frac{m_2 + 1}{2m_2} P_s , \tag{3.10}$$

where m_2 is the number of bits per symbol at the input of the RS decoder, which is five bits per symbol for the (31,15) RS decoder. Using (3.8), (3.9) and (3.10), we plot the probability of bit error for the first alternative JTIDS/Link-16 waveform in Figure 3.

For comparison purposes, the performance of both coded and uncoded waveforms are presented. The performance for the uncoded waveform is obtained using (2.5) and (2.16), where $E_s = 6E_b$.

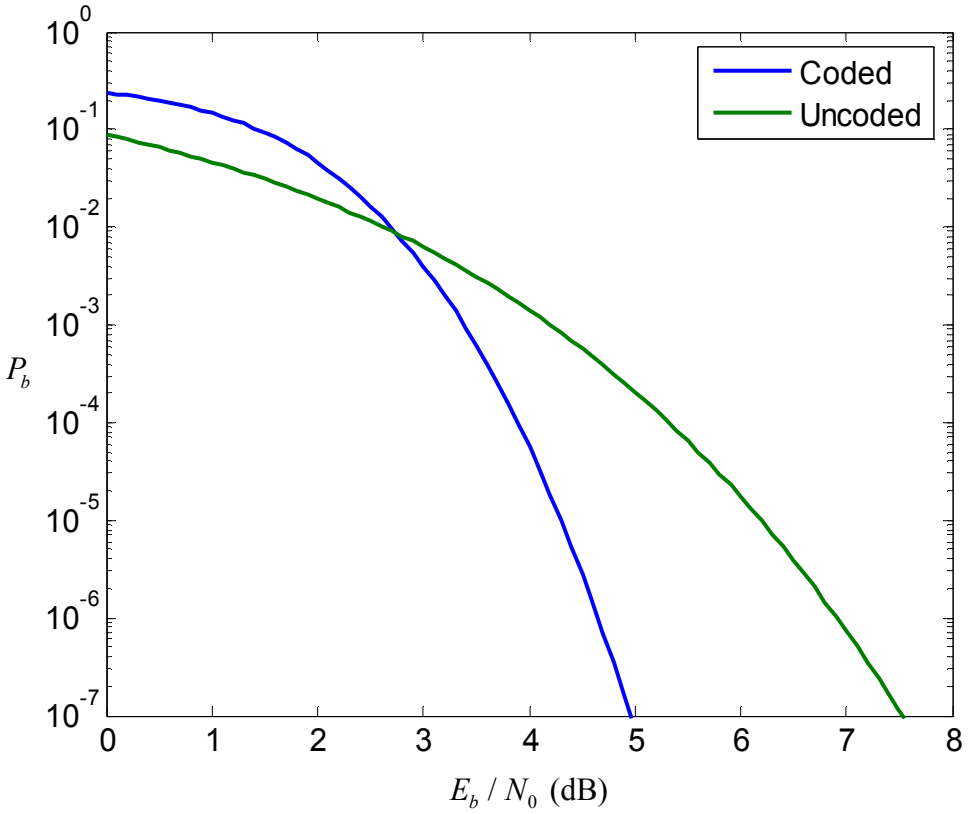

Figure 3. Performance in AWGN of the first alternative JTIDS/Link-16 waveform.

From Figure 3, we see that at $P_b = 10^{-5}$, the coded waveform requires $E_b / N_0 = 4.3$ dB, while the uncoded waveform requires $E_b / N_0 = 6.2$ dB, for a coding gain of 1.9 dB.

2. Performance in Both AWGN and Pulse-noise Interference

When both AWGN and PNI are present, combining (2.6), (2.8) and (3.8), we obtain the probability of five-bit channel symbol error as

$$p_{s5} = \rho\left\{1-\left[\frac{1}{\sqrt{2\pi}}\int_{-\sqrt{\frac{2rm_1}{\frac{N_I}{\rho E_b}+\frac{N_0}{E_b}}}}^{\infty} e^{\frac{-u^2}{2}}\left(1-2Q(u+\sqrt{\frac{2rm_1}{\frac{N_I}{\rho E_b}+\frac{N_0}{E_b}}}\right)^{\frac{M}{2}-1} du\right]^{\frac{5}{6}}\right\} \quad . \quad (3.11)$$
$$+(1-\rho)\left\{1-\left[\frac{1}{\sqrt{2\pi}}\int_{-\sqrt{2rm_1E_b/N_0}}^{\infty} e^{\frac{-u^2}{2}}\left(1-2Q(u+\sqrt{\frac{2rm_1E_b}{N_0}}\right)^{\frac{M}{2}-1} du\right]^{\frac{5}{6}}\right\}$$

Replacing E_b / N_I with γ_I and E_b / N_0 with γ_b in (3.11), we get

$$p_{s5} = \rho\left\{1-\left[\frac{1}{\sqrt{2\pi}}\int_{-\sqrt{\frac{2rm_1}{\frac{1}{\rho\gamma_I}+\frac{1}{\gamma_b}}}}^{\infty} e^{\frac{-u^2}{2}}\left(1-2Q(u+\sqrt{\frac{2rm_1}{\frac{1}{\rho\gamma_I}+\frac{1}{\gamma_b}}}\right)^{\frac{M}{2}-1} du\right]^{\frac{5}{6}}\right\} \quad . \quad (3.12)$$
$$+(1-\rho)\left\{1-\left[\frac{1}{\sqrt{2\pi}}\int_{-\sqrt{2rm_1\gamma_b}}^{\infty} e^{\frac{-u^2}{2}}\left[1-2Q(u+\sqrt{2rm_1\gamma_b}\right]^{\frac{M}{2}-1} du\right]^{\frac{5}{6}}\right\}$$

Now defining $\zeta = 1/\left(\gamma_b^{-1}+\left(\rho\gamma_I\right)^{-1}\right)$, we obtain

$$p_{s5} = \rho\left\{1-\left[\frac{1}{\sqrt{2\pi}}\int_{-\sqrt{2rm_1\zeta}}^{\infty} e^{\frac{-u^2}{2}}\left[1-2Q(u+\sqrt{2rm_1\zeta}\right]^{\frac{M}{2}-1} du\right]^{\frac{5}{6}}\right\}$$
$$+(1-\rho)\left\{1-\left[\frac{1}{\sqrt{2\pi}}\int_{-\sqrt{2rm_1\gamma_b}}^{\infty} e^{\frac{-u^2}{2}}\left[1-2Q(u+\sqrt{2rm_1\gamma_b}\right]^{\frac{M}{2}-1} du\right]^{\frac{5}{6}}\right\} \quad . \quad (3.13)$$

The probability of information channel symbol error is obtained by substituting (3.13) into (3.9) and (2.16). The performance for both the coded and the uncoded waveforms in AWGN and PNI for $E_b / N_0 = 9$ dB with $\rho = 1$ and $\rho = 0.2$ are shown in Figure 4 and Figure 5, respectively.

In Figure 4, at $P_b = 10^{-5}$, the E_b / N_I required for the coded waveform is 6.1 dB, while the uncoded waveform requires 9.4 dB, for a coding gain of 3.3 dB.

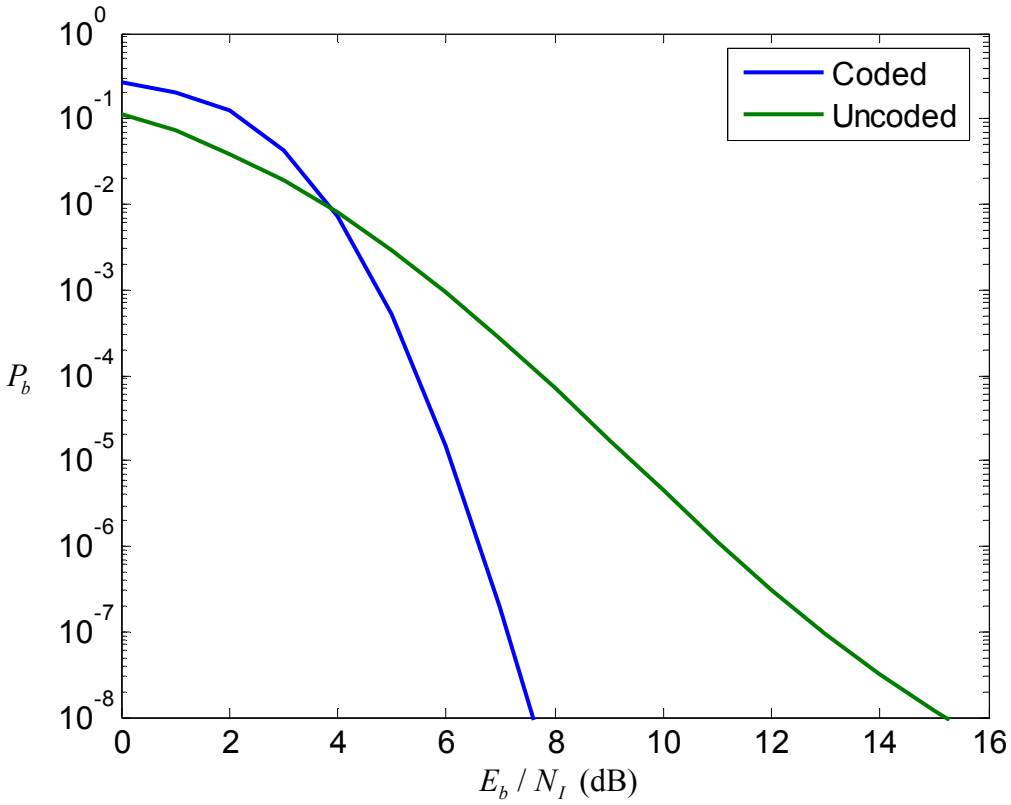

Figure 4. Performance of the first alternative JTIDS/Link-16 waveform for $\rho = 1$ and $E_b / N_0 = 9$ dB.

Similarly, in Figure 5, at $P_b = 10^{-5}$, the E_b / N_I required for the coded waveform is 8.9 dB, while the uncoded waveform requires 15.3 dB, for a coding gain of 6.4 dB. From the preceding results, the coded waveform performs better than the uncoded waveform in AWGN and PNI. Comparing the absolute performance of the coded waveform from Figure 4 and Figure 5, we see that when $\rho = 1$ performance is better than when $\rho = 0.2$; although, there is a larger coding gain when $\rho = 0.2$.

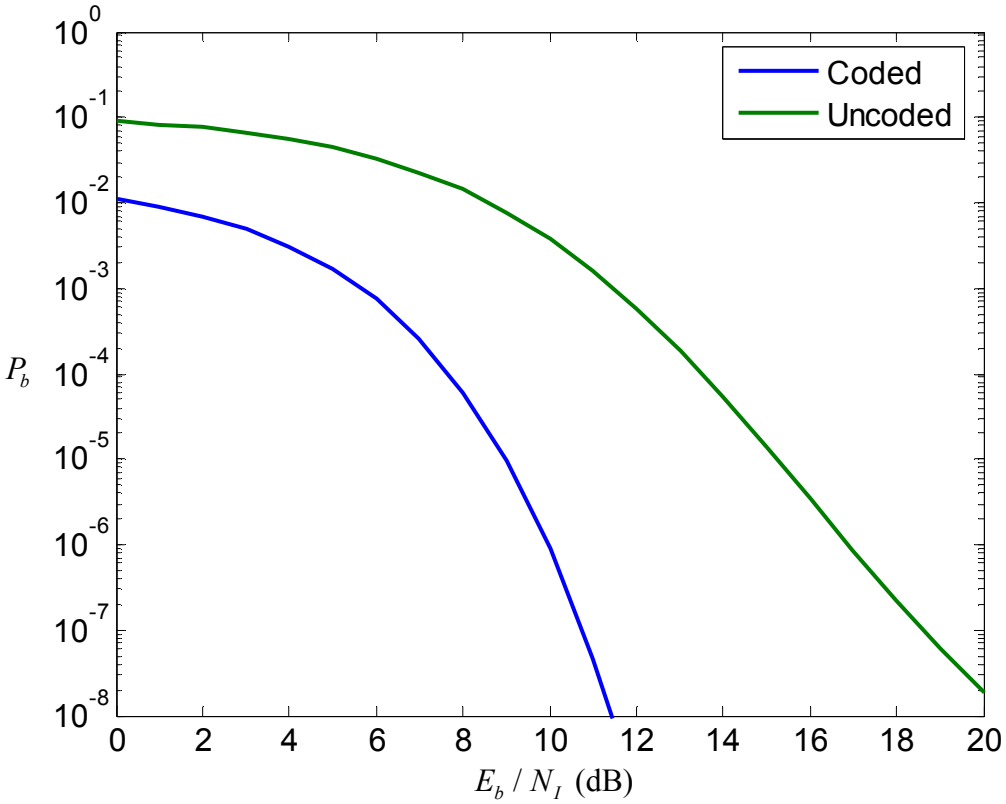

Figure 5. Performance of the first alternative JTIDS/Link-16 waveform for $\rho = 0.2$ and $E_b / N_0 = 9$ dB.

The performance of 64-BOK with (31, 15) RS coding in PNI for $E_b / N_0 = 6$ dB with different values of ρ is shown in Figure 6. Using $P_b = 10^{-5}$ as reference, we compare the required E_b / N_I for different values of ρ. When $\rho = 1$, which is equivalent to barrage noise interference, for $P_b = 10^{-5}$ performance is better ($E_b / N_I \approx 9.2$ dB) as compared to $\rho = 0.2$ and $\rho = 0.1$ ($E_b / N_I \approx 10$ dB); the degradation due to PNI is about 0.8 dB. In this particular case, there is small difference in performance between $\rho = 0.2$ and $\rho = 0.1$. From Figure 6, we see that the transition point when $\rho = 1$ yields better performance than $\rho = 0.2$ and 0.1 occurs for $P_b < 10^{-3}$ when $E_b / N_I > 6.9$ dB.

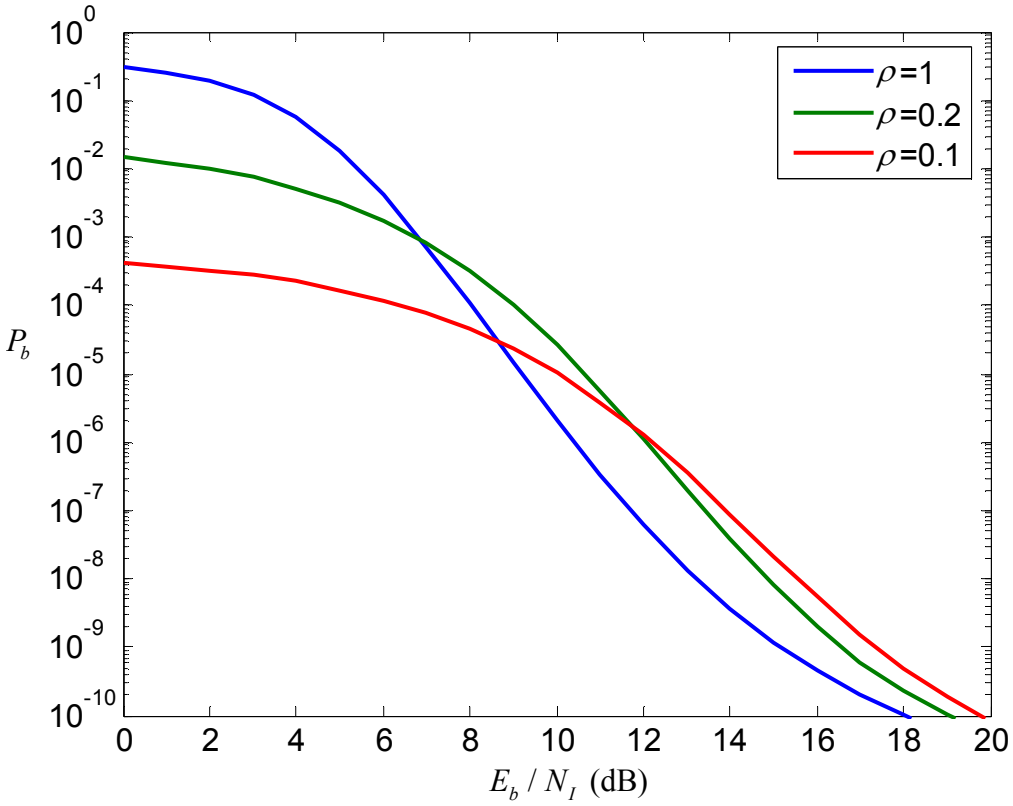

Figure 6. Performance of 64-BOK with (31,15) RS coding in PNI for different values of ρ with $E_b / N_0 = 6$ dB.

The performance of 64-BOK with (31, 15) RS coding in PNI for $E_b / N_0 = 9$ dB with different values of ρ is shown in Figure 7. When we compare the results in Figure 6 to those in Figure 7, we see an improvement in the overall performance as E_b / N_0 increases. When $P_b = 10^{-5}$, the required E_b / N_I for $\rho = 1$ and $\rho = 0.2$ are 6.1 dB and 8.9 dB, respectively; the degradation due to PNI is about 2.8 dB.

Comparing Figure 7 with Figure 6, where E_b / N_I for $\rho = 1$ and $\rho = 0.2$ are 9.2 dB and 10 dB, respectively, we see that smaller values of E_b / N_I are required for the same P_b. Thus, in Figure 7, the increase in E_b / N_0 improves the performance due to PNI but it also increases relative degradation.

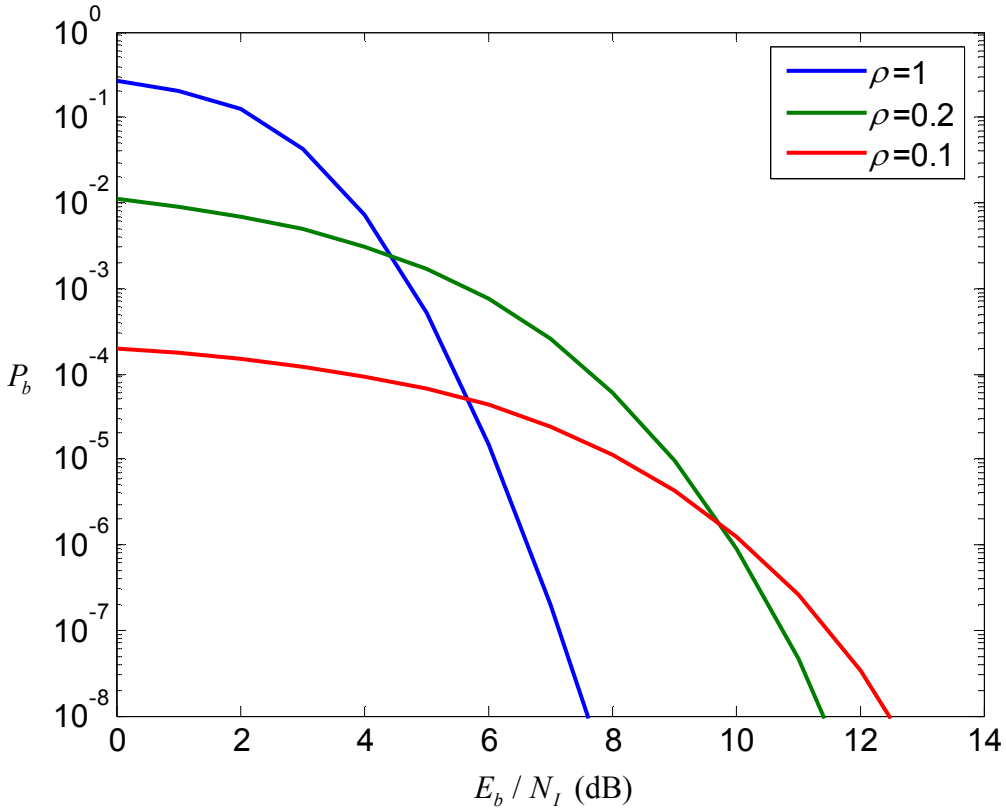

Figure 7. Performance of 64-BOK with (31,15) RS coding in PNI for different values of ρ with $E_b / N_0 = 9$ dB.

3. Conversion Between Five-bit Symbols and Six-bit Symbols with (31, 15) RS Encoding and EED

At the receiver, using 64-BOK with EED, we must convert the demodulated with erasures six-bit symbols into five-bit symbols with erasures prior to the RS decoder. This concept is shown in Figure 8.

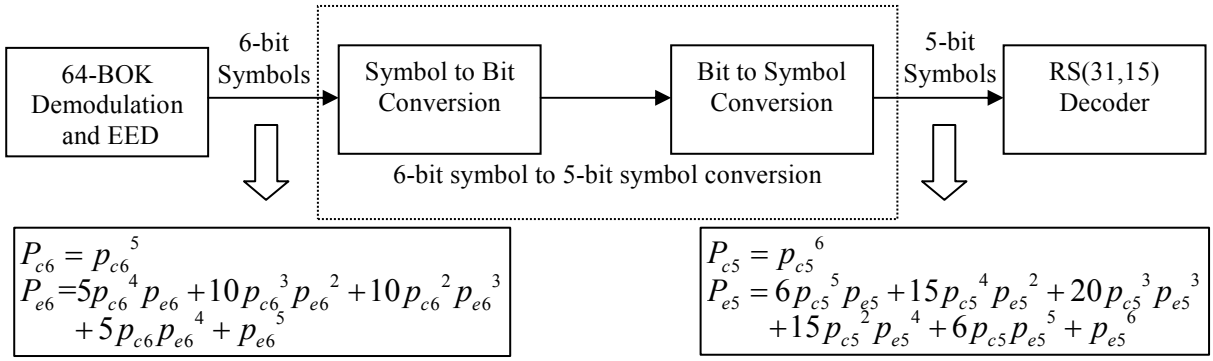

Figure 8. Conversion between five-bit symbol and six-bit symbols using 64-BOK with (31,15) RS encoding and EED.

From Figure 8, using 64-BOK with erasure demodulation, we obtain the total probability of correct six-bit symbol detection P_{c6} and, at the output of the six-bit symbol to five-bit symbol converter, the total probability of correct five-bit symbols P_{c5} just as when using errors-only detection. When each symbol is received independently, the total probability of six correct five-bit symbols and five six-bit symbols is identical and is given by (3.1). Using (3.1), we obtain the probability of correct five-bit symbol detection given in (3.2) and repeated here for convenience:

$$p_{c5} = (p_{c6})^{5/6}. \tag{3.14}$$

The total probability of six-bit symbol channel erasure at the output of the 64-BOK demodulator with EED in a block of five six-bit symbols is evaluated as

$$P_{e6}=5p_{c6}^{\ 4}p_{e6}+10p_{c6}^{\ 3}p_{e6}^{\ 2}+10p_{c6}^{\ 2}p_{e6}^{\ 3}+5p_{c6}p_{e6}^{\ 4}+p_{e6}^{\ 5}, \tag{3.15}$$

and the total probability of five-bit symbol channel erasure at the output of the six-bit symbol to five-bit converter in a block of six five-bit symbols is evaluated as

$$P_{e5}=6p_{c5}^{\ 5}p_{e5}+15p_{c5}^{\ 4}p_{e5}^{\ 2}+20p_{c5}^{\ 3}p_{e5}^{\ 3}+15p_{c5}^{\ 2}p_{e5}^{\ 4}+6p_{c5}p_{e5}^{\ 5}+p_{e5}^{\ 6}. \tag{3.16}$$

When each symbol is received independently, the total probability of channel erasure in a block of five six-bit symbols is identical to that of a block of six five-bit symbols; therefore,

$$P_{e6} = P_{e5}, \tag{3.17}$$

Substituting (3.15)and (3.16) into (3.17), we get

$$\begin{aligned} &5{p_{c6}}^4 p_{e6} + 10{p_{c6}}^3 {p_{e6}}^2 + 10{p_{c6}}^2 {p_{e6}}^3 + 5p_{c6}{p_{e6}}^4 + {p_{e6}}^5 \\ &= 6{p_{c5}}^5 p_{e5} + 15{p_{c5}}^4 {p_{e5}}^2 + 20{p_{c5}}^3 {p_{e5}}^3 + 15{p_{c5}}^2 {p_{e5}}^4 + 6p_{c5}{p_{e5}}^5 + {p_{e5}}^6 . \end{aligned} \tag{3.18}$$

which, using Mathcad, can be simplified to

$$p_{e5} = \left({p_{c5}}^6 + 5{p_{c6}}^4 p_{e6} + 10{p_{c6}}^3 {p_{e6}}^2 + 5{p_{c6}}^2 {p_{e6}}^3 + {p_{e6}}^5 \right)^{\frac{1}{6}} - p_{c5} . \tag{3.19}$$

4. Performance with Errors-and-Erasures Encoding in AWGN

At the receiver, the *M*BOK demodulator has to decide which of *M* symbols was received with sufficient or insufficient confidence. If the output of each integrator $V_T > X_i > -V_T,\ i = 1,2,...,M/2,$ then the receiver erases the symbol since it cannot decide with sufficient confidence.

Assuming that the original signal representing symbol '1' is transmitted and received at the receiver with errors-and-erasures demodulation, we get the probability of channel symbol erasure p_e and probability of correct symbol detection p_c as [10]

$$p_e = \Pr\left[(V_T > X_1 > -V_T) \cap (V_T > X_2 > -V_T) \cap ... \cap (V_T > X_{M/2} > -V_T) \,|\, 1 \right] \tag{3.20}$$

and

$$p_c = \Pr\left[(X_1 > V_T) \cap (|X_1| > |X_2|) \cap (|X_1| > |X_3|) \cap ... \cap (|X_1| > |X_{M/2}|) \,|\, 1 \right], \tag{3.21}$$

respectively. The probability of channel symbol error is obtained by substituting (3.20) and (3.21) into (2.21).

From (3.20), the probability of symbol erasure is given by

$$p_e = \int_{-V_T}^{V_T} \int_{-V_T}^{V_T} \int_{-V_T}^{V_T} ... \int_{-V_T}^{V_T} f_{X_1 X_2 ... X_{M/2}} \left(x_1, x_2, ..., x_{M/2} \,|\, 1 \right) dx_1 dx_2 dx_3 ... dx_{M/2} , \tag{3.22}$$

where $f_{X_1 X_2 ... X_{M/2}} \left(x_1, x_2, ..., x_{M/2} \,|\, 1 \right)$ is the joint probability density function of the random variables at the detector outputs. Considering that the random variables at the detector outputs are independent, we get from (3.22)

$$p_e = \int_{-V_T}^{V_T} f_{X_1}(x_1 \mid 1)dx_1 \int_{-V_T}^{V_T} f_{X_2}(x_2 \mid 1)dx_2 \times \int_{-V_T}^{V_T} f_{X_3}(x_3 \mid 1)dx_3 \ldots \int_{-V_T}^{V_T} f_{X_{M/2}}(x_{M/2} \mid 1)dx_{M/2} \quad . \tag{3.23}$$

Since $\int_{-V_T}^{V_T} f_{X_2}(x_2 \mid 1)dx_2 = \int_{-V_T}^{V_T} f_{X_3}(x_3 \mid 1)dx_3 = \ldots = \int_{-V_T}^{V_T} f_{X_{M/2}}(x_{M/2} \mid 1)dx_{M/2}$, (3.23) simplifies to

$$p_e = \left[\int_{-V_T}^{V_T} f_{X_1}(x_1 \mid 1)dx_1\right]\left[\int_{-V_T}^{V_T} f_{X_2}(x_2 \mid 1)dx_2\right]^{\frac{M}{2}-1} \tag{3.24}$$

Substituting (2.2), (2.3), and (2.4) into (3.24), we obtain

$$p_e = \left[\int_{-V_T}^{V_T} \frac{1}{\sqrt{2\pi}\sigma} e^{-\frac{(x_1-\sqrt{2}A_c)^2}{2\sigma^2}} dx_1\right]\left[2\int_{0}^{V_T} \frac{1}{\sqrt{2\pi}\sigma} e^{-\frac{x_2^2}{2\sigma^2}} dx_2\right]^{\frac{M}{2}-1}, \tag{3.25}$$

which can be evaluated to obtain

$$p_e = \left[1 - Q\left(\frac{V_T + \sqrt{2}A_c}{\sigma}\right) - Q\left(\frac{V_T + \sqrt{2}A_c}{\sigma}\right)\right]\left[1 - 2Q\left(\frac{V_T}{\sigma}\right)\right]^{\frac{M}{2}-1}. \tag{3.26}$$

Alternatively, (3.26) can be written as

$$p_e = \left[Q\left(\frac{\sqrt{2}A_c - V_T}{\sigma}\right) - Q\left(\frac{V_T + \sqrt{2}A_c}{\sigma}\right)\right]\left[1 - 2Q\left(\frac{V_T}{\sigma}\right)\right]^{\frac{M}{2}-1}. \tag{3.27}$$

Defining $V_T = a\sqrt{2}A_c$ where $0 < a < 1$ and $\sigma^2 = N_o / T_s$, we get

$$p_e = \left[Q\left(\frac{\sqrt{2}A_c - a\sqrt{2}A_c}{\sigma}\right) - Q\left(\frac{\sqrt{2}A_c + a\sqrt{2}A_c}{\sigma}\right)\right]\left[1 - 2Q\left(\frac{a\sqrt{2}A_c}{\sigma}\right)\right]^{\frac{M}{2}-1}. \tag{3.28}$$

Since $E_s = A_c^2 T_s$, the probability of symbol erasure for *M*BOK is

$$p_e = \left[Q\left((1-a)\sqrt{\frac{2E_s}{N_0}} \right) - Q\left((1+a)\sqrt{\frac{2E_s}{N_0}} \right) \right] \left[1 - 2Q\left(a\sqrt{\frac{2E_s}{N_0}} \right) \right]^{\frac{M}{2}-1}. \quad (3.29)$$

From (3.29), the probability of symbol erasure for *M*BOK with (n,k) RS coding with code rate r is

$$p_e = \left[Q\left((1-a)\sqrt{\frac{2rE_s}{N_0}} \right) - Q\left((1+a)\sqrt{\frac{2rE_s}{N_0}} \right) \right] \left[1 - 2Q\left(a\sqrt{\frac{2rE_s}{N_0}} \right) \right]^{\frac{M}{2}-1}, \quad (3.30)$$

and, in terms of E_b / N_0, we get

$$p_e = \left[Q\left((1-a)\sqrt{\frac{2rmE_b}{N_0}} \right) - Q\left((1+a)\sqrt{\frac{2rmE_b}{N_0}} \right) \right] \left[1 - 2Q\left(a\sqrt{\frac{2rmE_b}{N_0}} \right) \right]^{\frac{M}{2}-1}. \quad (3.31)$$

Next, we derive the probability of correct symbol detection from (3.21), where we have

$$p_c = \int_{V_T}^{\infty} \left[\int_{-x_1}^{x_1} \int_{-x_1}^{x_1} \cdots \int_{-x_1}^{x_1} f_{X_1 X_2 \ldots X_{M/2}}(x_1, x_2, \ldots, x_{M/2} \mid 1) dx_2 dx_3 \ldots dx_{M/2} \right] dx_1 \quad (3.32)$$

From (3.32) we get

$$p_c = \int_{V_T}^{\infty} f_{X_1}(x_1 \mid 1) \times \left[\int_{-x_1}^{x_1} f_{X_2}(x_2 \mid 1) dx_2 \int_{-x_1}^{x_1} f_{X_3}(x_3 \mid 1) dx_3 \ldots \int_{-x_1}^{x_1} f_{X_{M/2}}(x_{M/2} \mid 1) dx_{M/2} \right] dx_1, \quad (3.33)$$

since the $x_i s$ are modeled as independent random variables,

Simplifying (3.33) as in the derivation for p_e, we get

$$p_c = \int_{V_T}^{\infty} f_{X_1}(x_1 \mid 1) \left[\int_{-x_1}^{x_1} f_{X_2}(x_2 \mid 1) dx_2 \right]^{\frac{M}{2}-1} dx_1. \quad (3.34)$$

Substituting (2.2), (2.3) and (2.4) into (3.34), we obtain

$$p_c = \int_{V_T}^{\infty} \frac{1}{\sqrt{2\pi}\sigma} e^{-\frac{(x_1-\sqrt{2}A_c)^2}{2\sigma^2}} \left[\int_{-x_1}^{x_1} \frac{1}{\sqrt{2\pi}\sigma} e^{-\frac{x_2^2}{2\sigma^2}} dx_2 \right]^{\frac{M}{2}-1} dx_1, \tag{3.35}$$

which can be partially evaluated to get

$$p_c = \int_{V_T}^{\infty} \frac{1}{\sqrt{2\pi}\sigma} e^{-\frac{(x_1-\sqrt{2}A_c)^2}{2\sigma^2}} \left[1 - 2Q\left(\frac{x_1}{\sigma}\right) \right]^{\frac{M}{2}-1} dx_1. \tag{3.36}$$

Let $u = (x_1 - \sqrt{2}A_c)/\sigma$ in (3.36), and

$$p_c = \int_{\frac{V_T-\sqrt{2}A_c}{\sigma}}^{\infty} \frac{1}{\sqrt{2\pi}} e^{-\frac{u^2}{2}} \left[1 - 2Q\left(u + \frac{\sqrt{2}A_c}{\sigma} \right) \right]^{\frac{M}{2}-1} dx_1. \tag{3.37}$$

Defining $V_T = a\sqrt{2}A_c$ and $\sigma^2 = N_0/T_s$ as before, we obtain the probability of correct symbol detection for *M*BOK from (3.37) as

$$p_c = \frac{1}{\sqrt{2\pi}} \int_{-(1-a)\sqrt{\frac{2E_s}{N_0}}}^{\infty} e^{-\frac{u^2}{2}} \left[1 - 2Q\left(u + \sqrt{\frac{2E_s}{N_0}} \right) \right]^{\frac{M}{2}-1} du. \tag{3.38}$$

From (3.38), the probability of correct symbol detection with erasure demodulation for *M*BOK with (n,k) RS coding with code rate r is

$$p_c = \frac{1}{\sqrt{2\pi}} \int_{-(1-a)\sqrt{\frac{2rE_s}{N_0}}}^{\infty} e^{-\frac{u^2}{2}} \left[1 - 2Q\left(u + \sqrt{\frac{2rE_s}{N_0}} \right) \right]^{\frac{M}{2}-1} du. \tag{3.39}$$

In terms of E_b/N_0, (3.39) can be expressed as

$$p_c = \frac{1}{\sqrt{2\pi}} \int_{-(1-a)\sqrt{\frac{2rmE_b}{N_0}}}^{\infty} e^{-\frac{u^2}{2}} \left[1 - 2Q\left(u + \sqrt{\frac{2rmE_b}{N_0}} \right) \right]^{\frac{M}{2}-1} du. \tag{3.40}$$

Subsequently, the probability of channel symbol error for MBOK with EED can be obtained by substituting (3.31) and (3.40) into (2.21). Using the result for p_s from (2.21) and substituting (3.31) and (3.40) into (2.24), we obtain the probability of block error. Equation (2.24)is repeated here for convenience:

$$P_E = 1 - \left[\sum_{i=0}^{t} \binom{n}{i} {p_s}^i \sum_{j=0}^{d_{\min}-1-2i} \binom{n-i}{j} {p_e}^j {p_c}^{n-i-j} \right]. \tag{3.41}$$

Now, the probability of bit error for *M*BOK with RS coding and EED in the presence of AWGN is obtained by using (3.41) in (2.25) and then using that result in (2.16).

From (3.31), the probability of six-bit channel symbol erasure is

$$p_{e6} = \left[Q\left((1-a)\sqrt{\frac{2rm_1E_b}{N_0}} \right) - Q\left((1+a)\sqrt{\frac{2rm_1E_b}{N_0}} \right) \right] \left[1 - 2Q\left(a\sqrt{\frac{2rm_1E_b}{N_0}} \right) \right]^{\frac{M}{2}-1}, \tag{3.42}$$

where $m_1 = 6$ is the number of bits per symbol received by 64-BOK demodulator with EED. Similarly, the probability of correct six-bit channel symbol detection is obtained from (3.40) as

$$p_{c6} = \frac{1}{\sqrt{2\pi}} \int_{-(1-a)\sqrt{\frac{2rm_1E_b}{N_0}}}^{\infty} e^{-\frac{u^2}{2}} \left[1 - 2Q\left(u + \sqrt{\frac{2rm_1E_b}{N_0}} \right) \right]^{\frac{M}{2}-1} du\,. \tag{3.43}$$

Substituting (3.43) into (3.14), we obtain the probability of correct five-bit channel symbol detection as

$$p_{c5} = \left(\frac{1}{\sqrt{2\pi}} \int_{-(1-a)\sqrt{\frac{2rm_1E_b}{N_0}}}^{\infty} e^{-\frac{u^2}{2}} \left[1 - 2Q\left(u + \sqrt{\frac{2rm_1E_b}{N_0}} \right) \right]^{\frac{M}{2}-1} du \right)^{5/6}. \tag{3.44}$$

Using (3.42), (3.43) and (3.44) in (3.19), we obtain the probability of five-bit channel symbol erasure. Substituting this result and (3.44) into (2.21), we obtain the probability of five-bit channel symbol error as

$$p_{s5} = 1 - p_{e5} - p_{c5}. \tag{3.45}$$

Using the results for p_{s5}, $p_{e5,}$ and p_{c5} in (2.24), we obtain the probability of block error for 64-BOK with (31, 15) RS code and EED as

$$P_E = 1 - \sum_{i=0}^{t} \binom{n}{i} {p_{s5}}^{i} \sum_{j=0}^{d_{\min}-1-2i} \binom{n-i}{j} {p_{e5}}^{j} {p_{c5}}^{n-i-j}. \tag{3.46}$$

Now, we obtain the probability of symbol error and the probability of bit error for 64-BOK with (31, 15) RS coding and EED in the presence of AWGN using (2.25) and (3.10), respectively.

The results for 64-BOK with (31, 15) RS coding and EED in AWGN for different values of a are shown in Figure 9, where a varies from 0 (no EED) to 0.9 (with EED). In Figure 9, we see the degradation in performance for large values of a ($a \geq 0.8$) but not much difference for $a <$ 0.6. From these results, we conclude that there is no improvement in the performance when EED is used for the first alternative JTIDS/Link-16 waveform in the presence of AWGN. EED degrades performance if a is too large.

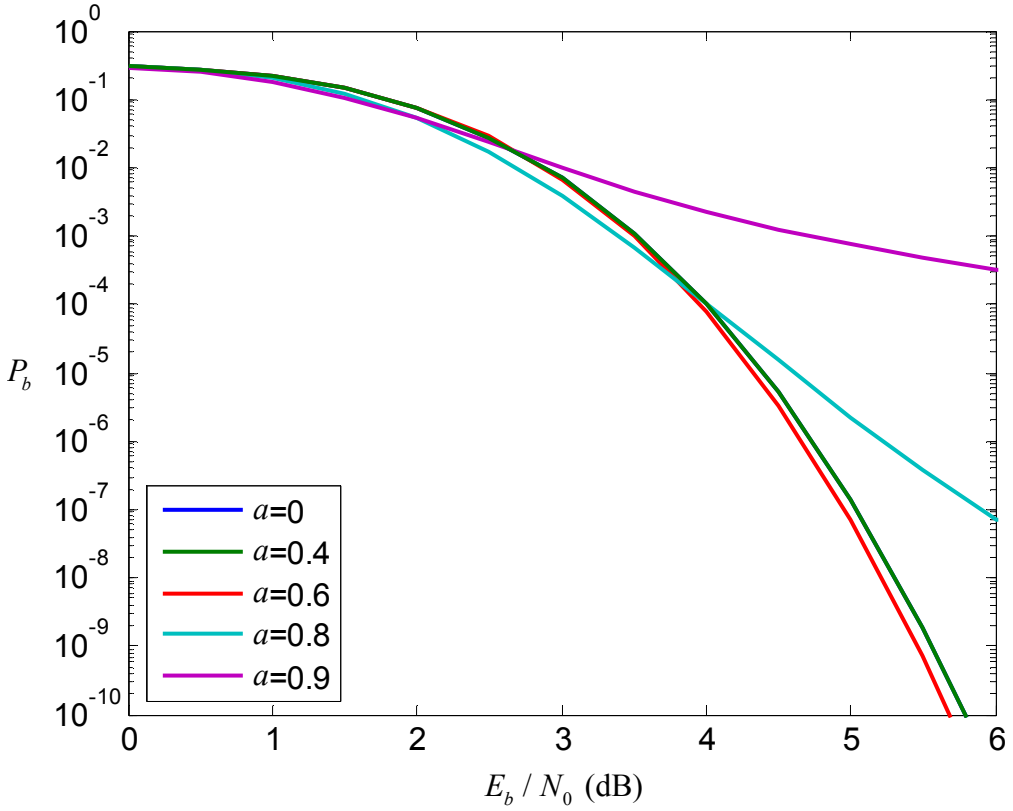

Figure 9. Performance of 64-BOK with (31,15) RS coding and EED for different values of a in the presence of AWGN.

5. Performance with Errors-and-Erasures Decoding in AWGN and Pulse-noise Interference

The probability of six-bit channel symbol erasure for 64-BOK and EED when PNI is also present is obtained from (2.6), (2.8) and (3.42) in terms of E_b as

$$p_{e6} = (1-\rho)\left[Q\left((1-a)\sqrt{\frac{2rm_1E_b}{N_0}}\right) - Q\left((1+a)\sqrt{\frac{2rm_1E_b}{N_0}}\right)\right]\left[1-2Q\left(a\sqrt{\frac{2rm_1E_b}{N_0}}\right)\right]^{\frac{M}{2}-1}$$
$$+\rho\left[Q\left((1-a)\sqrt{\frac{2rm_1E_b}{\frac{1}{\rho}N_I+N_0}}\right) - Q\left((1+a)\sqrt{\frac{2rm_1E_b}{\frac{1}{\rho}N_I+N_0}}\right)\right]\left[1-2Q\left(a\sqrt{\frac{2rm_1E_b}{\frac{1}{\rho}N_I+N_0}}\right)\right]^{\frac{M}{2}-1}. \quad (3.47)$$

Since $\gamma_I = E_b / N_I$ and $\gamma_b = E_b / N_0$ and defining $\zeta = 1/\left(\gamma_b^{-1} + (\rho\gamma_I)^{-1}\right)$, we obtain from (3.47)

$$p_{e6} = (1-\rho)\left[Q\left((1-a)\right)\sqrt{2rm_1\gamma_b}\right) - Q\left((1+a)\sqrt{2rm_1\gamma_b}\right)\right]\left[1-2Q\left(a\sqrt{2rm_1\gamma_b}\right)\right]^{\frac{M}{2}-1} + \rho\left[Q\left((1-a)\sqrt{2rm_1\zeta}\right) - Q\left((1+a)\sqrt{2rm_1\zeta}\right)\right]\left[1-2Q\left(a\sqrt{2rm_1\zeta}\right)\right]^{\frac{M}{2}-1}. \quad (3.48)$$

Similarly, the probability of six-bit correct channel symbol detection is obtained from (2.6), (2.8) and (3.43) as

$$p_{c6} = (1-\rho)\left\{\frac{1}{\sqrt{2\pi}}\int_{-(1-a)\sqrt{\frac{2rm_1E_b}{N_0}}}^{\infty} e^{-\frac{u^2}{2}}\left[1-2Q\left(u+\sqrt{\frac{2rm_1E_b}{N_0}}\right)\right]^{\frac{M}{2}-1} du\right\} + \rho\left\{\frac{1}{\sqrt{2\pi}}\int_{-(1-a)\sqrt{\frac{2rm_1E_b}{\frac{1}{\rho}N_I+N_0}}}^{\infty} e^{-\frac{u^2}{2}}\left[1-2Q\left(u+\sqrt{\frac{2rm_1E_b}{\frac{1}{\rho}N_I+N_0}}\right)\right]^{\frac{M}{2}-1} du\right\}, \quad (3.49)$$

which can be expressed as

$$p_{c6} = (1-\rho)\left\{\frac{1}{\sqrt{2\pi}}\int_{-(1-a)\sqrt{2rm_1\gamma_b}}^{\infty} e^{-\frac{u^2}{2}}\left[1-2Q\left(u+\sqrt{2rm_1\gamma_b}\right)\right]^{\frac{M}{2}-1} du\right\} + \rho\left\{\frac{1}{\sqrt{2\pi}}\int_{-(1-a)\sqrt{2rm_1\zeta}}^{\infty} e^{-\frac{u^2}{2}}\left[1-2Q\left(u+\sqrt{2rm_1\zeta}\right)\right]^{\frac{M}{2}-1} du\right\}. \quad (3.50)$$

The probability of correct five-bit channel symbol detection is obtained by substituting (3.50) into (3.14) to get

$$p_{c5} = \left[(1-\rho)\left\{\frac{1}{\sqrt{2\pi}}\int_{-(1-a)\sqrt{2rm_1\gamma_b}}^{\infty} e^{-\frac{u^2}{2}}\left[1-2Q\left(u+\sqrt{2rm_1\gamma_b}\right)\right]^{\frac{M}{2}-1} du\right\} + \rho\left\{\frac{1}{\sqrt{2\pi}}\int_{-(1-a)\sqrt{2rm_1\zeta}}^{\infty} e^{-\frac{u^2}{2}}\left[1-2Q\left(u+\sqrt{2rm_1\zeta}\right)\right]^{\frac{M}{2}-1} du\right\}\right]^{\frac{5}{6}}. \quad (3.51)$$

Now, substituting the results from (3.49), (3.50) and (3.51) into (3.19), we obtain the probability of five-bit channel symbol erasure p_{e5}. The probability of five-bit channel symbol error is obtained by substituting (3.51) and the result for p_{e5} into (3.45).

As previously, we obtain the probability of block error by substituting (3.45), (3.51) and the result for p_{e5} into (3.46). This result is then used to get the probability of symbol error expressed in (2.25). Using (3.10), we get the probability of bit error for 64-BOK with (31,15) RS coding and EED in both AWGN and PNI.

The performance of 64-BOK with (31,15) RS coding and EED for different values of a, $\rho = 1$ and $E_b / N_0 = 6$ dB is shown in Figure 10. From Figure 10, the performance for $a = 0.6$ is slightly better as compared to $a = 0$, $a = 0.2$, $a = 0.4$ and $a = 0.8$. The performance for $a = 0, a = 0.2$ and $a = 0.4$ are almost the same at $P_b = 10^{-5}$, while the performance for $a = 0.8$ is the worst. Note that $a = 0$ corresponds to no EED.

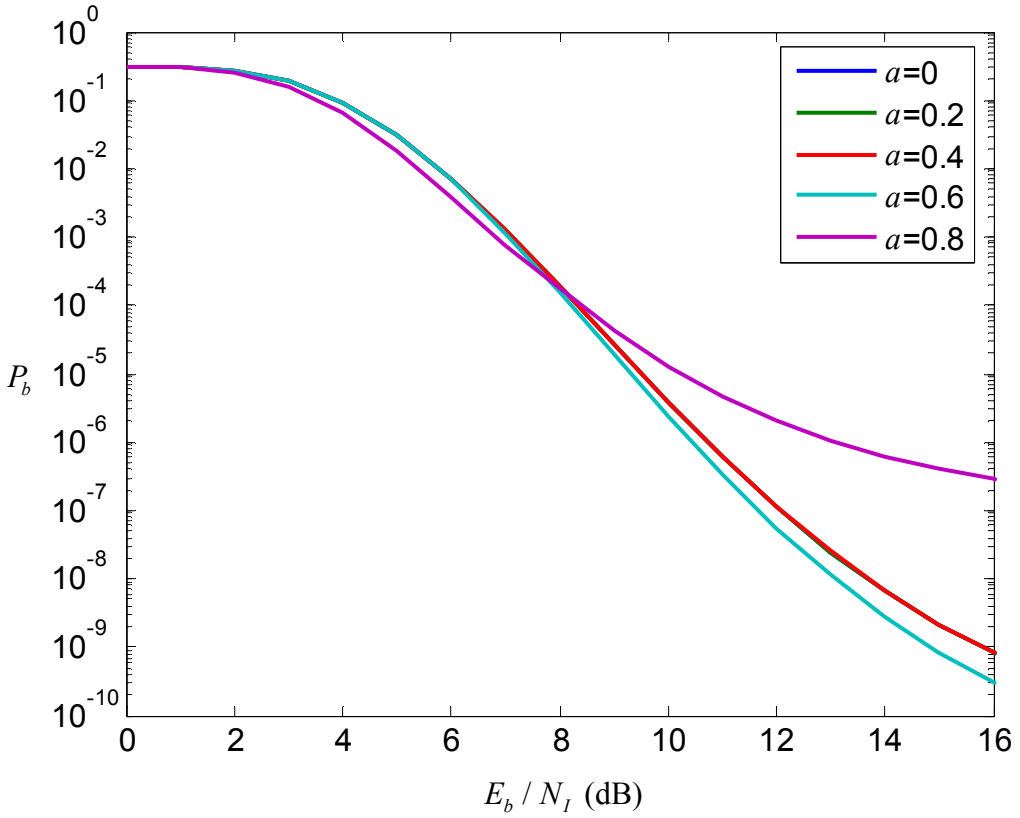

Figure 10. Performance of 64-BOK with (31,15) RS coding and EED for $\rho = 1$ and $E_b / N_0 = 6$ dB for different values of a in both AWGN and PNI.

The performance of 64-BOK with (31,15) RS coding and EED in both AWGN and PNI environment for different values of ρ, $a = 0.6$ and $E_b / N_0 = 6$ dB is shown in Figure 11. At $P_b = 10^{-5}$, the performance is degraded as ρ decreases and the degradation is limited to about 2 dB.

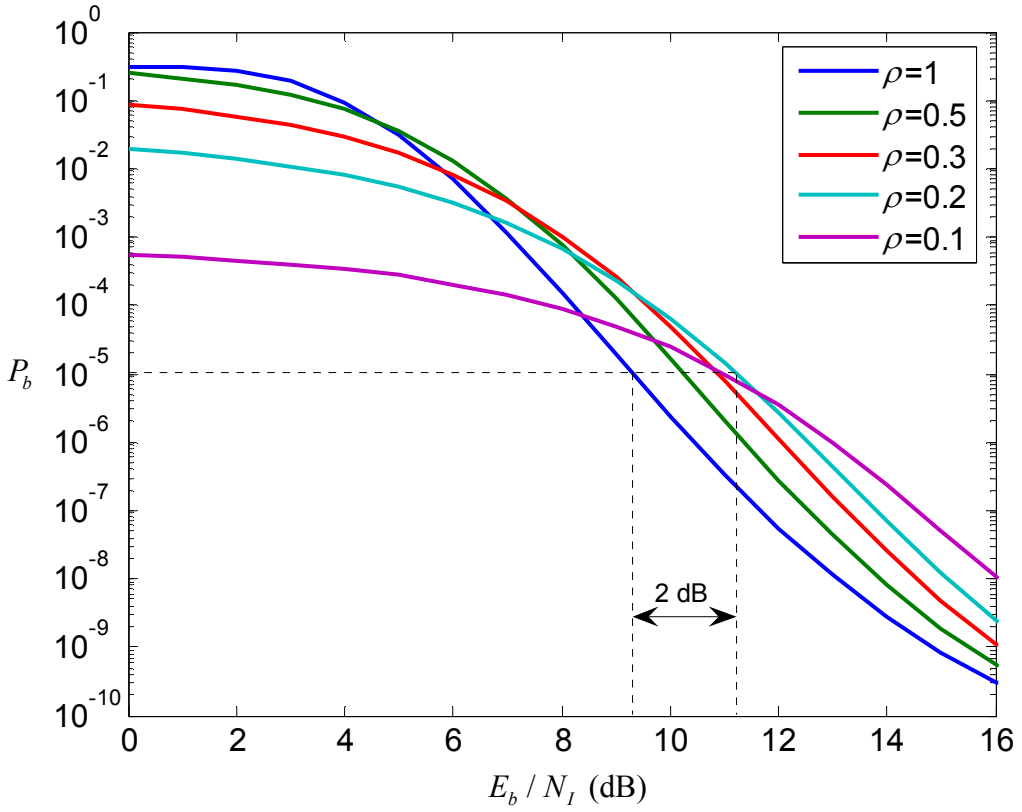

Figure 11. Performance of 64-BOK with (31,15) RS coding and EED for $E_b / N_0 = 6$ dB with different ρ for $a = 0.6$ in both AWGN and PNI.

The performance for 64-BOK with (31, 15) RS coding both with and without EED in a AWGN and PNI environment for $a = 0.6$, $E_b / N_0 = 6$ dB and different values of ρ is shown in Figure 12. At $P_b = 10^{-5}$, we see that there is a degradation of 0.1 to 0.9 dB and no improvement in performance due to EED. The worst performance is when $\rho = 0.2$, where the degradation is 0.9 dB. When $\rho = 1$, the degradation is 0.1 dB.

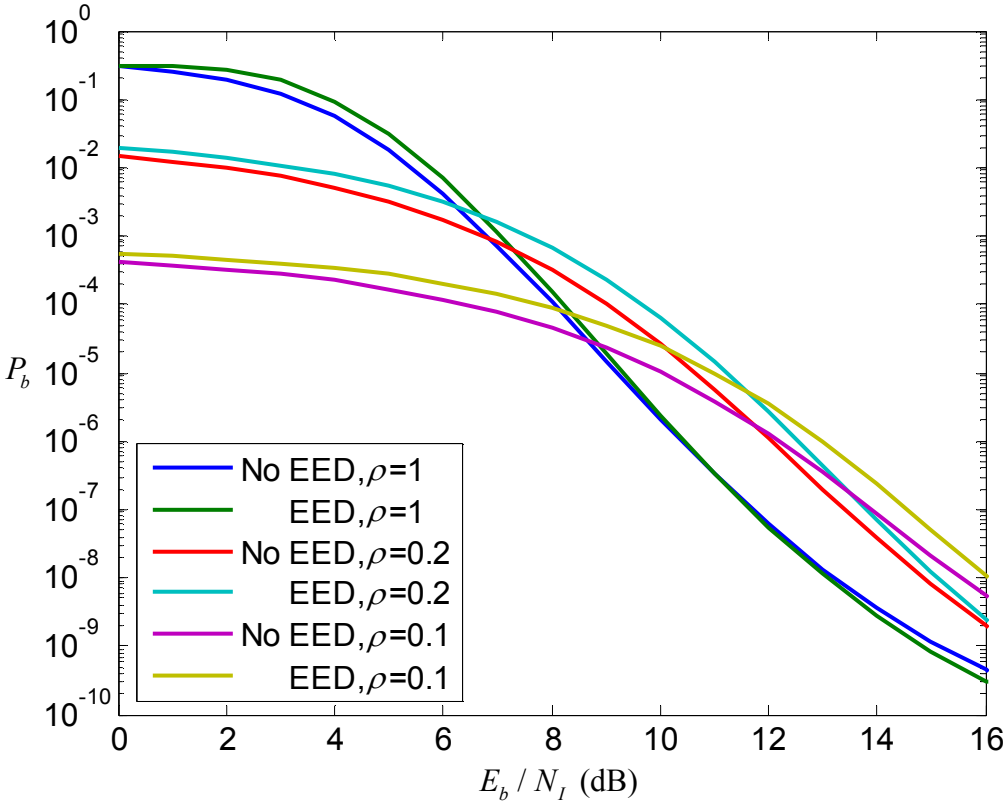

Figure 12. Performance of 64-BOK with (31,15) RS coding with and without EED for $E_b / N_0 = 6$ dB with different ρ for $a = 0.6$ in PNI.

In Figure 13, when $a = 0.4$, the results are similar to those shown in Figure 12, where there is no improvement in performance for different values of ρ due to EED.

From the results shown in Figure 12 and Figure 13, we conclude that EED used with 64-BOK and (31,15) RS coding does not improve performance but instead degrades it .

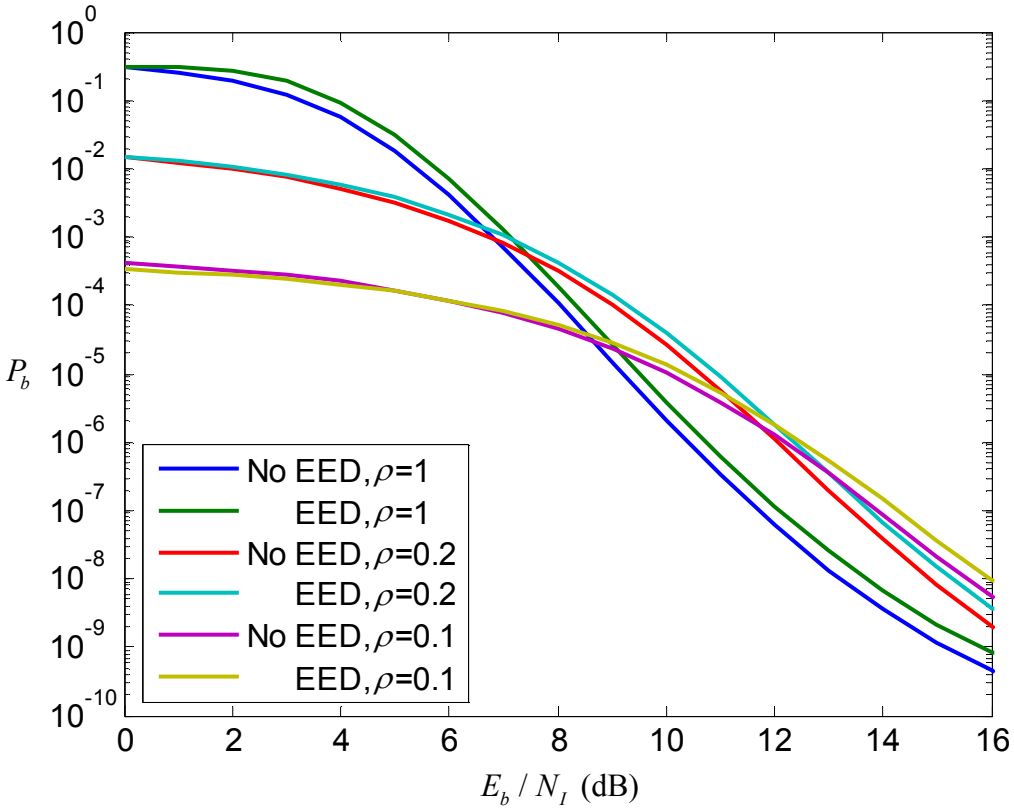

Figure 13. Performance of 64-BOK with (31,15) RS coding with and without EED for $E_b / N_0 = 6$ dB with different ρ for $a = 0.4$ in PNI.

6. Section Summary

The performance of the first alternative JTIDS/Link-16 waveform with the single-pulse structure (no diversity), both with and without EED and in an environment with both AWGN only as well as AWGN plus PNI, was evaluated in this section. We found that the waveform in a barrage noise interference environment performs better than with PNI. We also concluded that EED decoding does not improve the performance at the receiver when both AWGN and PNI are present. In the next section of the chapter, we investigate the performance of the first alternative JTIDS/Link-16 waveform with the double-pulse structure (with diversity of two).

C. PERFORMANCE OF 64-BOK WITH (31,15) RS CODING AND A DIVERSITY OF TWO (DOUBLE-PULSE STRUCTURE)

In this section, the performance of the first alternative JTIDS/Link-16 waveform with the double-pulse structure (with diversity of two) is investigated. Diversity is a widely used method for minimizing the effect of PNI and/or fading. It increases the redundancy of the system by transmitting the same symbol twice at different carrier frequencies.

1. Performance in AWGN with Diversity of Two

In Chapter II, we mentioned that JTIDS/Link-16 employs diversity in its pulse structure to improve its resistance to interference. The double-pulse structure improves the performance of the system, while the single-pulse structure allows for higher throughput. In this section, the performance of the first alternative waveform with the double-pulse structure is investigated.

With diversity, the received energy per bit is L times the average received energy per chip, $E_b = LE_c$, where we define E_c as the average energy per bit per pulse. For the double-pulse structure, diversity is two ($L = 2$), and the received energy per bit is the combination of two chip's energy to double the energy per bit received. Hence, the probability of correct six-bit channel symbol detection with a diversity of L for 64-BOK in AWGN can be obtained from (3.5) as

$$p_{c6} = \frac{1}{\sqrt{2\pi}} \int_{-\sqrt{2Lrm_1E_c/N_0}}^{\infty} e^{-\frac{u^2}{2}} \left[1 - 2Q\left(u + \sqrt{\frac{2Lrm_1E_c}{N_0}} \right) \right]^{\frac{M}{2}-1} du, \tag{3.52}$$

where E_c is the average energy per bit per pulse, $L = 2$ and $m_1 = 6$ bits per symbol. Since $L = 2$, (3.52) can be simplified to

$$p_{c6} = \frac{1}{\sqrt{2\pi}} \int_{-\sqrt{4rm_1E_c/N_0}}^{\infty} e^{-\frac{u^2}{2}} \left[1 - 2Q\left(u + \sqrt{\frac{4rm_1E_c}{N_0}} \right) \right]^{\frac{M}{2}-1} du. \tag{3.53}$$

The demodulated six-bit symbols are converted to five-bit symbols before being decoded by the (31,15) RS decoder. Substituting (3.53) into (3.2), we obtain the probability of correct five-bit symbol detection before RS decoding as

$$p_{c5} = \left\{ \frac{1}{\sqrt{2\pi}} \int_{-\sqrt{4rm_1E_c/N_0}}^{\infty} e^{-\frac{u^2}{2}} \left[1 - 2Q\left(u + \sqrt{\frac{4rm_1E_c}{N_0}} \right) \right]^{\frac{M}{2}-1} du \right\}^{\frac{5}{6}} . \quad (3.54)$$

Using (3.3) and (3.54), we obtain the probability of five-bit channel symbol error as

$$p_{s5} = 1 - \left\{ \frac{1}{\sqrt{2\pi}} \int_{-\sqrt{4rm_1E_c/N_0}}^{\infty} e^{-\frac{u^2}{2}} \left[1 - 2Q\left(u + \sqrt{\frac{4rm_1E_c}{N_0}} \right) \right]^{\frac{M}{2}-1} du \right\}^{\frac{5}{6}} . \quad (3.55)$$

Subsequently, the probability of information symbol error and information bit error can be obtained by substituting (3.55) into (3.9) and into (3.10).

The performance of 64-BOK with (31,15) RS coding for both the single-pulse and the double-pulse structure in AWGN is shown in Figure 14. At $P_b = 10^{-5}$, the difference in the required E_c / N_0 between the double-pulse and the single-pulse structure is 3 dB. From Figure 14, we see that a diversity of two gives a 3 dB improvement in the performance when compared to no diversity in terms of E_c.

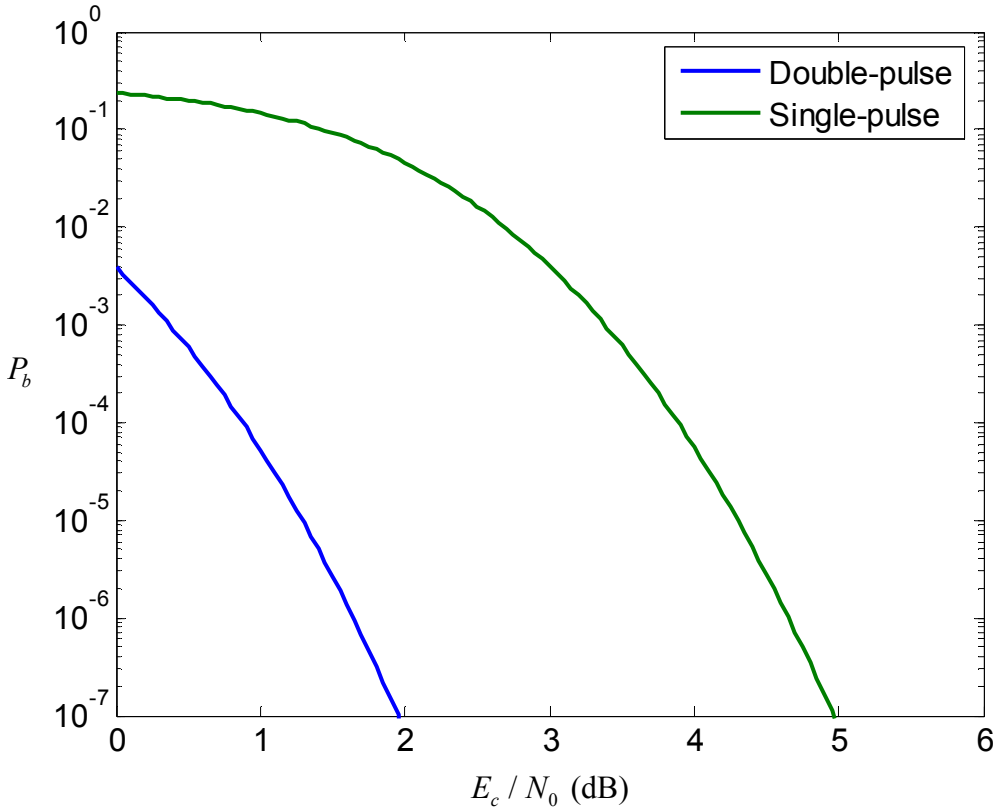

Figure 14. Performance of 64-BOK modulation with (31, 15) RS encoding for both the single-pulse and the double-pulse structure in AWGN.

2. Performance in Both AWGN and PNI with a Diversity of Two

The probability of channel symbol error for *M*BOK with (n,k) RS coding and a diversity of two in both AWGN and PNI is given by

$$p_s = \sum_{i=0}^{2} \binom{2}{i} \rho^i (1-\rho)^{2-i} \, p_s(i), \tag{3.56}$$

where $p_s(i)$ is the conditional probability of channel symbol error given that i symbols experience PNI.

The conditional probability density functions for the random variables X_m, where $m = 1, 2, ..., M/2$, that represent the decision variables are obtained assuming soft combination of the integrator outputs and are given by

$$f_{X_m}(x_m \mid m,i) = \frac{1}{\sqrt{2\pi}\sigma_m(i)} e^{-\frac{\left(x_m - 2\sqrt{2}A_c\right)^2}{2\sigma_m{}^2(i)}} \quad \text{for } m \le M/2, \tag{3.57}$$

$$f_{X_m}(x_m \mid m,i) = \frac{1}{\sqrt{2\pi}\sigma_m(i)} e^{-\frac{\left(x_m + 2\sqrt{2}A_c\right)^2}{2\sigma_m{}^2(i)}} \quad \text{for } (M/2)+1 \le m \le M, \tag{3.58}$$

and

$$f_{X_n}(x_n \mid n, n \ne m,i) = \frac{1}{\sqrt{2\pi}\sigma_m(i)} e^{-\frac{x_n{}^2}{2\sigma_m{}^2(i)}}, \tag{3.59}$$

where

$$\sigma_m{}^2(i) = i\sigma_T{}^2 + (2-i)\sigma_0{}^2, \tag{3.60}$$

and

$$\sigma_T{}^2 = \sigma_I{}^2 + \sigma_0{}^2. \tag{3.61}$$

Substituting (3.61) into (3.60) and defining $\sigma_0{}^2 = N_0 / rT_s$ and $\sigma_I{}^2 = N_I / \rho rT_s$, we obtain

$$\sigma_m{}^2(i) = i\frac{N_I}{\rho rT_s} + 2\frac{N_0}{rT_s}. \tag{3.62}$$

The conditional probability of channel symbol error is obtained by comparing (3.57) through (3.62) to (2.2) through (2.4). Adapting into (2.5), we get

$$p_s(i) = 1 - \int_0^\infty \frac{1}{\sqrt{2\pi}\sigma_m(i)} e^{-\frac{\left(x_1 - 2\sqrt{2}A_c\right)^2}{2\sigma_m{}^2(i)}} \left[1 - 2Q\left(\frac{x_1}{\sigma_m(i)}\right)\right]^{\frac{M}{2}-1} dx_1, \tag{3.63}$$

which can also be expressed as

$$p_s(i) = 1 - \frac{1}{\sqrt{2\pi}} \int_{-2\sqrt{\frac{2E_s}{\frac{iN_I}{\rho}+2N_0}}}^{\infty} e^{-\frac{u^2}{2}} \left[1 - 2Q\left(u + 2\sqrt{\frac{2E_s}{i\frac{N_I}{\rho}+2N_0}}\right)\right]^{\frac{M}{2}-1} du. \tag{3.64}$$

Expressed in terms of E_c, (3.64) is given by

$$p_s(i) = 1 - \frac{1}{\sqrt{2\pi}} \int_{-2\sqrt{\frac{2rmE_c}{\frac{iN_I}{\rho}+2N_0}}}^{\infty} e^{-\frac{u^2}{2}} \left[1 - 2Q\left(u + 2\sqrt{\frac{2rmE_c}{i\frac{N_I}{\rho}+2N_0}} \right) \right]^{\frac{M}{2}-1} du \,, \qquad (3.65)$$

which can also be represented as

$$p_s(i) = 1 - \frac{1}{\sqrt{2\pi}} \int_{-2\sqrt{\frac{2rm}{\frac{i}{\rho}\gamma_I^{-1}+2\gamma_c^{-1}}}}^{\infty} e^{-\frac{u^2}{2}} \left[1 - 2Q\left(u + 2\sqrt{\frac{2rm}{\frac{i}{\rho}\gamma_I^{-1}+2\gamma_c^{-1}}} \right) \right]^{\frac{M}{2}-1} du \,, \qquad (3.66)$$

where $\gamma_I = E_c / N_I$ and $\gamma_c = E_c / N_0$. Substituting (3.66) into (3.56), we obtain the probability of channel symbol error. The probability of information symbol error and information bit error for *M*BOK with (n,k) RS coding in both AWGN and PNI with a diversity of two is obtained by substituting (3.56) into (2.14) and (2.14) into (2.16), respectively.

For 64-BOK with (31,15) RS coding, we apply the concept of mapping from six-bit symbols into five-bit symbols at the receiver. Comparing (3.3) to (3.66), we get the probability of five-bit channel symbol error based as

$$p_{chip5}(i) = 1 - \left\{ \frac{1}{\sqrt{2\pi}} \int_{-2\sqrt{\frac{2rm_1}{\frac{i}{\rho}\gamma_I^{-1}+2\gamma_c^{-1}}}}^{\infty} e^{-\frac{u^2}{2}} \left[1 - 2Q\left(u + 2\sqrt{\frac{2rm_1}{\frac{i}{\rho}\gamma_I^{-1}+2\gamma_c^{-1}}} \right) \right]^{\frac{M}{2}-1} du \right\}^{\frac{5}{6}} \qquad (3.67)$$

where $m_1 = 6$ is the number of bits per symbol received by the 64-BOK demodulator.

Substituting (3.67) into (3.56), we obtain the probability of five-bit channel symbol error as

$$p_{s5} = \sum_{i=0}^{2} \binom{2}{i} \rho^i (1-\rho)^{2-i} \, p_{s5}(i) \,. \qquad (3.68)$$

The probability of information symbol error and information bit error for 64-BOK with (31,15) RS coding with a diversity of two in AWGN and PNI is obtained by substituting (3.68) into (3.9) and (3.9) into (3.10), respectively.

The performance for different values of ρ with $E_c / N_0 = 2$ dB is shown in Figure 15. The E_c / N_0 is chosen to be 2 dB since this gives $P_b = 10^{-7}$ at $E_c / N_I = 25$ dB. From Figure 15, we see that varying the ρ does not degrade performance significantly as compared to barrage noise interference ($\rho = 1$). At $P_b = 10^{-5}$, $\rho = 0.02$ gives the best performance as compared to larger ρ, and the degradation due to PNI is only about 1 dB.

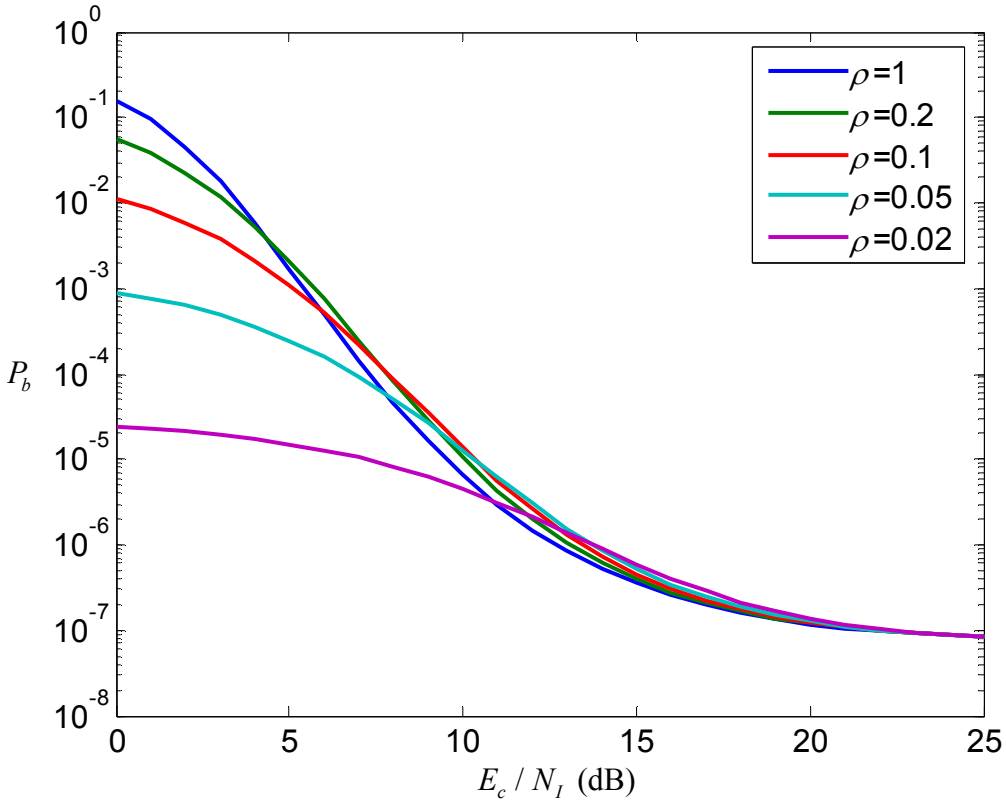

Figure 15. Performance of 64-BOK with (31,15) RS coding and the double-pulse structure for different ρ with $E_c / N_0 = 2$ dB and PNI.

In Figure 16, $E_c / N_0 = 2.5$ dB is chosen to yield $P_b = 10^{-9}$ at $E_c / N_I = 25$ dB. From Figure 16, we see that the degradation due to PNI increases to about 2 dB, but the absolute performance improves by about 2 dB.

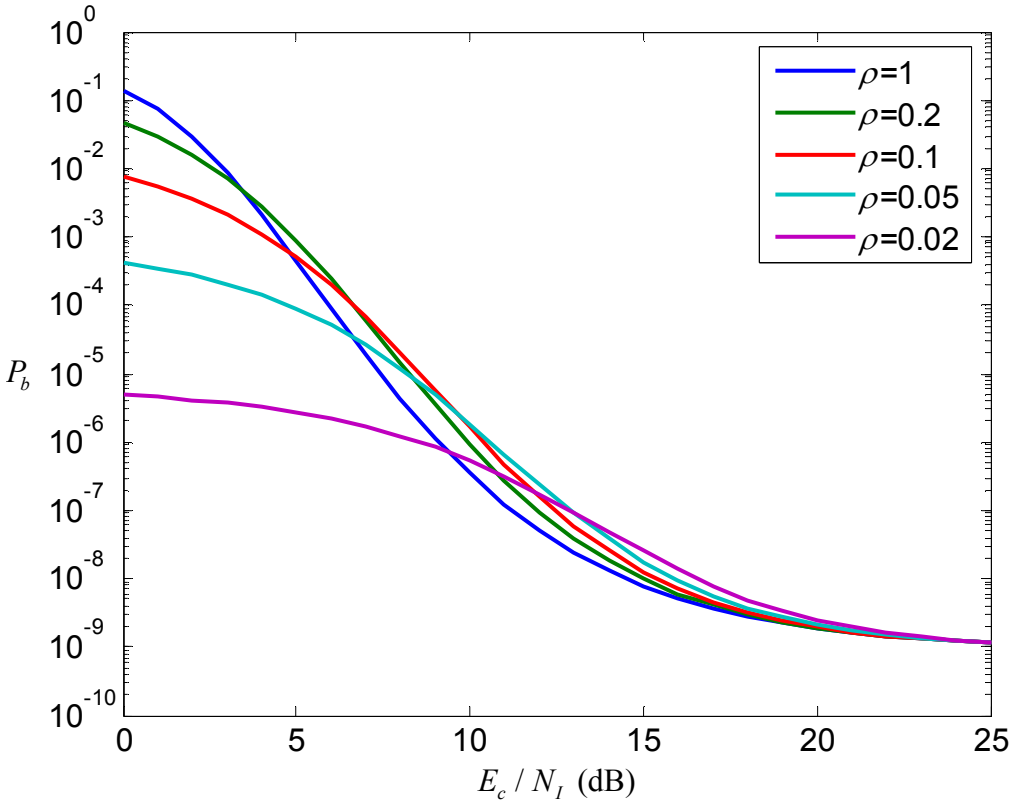

Figure 16. Performance of 64-BOK with (31,15) RS coding and the double-pulse structure for different ρ with $E_c / N_0 = 2.5$ dB and PNI.

In Figure 17, we compare the performance for receivers both with and without diversity where the probability of bit error approaches 10^{-7} at $E_c / N_I = 25$ dB. For the receiver without diversity, $E_c / N_0 = 5$ dB is required, while with diversity, the required E_c / N_0 is 3 dB less. The difference in performance between the waveforms with and without diversity is about 3 dB for both $\rho = 1$ and 0.1 at $P_b = 10^{-5}$.

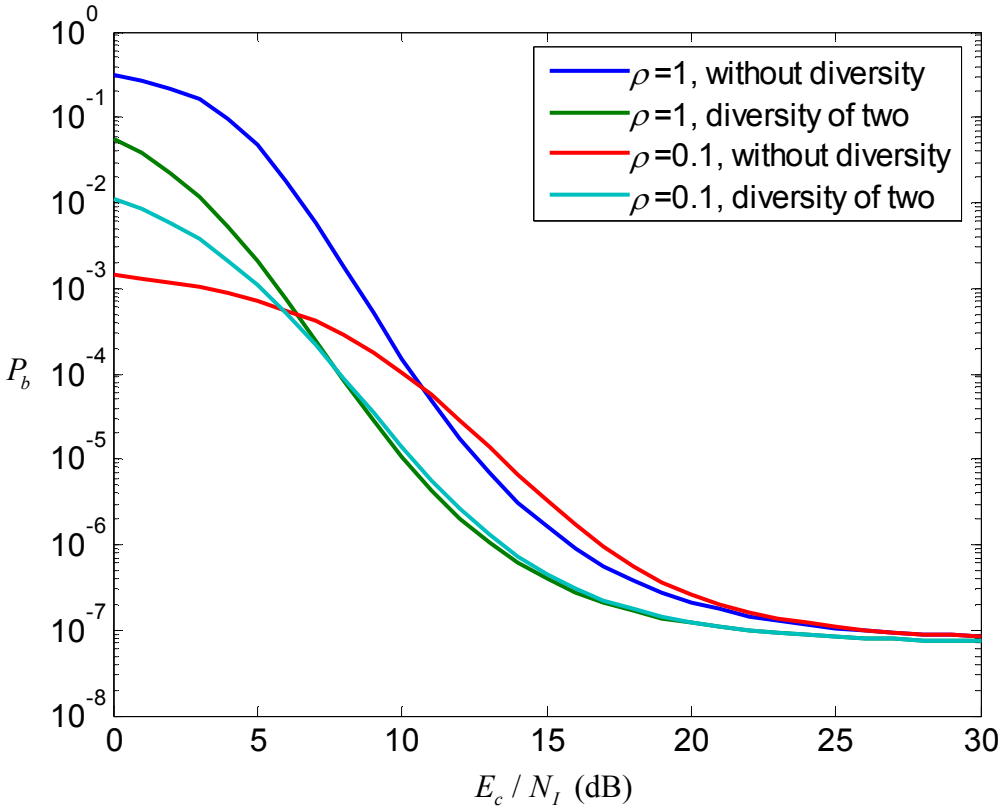

Figure 17. Performance of 64-BOK with (31,15) RS coding for both the double-pulse $(E_c / N_0 = 2 \text{ dB})$ and the single-pulse structure $(E_b / N_0 = 5 \text{ dB})$ in PNI.

3. Performance in Both AWGN and PNI with a Diversity of Two and EED

The probability of bit error for *M*BOK with (n,k) RS coding and EED with a diversity of two in AWGN and PNI is obtained by using a similar approach to that without diversity. We first obtain the probability of correct channel detection, the probability of channel erasure, and the probability of channel symbol error.

Recalling from (3.24), we have the probability of channel erasure as

$$p_e = \left[\int_{-V_T}^{V_T} f_{X_1}(x_1 \mid 1)dx_1\right]\left[\int_{-V_T}^{V_T} f_{X_2}(x_2 \mid 1)dx_2\right]^{\frac{M}{2}-1}. \qquad (3.69)$$

From (3.57), (3.58), (3.59) and (3.69), the conditional probability of channel erasure given that i diversity receptions experience PNI is obtained as

$$p_e(i)=\left[\int_{-V_T}^{V_T}\frac{1}{\sqrt{2\pi}\sigma_m(i)}e^{-\frac{(x_1-2\sqrt{2}A_c)^2}{2\sigma_m^2(i)}}dx_1\right]\times\left[2\int_0^{V_T}\frac{1}{\sqrt{2\pi}\sigma_m(i)}e^{-\frac{x_2^2}{2\sigma_m^2(i)}}dx_2\right]^{\frac{M}{2}-1}, \tag{3.70}$$

which can be evaluated to get

$$p_e(i)=\left[Q\left(\frac{2\sqrt{2}A_c-V_T}{\sigma_m(i)}\right)-Q\left(\frac{2\sqrt{2}A_c+V_T}{\sigma_m(i)}\right)\right]\left[1-Q\left(\frac{V_T}{\sigma_m(i)}\right)\right]^{\frac{M}{2}-1}. \tag{3.71}$$

Using (3.62) and defining $V_T=a\left(2\sqrt{2}A_c\right)$, where $0<a<1,$ we obtain

$$p_e(i)=\left[Q\left((1-a)2\sqrt{\frac{2E_s}{iN_I+2N_0}}\right)-Q\left((1+a)2\sqrt{\frac{2E_s}{iN_I+2N_0}}\right)\right]\times\left[1-2Q\left(2a\sqrt{\frac{2E_s}{iN_I+2N_0}}\right)\right]^{\frac{M}{2}-1}. \tag{3.72}$$

With RS coding, (3.72) can be expressed as

$$p_e(i)=\left[Q\left((1-a)2\sqrt{\frac{2rmE_c}{\frac{i}{\rho}N_I+2N_0}}\right)-Q\left((1+a)2\sqrt{\frac{2rmE_c}{\frac{i}{\rho}N_I+2N_0}}\right)\right]\times\left[1-2Q\left(2a\sqrt{\frac{2rmE_c}{\frac{i}{\rho}N_I+2N_0}}\right)\right]^{\frac{M}{2}-1}. \tag{3.73}$$

The probability of channel erasure for the double-pulse structure with EED is obtained by substituting (3.73) into an equation analogous to (3.56) and is

$$p_e = \sum_{i=0}^{2} \binom{2}{i} \rho^i (1-\rho)^{2-i} \times \left[Q\left((1-a) 2 \sqrt{\frac{2rmE_c}{\frac{i}{\rho} N_I + 2N_0}} \right) - Q\left((1-a) 2 \sqrt{\frac{2rmE_c}{\frac{i}{\rho} N_I + 2N_0}} \right) \right] \times \left[1 - 2Q\left(2a \sqrt{\frac{2rmE_c}{\frac{i}{\rho} N_I + 2N_0}} \right) \right]^{\frac{M}{2}-1} . \quad (3.74)$$

Similarly, the conditional probability of channel detection given that i diversity receptions experience PNI is obtained from (3.57), (3.58), (3.59) and (3.34) as

$$p_c(i) = \int_{-V_T}^{\infty} \frac{1}{\sqrt{2\pi}\sigma_m(i)} e^{-\frac{(x_1 - 2\sqrt{2}A_c)^2}{2\sigma_m^2(i)}} \times \left[\int_{-x_1}^{x_1} \frac{1}{\sqrt{2\pi}\sigma_m(i)} e^{-\frac{x_2^2}{2\sigma_m^2(i)}} dx_2 \right]^{\frac{M}{2}-1} dx_1 , \quad (3.75)$$

which can be partially evaluated to get

$$p_c(i) = \int_{V_T}^{\infty} \frac{1}{\sqrt{2\pi}\sigma_m(i)} e^{-\frac{\left(x_1 - 2\sqrt{2}A_c\right)^2}{2\sigma_m^2(i)}} \left[1 - 2Q\left(\frac{x_1}{\sigma_m(i)} \right) \right]^{\frac{M}{2}-1} dx_1 . \quad (3.76)$$

Letting $u = \left(x_1 - 2\sqrt{2}A_c \right) / \sigma_m(i)$ in (3.76), we obtain

$$p_c(i) = \int_{\frac{V_T - 2\sqrt{2}A_c}{\sigma_m(i)}}^{\infty} \frac{1}{\sqrt{2\pi}} e^{-\frac{u^2}{2}} \left[1 - 2Q\left(\frac{2\sqrt{2}A_c}{\sigma_m(i)} \right) \right]^{\frac{M}{2}-1} du . \quad (3.77)$$

Using (3.62) and $V_T = a\left(2\sqrt{2}A_c\right)$, we obtain the conditional probability of correct channel detection for *M*BOK with FEC coding expressed in terms of E_c / N_0 given that i diversity receptions experience PNI as

$$p_c(i)=\frac{1}{\sqrt{2\pi}}\int_{-(1-a)2\sqrt{\frac{2rmE_c}{\frac{iN_I}{\rho}+2N_0}}}^{\infty}\frac{1}{\sqrt{2\pi}}\,e^{-\frac{u^2}{2}}\left[1-2Q\left(\frac{2rmE_c}{\frac{iN_I}{\rho}+2N_0}\right)\right]^{\frac{M}{2}-1}du\,. \quad (3.78)$$

Substituting (3.78) into an equation analogous to (3.56), we obtain the probability of correct channel detection for the double-pulse structure with EED as

$$p_c=\sum_{i=0}^{2}\binom{2}{i}\rho^i(1-\rho)^{2-i}$$
$$\times\frac{1}{\sqrt{2\pi}}\int_{-(1-a)2\sqrt{\frac{2rmE_c}{\frac{iN_I}{\rho}+2N_0}}}^{\infty}e^{-\frac{u^2}{2}}\left[1-2Q\left(u+2\sqrt{\frac{2rmE_c}{\frac{iN_I}{\rho}+2N_0}}\right)\right]^{\frac{M}{2}-1}du\,. \quad (3.79)$$

From the results of (3.74) and (3.79), we can obtain the probability of channel symbol error with EED as

$$p_s=1-p_e-p_c\,. \quad (3.80)$$

Using the results of p_e, p_c and p_s, we obtain the probability of block error as

$$P_E=1-\left[\sum_{i=0}^{t}\binom{n}{i}{p_s}^i\sum_{j=0}^{d_{\min}-1-2i}\binom{n-i}{j}{p_e}^j{p_c}^{n-i-j}\right], \quad (3.81)$$

and the probability of information symbol error and information bit error are obtained from (2.25) and (2.16), respectively.

For 64-BOK with (31,15) RS coding, we apply the concept of mapping from six-bit symbols into five-bit symbols at the receiver. Hence, using (3.79), we get the probability of correct six-bit channel symbol detection as

$$p_{c6}=\sum_{i=0}^{2}\binom{2}{i}\rho^i(1-\rho)^{2-i}$$
$$\times\frac{1}{\sqrt{2\pi}}\int_{-(1-a)2\sqrt{\frac{2rm_1E_c}{\frac{iN_I}{\rho}+2N_0}}}^{\infty}e^{-\frac{u^2}{2}}\left[1-2Q\left(u+2\sqrt{\frac{2rm_1E_c}{\frac{iN_I}{\rho}+2N_0}}\right)\right]^{\frac{M}{2}-1}du\,, \quad (3.82)$$

where $m_1 = 6$ is the number of bits per symbol received by the 64-BOK demodulator.

Substituting (3.82) into (3.2), we obtain the probability of five-bit correct channel symbol detection as

$$p_{c5} = \left\{ \begin{array}{l} \sum_{i=0}^{2} \binom{2}{i} \rho^i (1-\rho)^{2-i} \\ \times \frac{1}{\sqrt{2\pi}} \int_{-(1-a)2\sqrt{\frac{2rm_1E_c}{\frac{iN_I}{\rho}+2N_0}}}^{\infty} e^{-\frac{u^2}{2}} \left[1-2Q\left(u+2\sqrt{\frac{2rm_1E_c}{\frac{iN_I}{\rho}+2N_0}} \right) \right]^{\frac{M}{2}-1} du \end{array} \right\}^{\frac{5}{6}}. \quad (3.83)$$

Next, the probability of six-bit channel symbol erasure is obtained from (3.74) as

$$\begin{aligned} p_{e6} &= \sum_{i=0}^{2} \binom{2}{i} \rho^i (1-\rho)^{2-i} \\ &\times \left[Q\left((1-a)2\sqrt{\frac{2rm_1E_c}{\frac{i}{\rho}N_I+2N_0}} \right) - Q\left((1-a)2\sqrt{\frac{2rm_1E_c}{\frac{i}{\rho}N_I+2N_0}} \right) \right] \\ &\times \left[1-2Q\left(2a\sqrt{\frac{2rm_1E_c}{\frac{i}{\rho}N_I+2N_0}} \right) \right]^{\frac{M}{2}-1} \end{aligned} \quad (3.84)$$

Substituting (3.19) with results from (3.82), (3.83) and (3.84) into (3.19), we get the probability of five-bit channel symbol erasure p_{e5}. Substituting (3.83) and p_{e5} into (3.80), we obtain the probability of five-bit channel symbol error as

$$p_{s5} = 1 - p_{e5} - p_{c5}. \quad (3.85)$$

Using the results for p_{s5}, p_{c5} and p_{e5} in (3.81), we obtain the probability of block error for 64-BOK with (31,15) RS code and EED for the double-pulse structure. Finally, we obtain the probability of symbol error and the probability of bit error for 64-BOK with (31,15) RS coding and EED with a diversity of two and both AWGN and PNI using (2.25) and (3.10), respectively.

The results for 64-BOK with (31, 15) RS coding and EED and a diversity of two in AWGN and PNI for different values of a are shown in Figure 18 and Figure 19, where E_c / N_0 is 2 dB and 14 dB, respectively. From Figure 18 and Figure 19, we see that there is not much difference in performance for $0 \le a \le 0.7$. However, performance degrades for $a > 0.7$. This degradation is expected since, when a reaches a large value, more received symbols are erased and overwhelm the erasure correction capability of the RS code. The subsequent analyses use $a = 0.7$ as it provides the best performance.

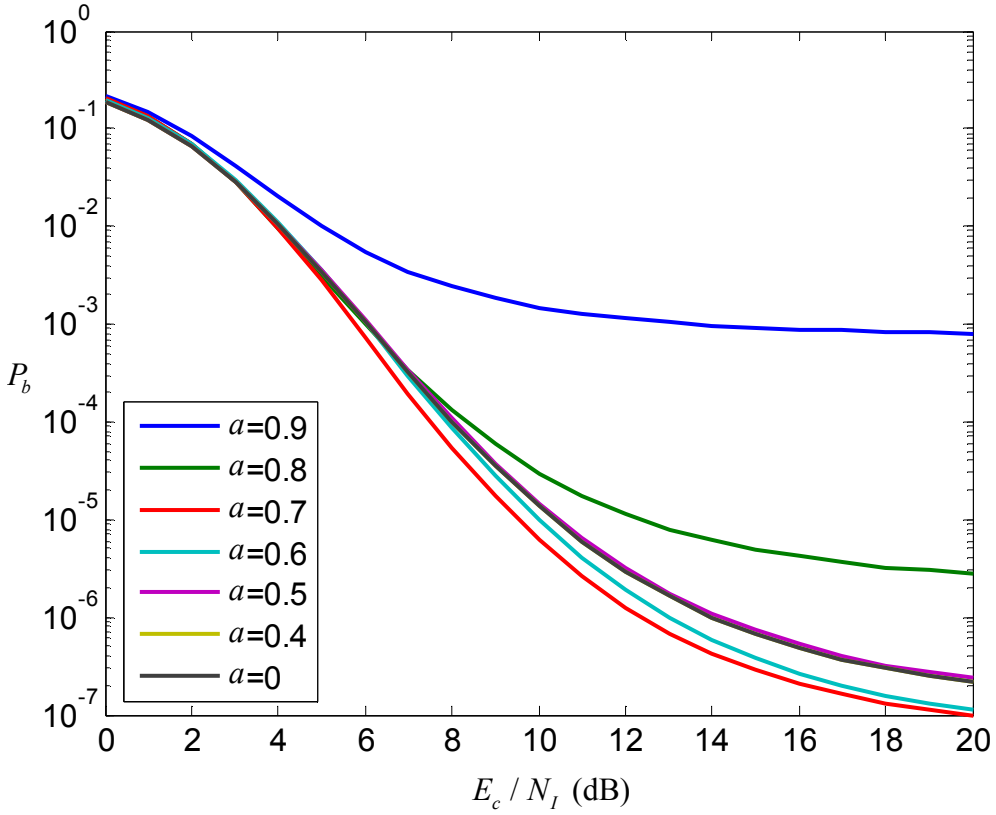

Figure 18. Performance of 64-BOK with (31,15) RS coding and EED for the double-pulse structure with $\rho = 0.5$ and $E_c / N_0 = 2$ dB for different values of a.

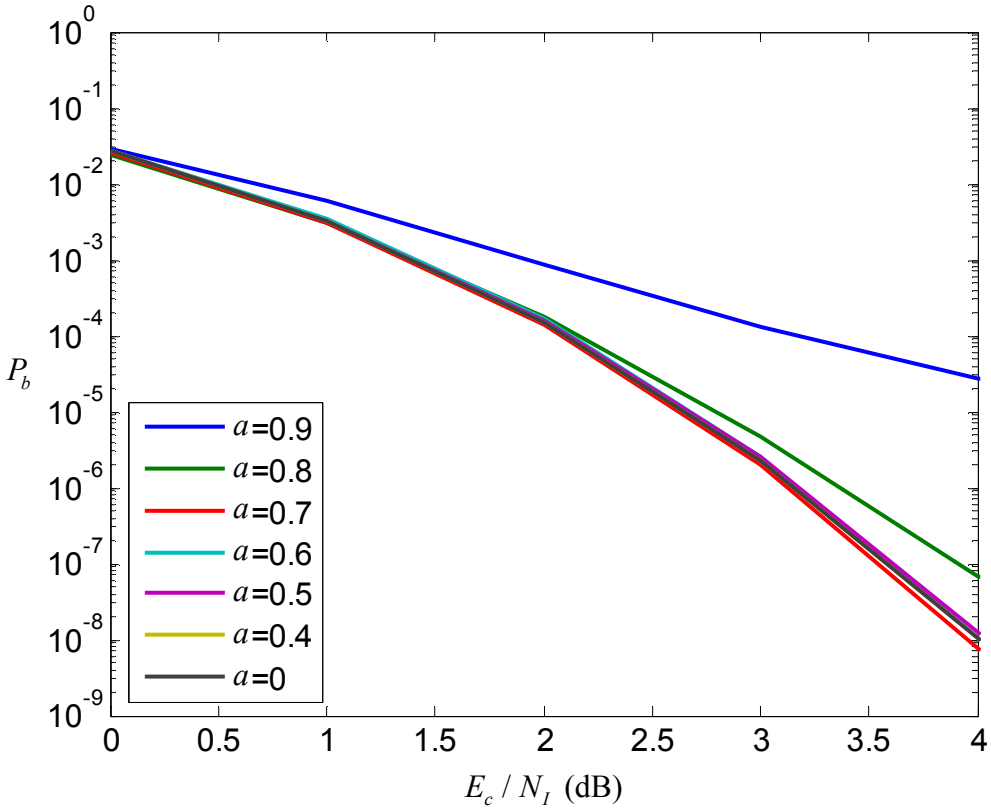

Figure 19. Performance of 64-BOK with (31,15) RS coding and EED for the double-pulse structure with $\rho = 0.5$ and $E_c / N_0 = 14$ dB for different values of a.

The performance of 64-BOK with (31,15) RS coding and EED with a diversity of two when $E_c / N_0 = 2$ dB for $a = 0.7$ and different values of ρ is shown in Figure 20. At $P_b = 10^{-5}$, there is a difference of 1.7 dB in E_c / N_I between the best and the worst performance. The best performance occurs for $\rho = 1$ at $E_c / N_I = 9.1$ dB, and the worst performance occurs for $\rho = 0.1$ at $E_c / N_I = 10.8$ dB.

In Figure 21, we can see that the difference in performance increases when E_c / N_0 increases to 14 dB. At $P_b = 10^{-5}$, the best performance occurs for $\rho = 1$ at $E_c / N_I = 1.4$ dB, and the worst performance occurs for $\rho = 0.1$ at $E_c / N_I = 5.3$ dB. This gives a difference of 3.9 dB.

From Figure 20 and Figure 21, we can see that although there is an improvement in absolute performance for larger E_b / N_0, there is also a significant increase in the relative performance gap between $\rho = 1$ and $\rho = 0.1$.

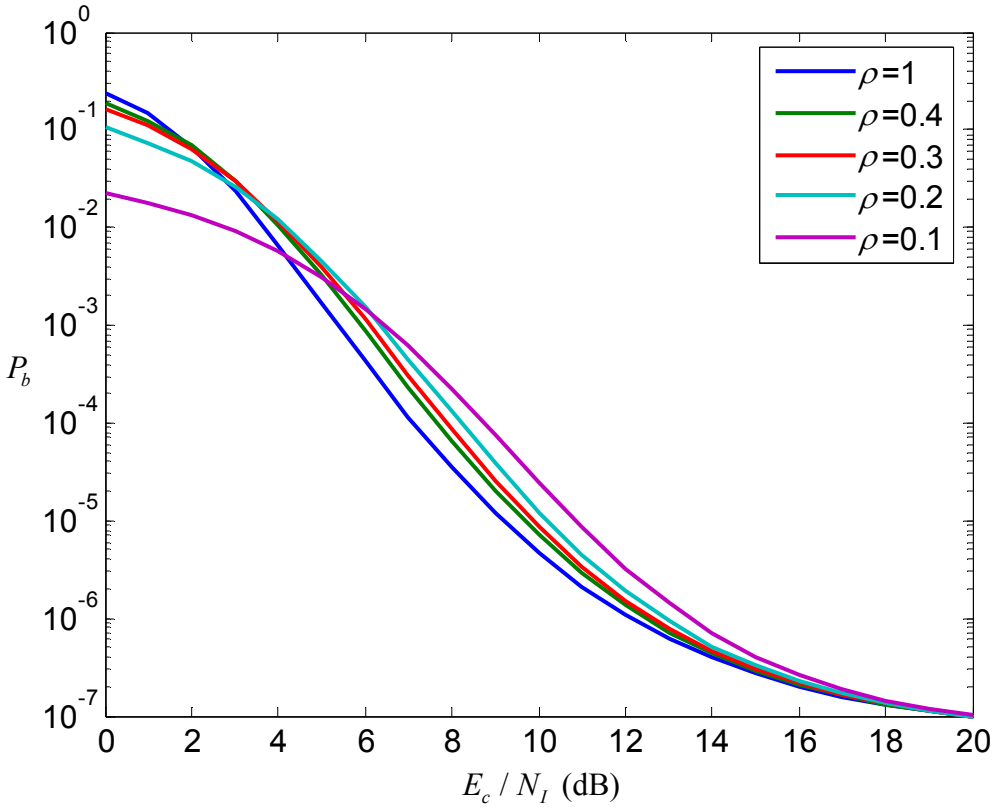

Figure 20. Performance of 64-BOK with (31,15) RS coding and EED for the double-pulse structure with $a = 0.7$ and $E_c / N_0 = 2$ dB for different values of ρ.

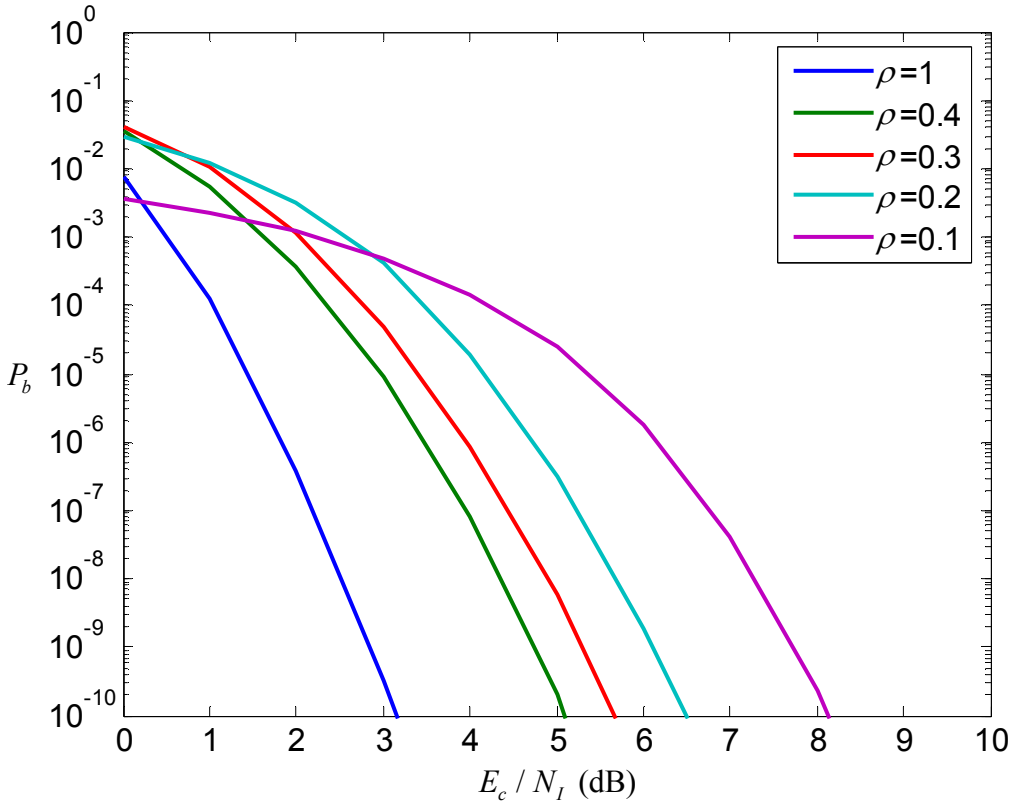

Figure 21. Performance of 64-BOK with (31,15) RS coding and EED for the double-pulse structure with $a = 0.7$ and $E_c / N_0 = 14$ dB for different values of ρ.

The performance for 64-BOK with (31,15) RS coding and EED, both with and without diversity, for the case of an asymptotic convergence to 10^{-7}, is shown in Figure 22. As expected, from the results at $P_b = 10^{-5}$, we see that there is about a 3 dB difference in performance between the single-pulse and the double-pulse structure. The 3 dB improvement is due to the power advantage of the double-pulse structure.

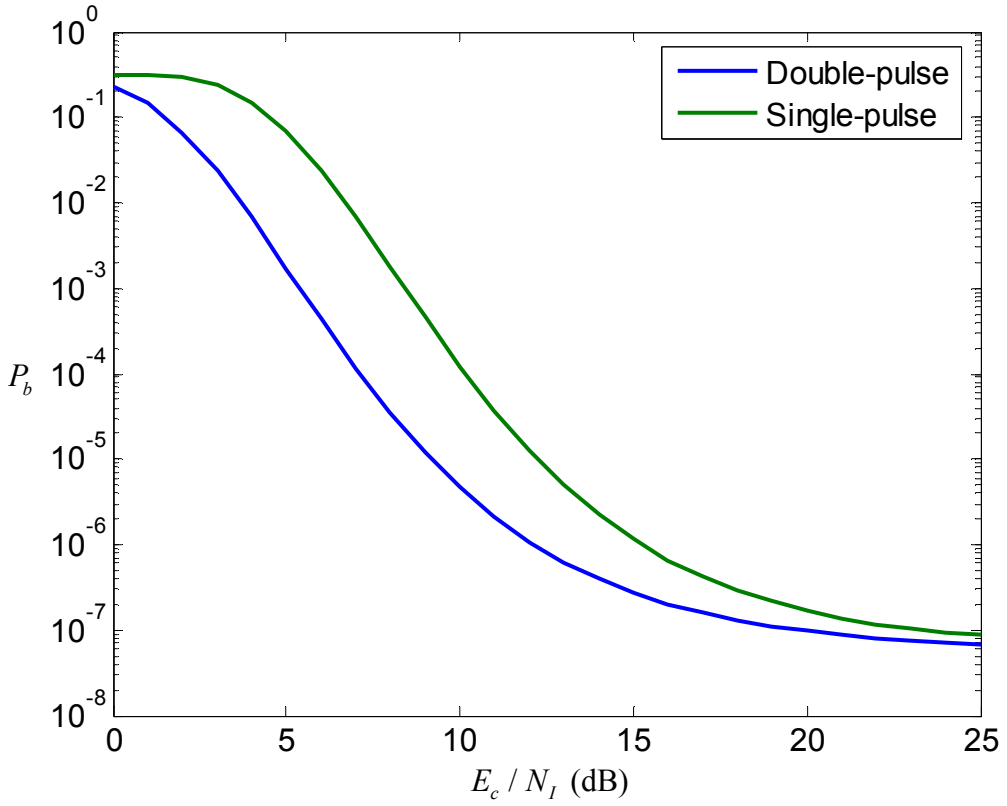

Figure 22. Performance of 64-BOK with (31,15) RS coding and EED, $a = 0.7$, ρ=1 for both the double-pulse structure $(E_c / N_0 = 2 \text{ dB})$ and single-pulse structure $(E_b / N_0 = 5 \text{ dB})$.

The performance of 64-BOK with (31,15) RS coding both with and without EED for $E_c / N_0 = 2$ dB is shown in Figure 23. From Figure 23, at $P_b = 10^{-5}$, the difference in performance when using EED is less than 0.5 dB.

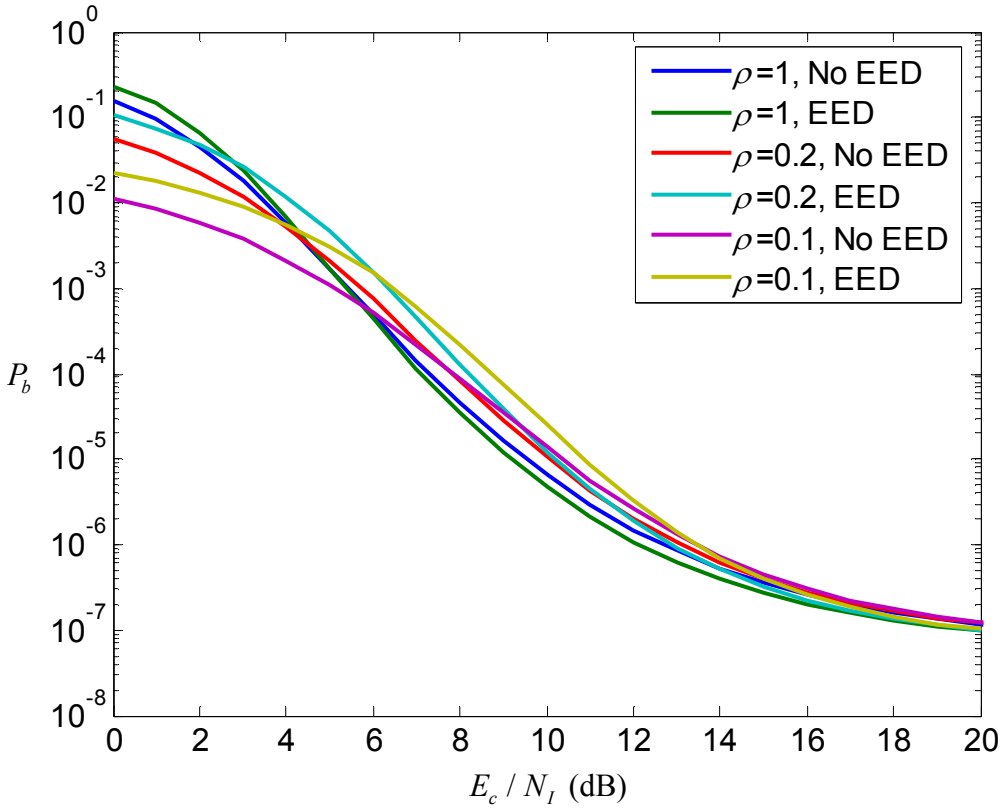

Figure 23. Performance of 64-BOK with (31,15) RS coding with and without EED with $E_c / N_0 = 2$ dB and $a = 0.7$ for different values of ρ.

Next, we increase E_c / N_0 to 14 dB, and the result is shown in Figure 24. From Figure 24, we observe that there is no difference in performance when using EED. This comparison shows that there is no benefit to EED for the double-pulse structure, which is also the case for the single-pulse structure.

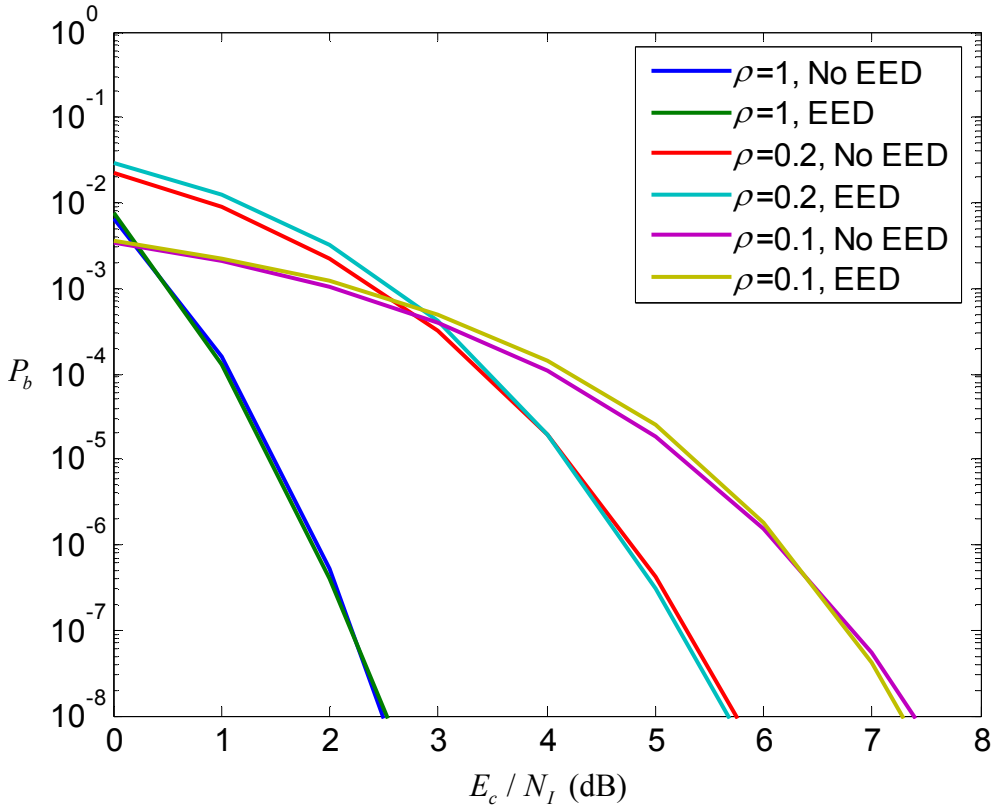

Figure 24. Performance of 64-BOK with (31,15) RS coding with and without EED with $E_c / N_0 = 14$ dB and $a = 0.7$ for different values of ρ.

4. Performance with Perfect-side Information in Both AWGN and PNI

PSI modulation can be considered for a system with a diversity of two when the diversity receptions are received independently. When only one diversity reception is affected by PNI, the decoding decision is based on the diversity reception that is free from PNI. Using (2.11), we obtain the probability of channel symbol error with a diversity of two as

$$P_s = (1-\rho)^2 p_s(0) + \rho^2 p_s(2) + \rho(1-\rho) p_s(1). \tag{3.86}$$

In (3.86), $p_s(0)$ is the conditional probability of channel symbol error when there is no PNI present in either diversity reception and is obtained from (3.53) as

$$p_s(0) = 1 - \frac{1}{\sqrt{2\pi}} \int_{-\sqrt{\frac{4rmE_c}{N_0}}}^{\infty} e^{-\frac{u^2}{2}} \left[1 - 2Q(u + \sqrt{\frac{4rmE_c}{N_0}} \right]^{\frac{M}{2}-1} du \,. \tag{3.87}$$

The conditional probability of channel symbol error when only one of the diversity receptions suffer from PNI and is discarded is obtained from (2.5) as

$$p_s(1) = 1 - \frac{1}{\sqrt{2\pi}} \int_{-\sqrt{\frac{2rmE_c}{N_0}}}^{\infty} e^{-\frac{u^2}{2}} \left[1 - 2Q(u + \sqrt{\frac{2rmE_c}{N_0}} \right]^{\frac{M}{2}-1} du \,. \tag{3.88}$$

Finally, the conditional probability of channel symbol error when both diversity receptions suffer from PNI is obtained from (3.64) as

$$p_s(2) = 1 - \frac{1}{\sqrt{2\pi}} \int_{-2\sqrt{\frac{2rm}{\frac{2}{\rho}\gamma_I^{-1} + 2\gamma_c^{-1}}}}^{\infty} e^{-\frac{u^2}{2}} \left[1 - 2Q\left(u + 2\sqrt{\frac{2rm}{\frac{2}{\rho}\gamma_I^{-1} + 2\gamma_c^{-1}}} \right) \right]^{\frac{M}{2}-1} du \,. \tag{3.89}$$

For 64-BOK with (31,15) RS coding and PSI, the concept of mapping from six-bit symbols to five-bit symbols at the receiver is applied to obtain the probability of five-bit channel symbol error (with a diversity of two) from (3.86) as

$$P_s = (1-\rho)^2 p_{s5}(0) + \rho^2 p_{s5}(2) + \rho(1-\rho) p_{s5}(1) \,. \tag{3.90}$$

The conditional probability of five-bit channel symbol error when PNI is not present in either diversity reception is obtained from (3.55) as

$$p_{s5}(0) = 1 - \left\{ \frac{1}{\sqrt{2\pi}} \int_{-\sqrt{4rm_1E_c/N_0}}^{\infty} e^{-\frac{u^2}{2}} \left[1 - 2Q\left(u + \sqrt{\frac{4rm_1E_c}{N_0}} \right) \right]^{\frac{M}{2}-1} du \right\}^{\frac{5}{6}} . \tag{3.91}$$

The conditional probability of five-bit channel symbol error when only one of the diversity receptions suffers PNI and is discarded, is obtained from (3.8) as

$$p_{s5}(1) = 1 - \left\{ \frac{1}{\sqrt{2\pi}} \int_{-\sqrt{2rm_1E_c/N_0}}^{\infty} e^{-\frac{u^2}{2}} \left[1 - 2Q\left(u + \sqrt{\frac{2rm_1E_c}{N_0}} \right) \right]^{\frac{M}{2}-1} du \right\}^{\frac{5}{6}}. \qquad (3.92)$$

Finally, the conditional probability of channel symbol error when both diversity receptions suffer from PNI, is obtained from (3.67) as

$$p_{s5}(2) = 1 - \left\{ \frac{1}{\sqrt{2\pi}} \int_{-2\sqrt{\frac{2rm_1}{\frac{2}{\rho}\gamma_I^{-1}+2\gamma_c^{-1}}}}^{\infty} e^{-\frac{u^2}{2}} \left[1 - 2Q\left(u + 2\sqrt{\frac{2rm_1}{\frac{2}{\rho}\gamma_I^{-1} + 2\gamma_c^{-1}}} \right) \right]^{\frac{M}{2}-1} du \right\}^{\frac{5}{6}} \qquad (3.93)$$

The performance of 64-BOK with (31,15) RS coding both with and without PSI is shown in Figure 25. From Figure 25, there is no difference in performance when $\rho = 1$ with PSI. This makes sense since the channel is experiencing barrage noise interference. At $P_b = 10^{-6}$, $\rho = 0.2$, the E_c / N_I required with and without PSI is 6.5 dB and 13.2 dB, respectively. Hence, there is a gain of 6.7 dB when PSI is used, and there is a significant improvement in performance.

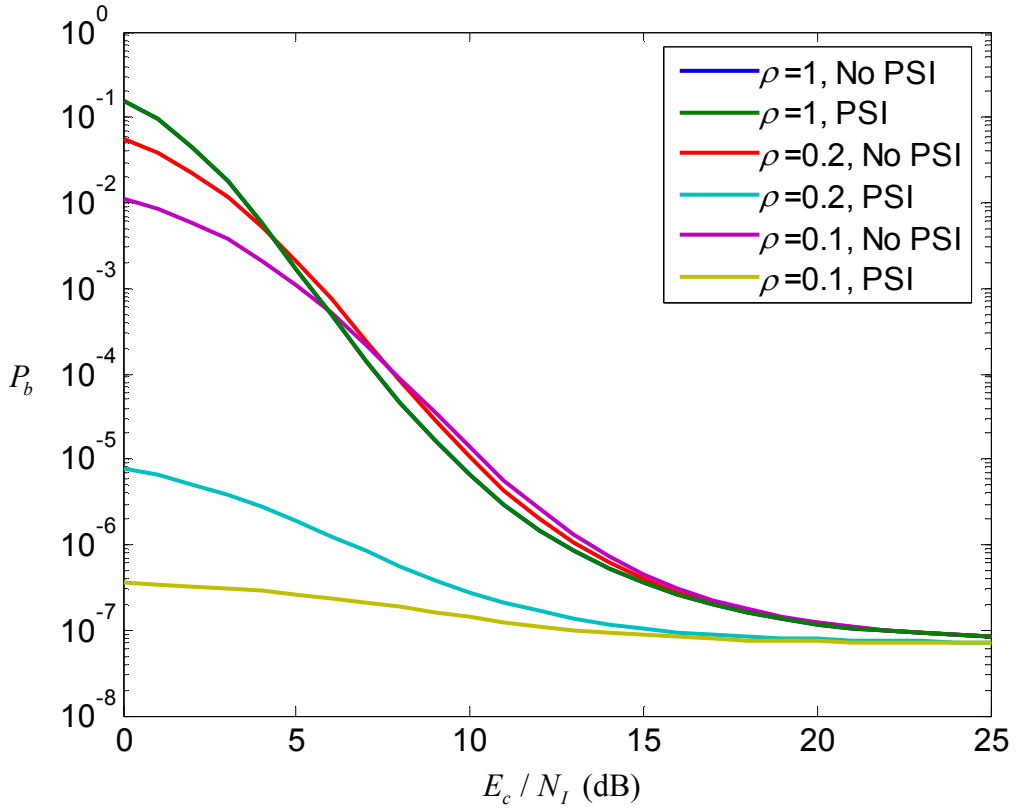

Figure 25. Performance for 64-BOK with (31,15) RS coding with and without PSI for different ρ with $E_c / N_0 = 2$ dB.

Next, we increase E_c / N_0 to 9 dB, and the result is shown in Figure 26. From Figure 26, we again see identical results for $\rho = 1$, where there is no difference in performance with PSI. At $P_b = 10^{-9}$, $\rho = 0.2$, the E_c / N_I required with and without PSI is 2.9 dB and 6.7 dB, respectively. Hence, there is a gain of 3.8 dB when PSI is used, and there is a significant improvement in performance. Thus, PSI forces a jammer to adopt a barrage noise jamming strategy, where the benefit of PSI is negated.

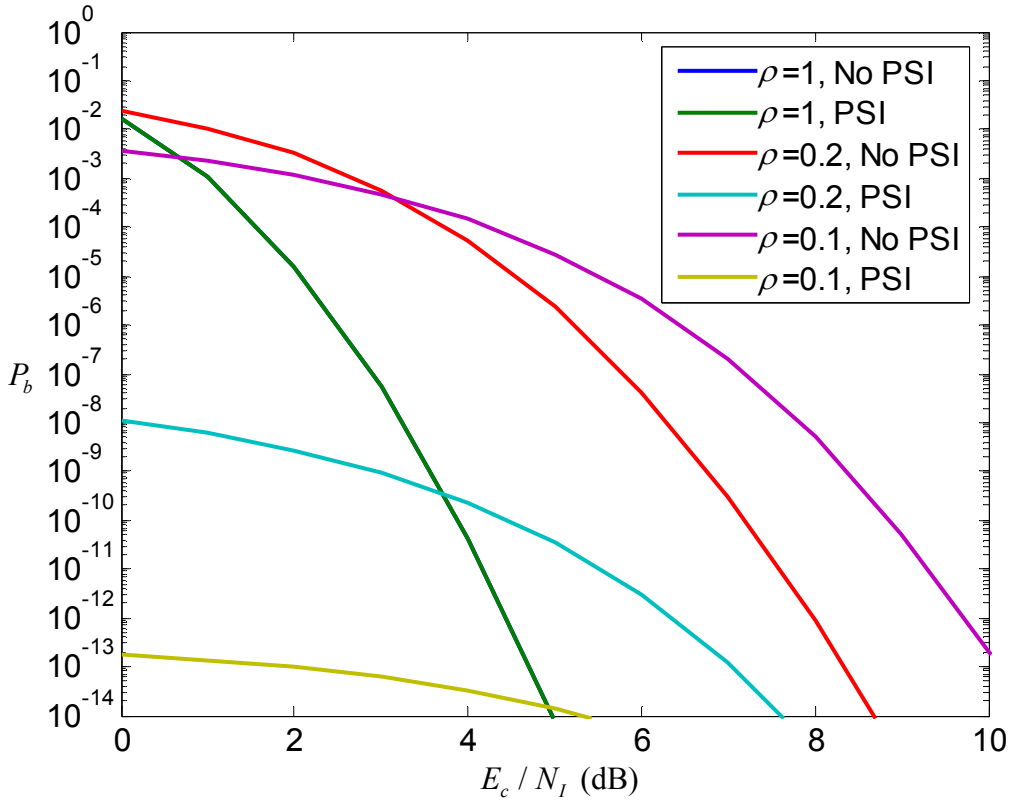

Figure 26. Performance for 64-BOK with (31,15) RS coding with and without PSI for different ρ with $E_c / N_0 = 9$ dB.

5. Section Summary

This section covered the analyses of the performance of the first alternative JTIDS/Link-16 waveform with a diversity of two (double-pulse structure), both with and without EED for both AWGN as well as AWGN plus PNI. From the analyses, the performance of the waveform is better when $\rho = 1$ (barrage noise interference) than for $\rho < 1$. We saw that EED does not substantially improve performance in the presence of both AWGN and PNI. The performance with PSI was analyzed, and the results showed a significant improvement in performance for a channel with AWGN and PNI.

D. COMPARISON OF FIRST ALTERNATIVE JTIDS/LINK-16 WAVEFORM TO JTIDS/LINK-16 WAVEFORMS IN BOTH AWGN ONLY AND AWGN PLUS PNI

In this section, we compare the performance of the first alternative JTIDS/Link-16 waveform to the original JTIDS/Link-16 waveform. The analyses are based on both single-pulse and double-pulse structures and in an environment with both AWGN only, and AWGN plus PNI. Detailed analyses of the original JTIDS/Link-16 waveform can be found in [7] respectively. Results from [7] are used to obtain the performance of the original JTIDS/Link-16 waveform for comparison with the first alternative JTIDS/Link-16 waveform.

1. Comparison of 64-BOK with (31,15) RS Coding to the JTIDS/Link-16 Waveform for AWGN, Single-pulse Structure

The performance of the alternative waveform with 64-BOK with (31,15) RS coding compared to that of the original JTIDS/LINK-16 waveform for the single-pulse structure and in AWGN is shown in Figure 27. At $P_b = 10^{-3}$, $E_b / N_0 = 6.1$ dB and $E_b / N_0 = 3.4$ dB for the JTIDS/Link-16 waveform and the first alternative JTIDS/Link-16 waveform, respectively. This is a gain of 2.7 dB for the 64-BOK waveform over the JTIDS/Link-16 waveform in AWGN. Similarly, at $P_b = 10^{-5}$, there is an identical gain of 2.7 dB for the first alternative JTIDS/Link-16 waveform over the JTIDS/Link-16 waveform, with $E_b / N_0 = 4.3$ dB and $E_b / N_0 = 7.0$ dB for the first alternative JTIDS/Link-16 waveform and the JTIDS/Link-16 waveform, respectively.

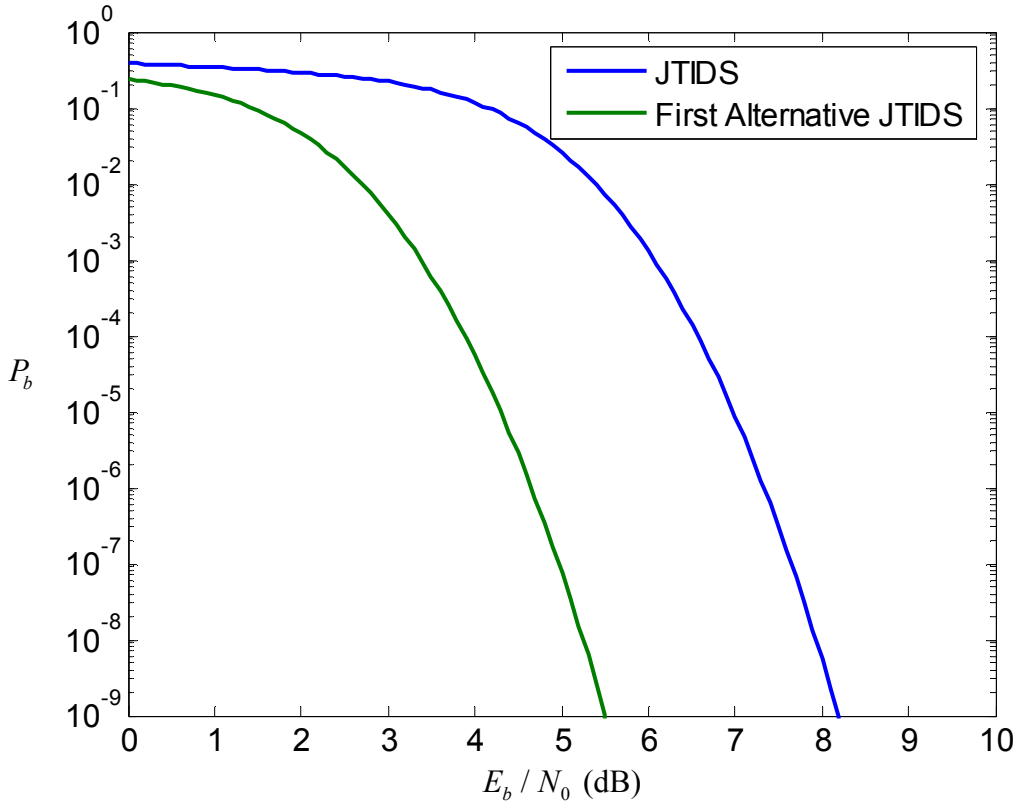

Figure 27. Performance of the first alternative JTIDS/Link-16 waveform and the JTIDS waveform for the single-pulse structure.

2. Comparison of 64-BOK with (31,15) RS Coding to the JTIDS/Link-16 Waveform for AWGN and PNI, Single-pulse Structure

The performance for both the first alternative JTIDS/Link-16 waveform and the JTIDS/Link-16 waveform in both AWGN and PNI for different values of ρ is shown in Figure 28. We consider the case where the performance of the two waveforms both converge to $P_b = 10^{-7}$; the required E_b / N_0 for the first alternative waveform and the JTIDS/Link-16 waveform is 5 dB and 7.7 dB, respectively. At $P_b = 10^{-5}$ and $\rho = 1$, the E_b / N_I required when for the alternative waveform and the JTIDS/Link-16 waveform is 12.4 dB and 15 dB, respectively. For $\rho = 0.2$ and $\rho = 0.1$, the difference in E_b / N_I between the alternative JTIDS/Link-16 waveform ($E_b / N_I = 13.3$ dB) and the JTIDS/Link-16 waveform ($E_b / N_I = 16$ dB) is 2.7 dB. Comparing the performance of the

two waveforms, we see that the first alternative JTIDS/Link-16 waveform performs better than the JTIDS/Link-16 waveform by about 2.6 to 2.7 dB at $P_b = 10^{-5}$. Clearly, the JTIDS/Link-16 waveform will have substantially inferior performance as compared to the first alternative waveform based on equal E_b / N_0. This is shown in Figure 29 for $E_b / N_0 = 7.7$ dB.

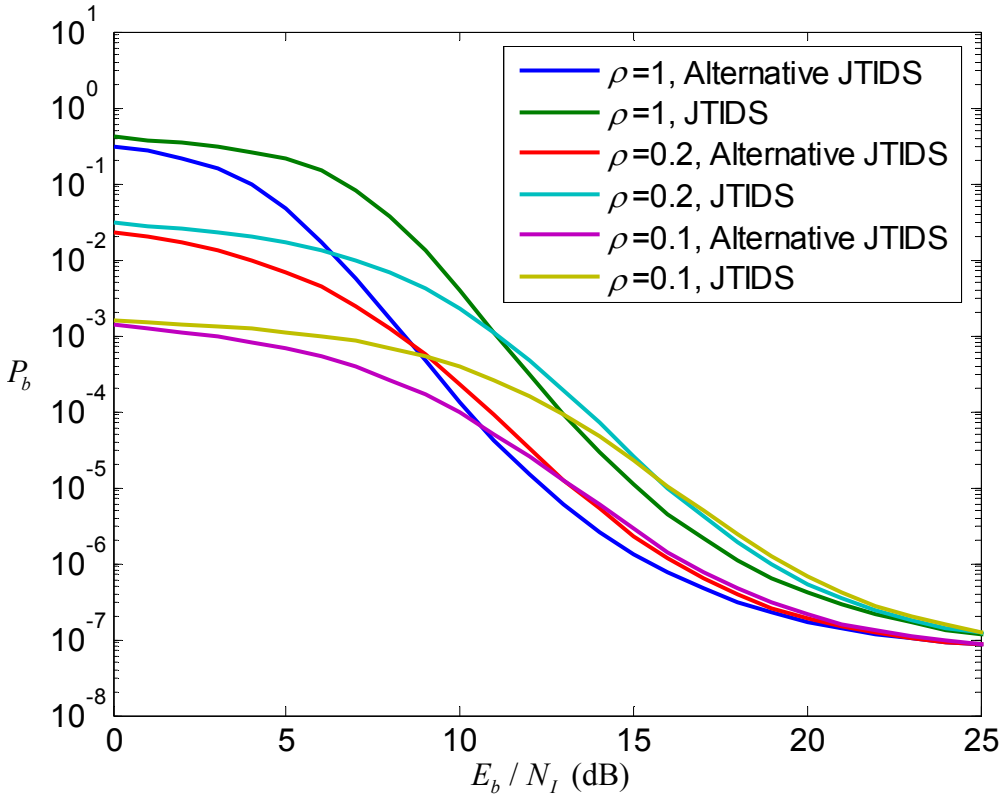

Figure 28. Performance of the first alternative JTIDS/Link-16 waveform ($E_b / N_0 = 5$ dB) and the JTIDS waveform ($E_b / N_0 = 7.7$ dB) for different values of ρ with the single-pulse structure.

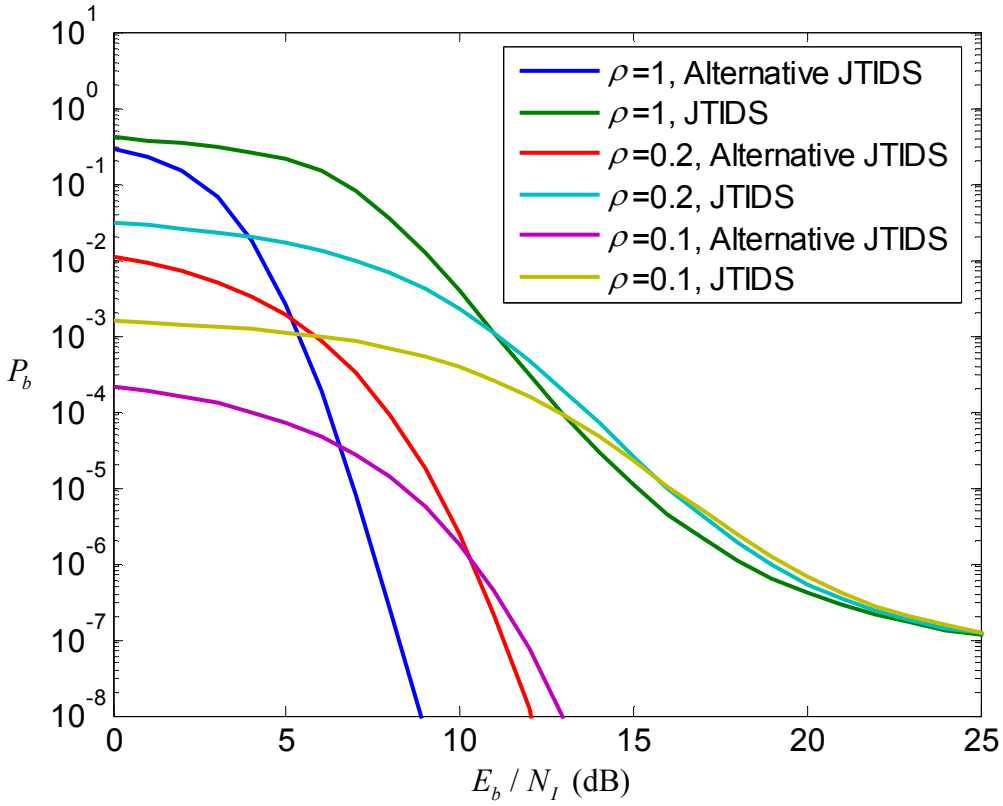

Figure 29. Performance of the first alternative JTIDS/Link-16 waveform and the JTIDS waveform, both with $E_b / N_0 = 7.7$ dB, for different values of ρ with the single-pulse structure.

3. Comparison of 64-BOK with (31,15) RS Coding to the JTIDS/Link-16 Waveform for AWGN, Double-pulse Structure

The performance of the first alternative JTIDS/Link-16 waveform and the original JTIDS/Link-16 waveform in AWGN for the double-pulse structure is shown in Figure 30. At $P_b = 10^{-5}$, $E_c / N_0 = 4$ dB and $E_c / N_0 = 1.3$ dB for the JTIDS/Link-16 waveform and the 64-BOK waveform, respectively. This yields a 2.7 dB gain for the first alternative JTIDS/Link-16 waveform over the JTIDS/Link-16 waveform, which is the same as was found for the single-pulse structure. Comparing Figure 27 and Figure 30, the single-pulse structure 64-BOK waveform has a 3 dB advantage over the double-pulse JTIDS/Link-16 waveform.

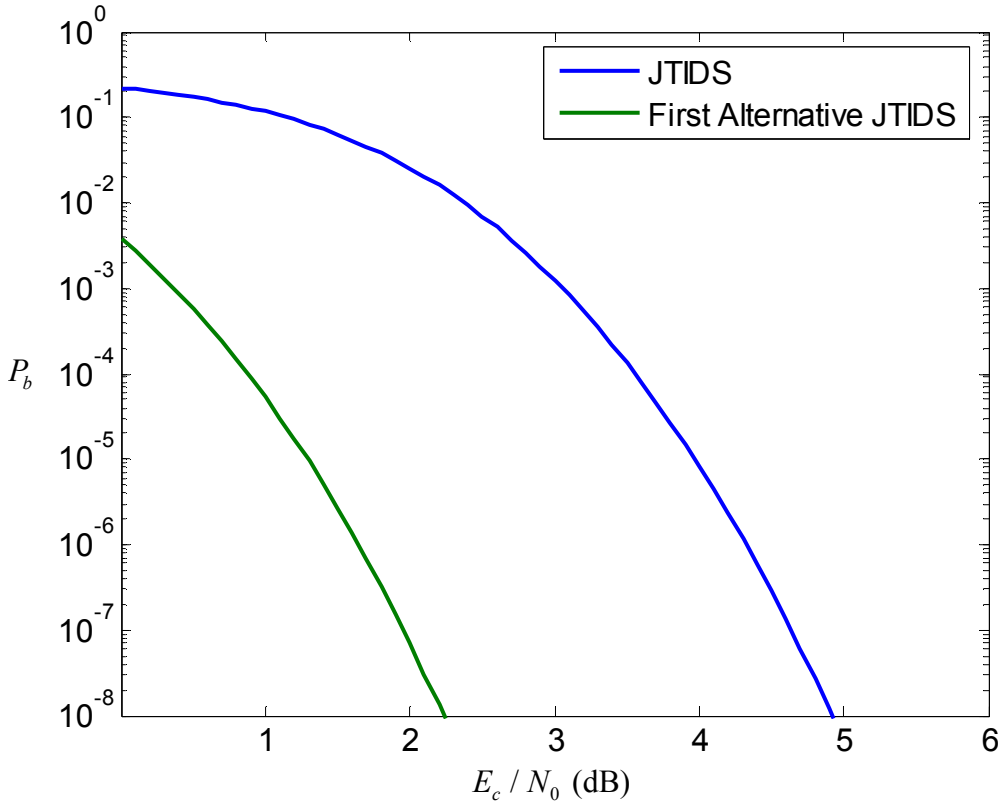

Figure 30. Performance of the first alternative JTIDS/Link-16 waveform and the JTIDS waveform for the double-pulse structure.

4. Comparison of 64-BOK with (31,15) RS Coding to the JTIDS/Link-16 Waveform for AWGN and PNI, Double-pulse Structure

The performance for both the first alternative JTIDS/Link-16 and the JTIDS/Link-16 waveform for the double-pulse structure in both AWGN and PNI for different values of ρ is shown in Figure 31. We consider the performance when the two waveforms both asymptotically converge to $P_b = 10^{-9}$. The required E_c / N_0 for the first alternative waveform and the JTIDS/Link-16 waveforms are 2.5 dB and 5.2 dB, respectively. We see a 2.7 dB gain for the first alternative JTIDS/Link-16 waveform over the JTIDS/Link-16 waveform.

At $P_b = 10^{-5}$ and $\rho = 1$, the E_c / N_I required for the alternative JTIDS/Link-16 waveform and the JTIDS/Link-16 waveform are 7.5 dB and 10 dB, respectively. This gives a difference of 2.5 dB between the two waveforms. When $\rho = 0.2$,

$E_c / N_I = 8.3$ dB is required for both the alternative JTIDS/Link-16 waveform and the JTIDS/Link-16 waveform. The JTIDS/Link-16 waveform performs better than the first alternative waveform when $E_c / N_I < 8.3$ dB and $\rho \le 0.2$.

For $\rho = 0.1$, at $P_b = 10^{-6}$, the JTIDS/Link-16 waveform performs better than the second alternative waveform when $E_c / N_I < 12.5$ dB . The difference in E_c / N_I between the alternative JTIDS/Link-16 waveform ($E_c / N_I = 10.4$ dB) and the JTIDS/Link-16 waveform ($E_c / N_I = 7.9$ dB) is 2.5 dB.

Comparing the performance of the two waveforms, we see that the first alternative JTIDS/Link-16 waveform performs better than the JTIDS/Link-16 waveform by about 2.5 dB at $P_b = 10^{-5}$ when $\rho = 1$. The JTIDS/Link-16 waveform outperforms the first alternative waveform when $\rho = 0.1$ and $\rho = 0.2$ for $E_c / N_I < 12.5$ dB and $E_c / N_I < 8.3$ dB, respectively. As can be seen in Figure 32, where $E_c / N_0 = 5.2$ dB, the first alternative JTIDS/Link-16 waveform outperforms the JTIDS/Link-16 waveform if the two waveforms are compared on equal E_c / N_0 basis.

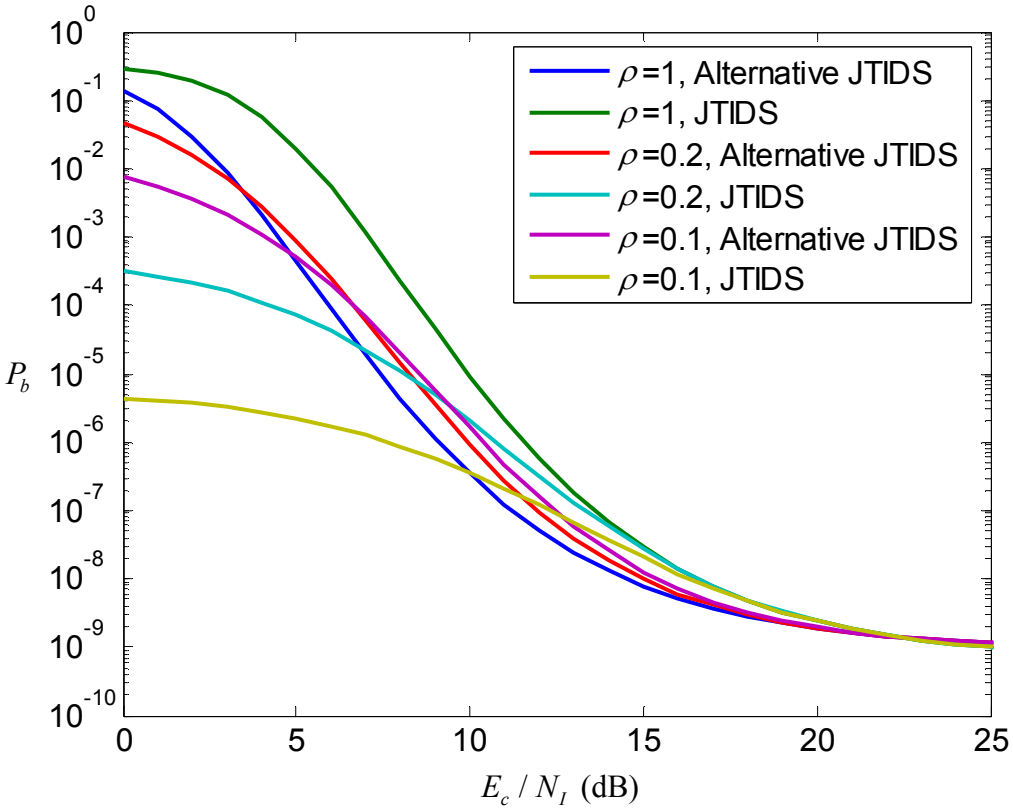

Figure 31. Performance of the first alternative JTIDS/Link-16 waveform ($E_c / N_0 = 2.5$ dB) and the JTIDS waveform ($E_c / N_0 = 5.2$ dB) for different values of ρ with the double-pulse structure.

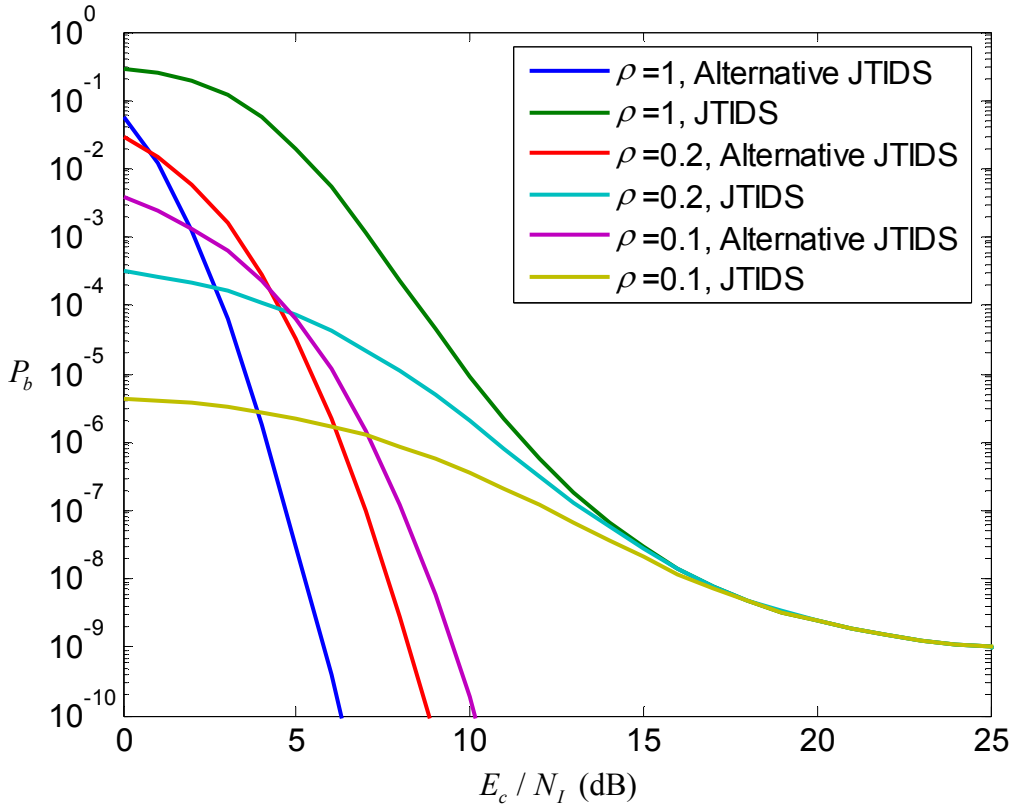

Figure 32. Performance of the first alternative JTIDS/Link-16 waveform and the JTIDS waveform, both with $E_c / N_0 = 5.2$ dB, for different values of ρ with the double-pulse structure.

5. Section Summary

In this section, we compared the performance of the first alternative JTIDS/Link-16 waveform to the original JTIDS/Link-16 waveform for a channel with both AWGN only as well as AWGN and PNI. Both single-pulse and double-pulse structures were considered. The result shows significant improvement of 2.7 dB gain for the 64-BOK waveform over the original JTIDS/Link-16 waveform. The primary advantage of the 64-BOK waveform is the 140 percent increase in data rate over the original JTIDS/Link-16 waveform.

E. CHAPTER SUMMARY

The performance of the first alternative JTIDS/Link-16 waveform, 64-BOK with (31,15) RS coding was examined in this chapter. In Section B, we analyzed the performance of the proposed waveform with a single-pulse structure (no diversity) for both AWGN only as well as AWGN plus PNI. The analyses of the performance of the waveform with EED were also conducted for both AWGN as well as AWGN plus PNI.

In Section C of this chapter, we investigated the performance of the first alternative JTIDS/Link-16 waveform with a double-pulse structure (a diversity of two). We analyzed the performance of the proposed waveform for both AWGN as well as AWGN plus PNI, and also conducted analyses both with and without EED. Perfect-side information (PSI) was also analyzed for the proposed waveform for the double-pulse structure.

In Section D, we compared the performance of the first alternative JTIDS/Link-16 waveform to that of the original JTIDS/Link-16 waveform in both AWGN only as well as AWGN plus PNI for both the single-pulse and the double-pulse structure. The results show a significant improvement for the proposed waveform as compared to the original JTIDS/Link-16 waveform when PNI is present. The primary advantage of the alternative waveform is an overall increase in data rate of 2.4 as compared to the original JTIDS/Link-16 waveform.

In the next chapter, we examine the performance of the second alternative JTIDS/Link-16 waveform that utilizes complex 64-BOK modulation and (63,47) RS coding. The performance of the second alternative waveform is also compared to that of the original JTIDS/Link-16 waveform.

IV. ALTERNATIVE JTIDS/LINK-16 WAVEFORM WITH 64-BOK AND (63,47) RS ENCODING

In this chapter, we examine the performance of the second alternative JTIDS/Link-16 waveform for both AWGN as well as AWGN plus PNI. The alternative waveform uses 64-BOK modulation with (63,47) RS encoding instead of the (31,15) RS encoding used for the original JTIDS/Link-16 waveform. We also examine the performance when EED is used. In Section A of this chapter, we compare different RS code rates; the analyses of the performance of the waveform are based on the single-pulse (no diversity) structure. In Section B, the double-pulse (with diversity) structure is taken into account. In the last section, Section C, the second alternative JTIDS/Link-16 waveform is compared to the original JTIDS/Link-16 waveform for both AWGN and AWGN plus PNI.

A. PERFORMANCE OF THE SECOND ALTERNATIVE WAVEFORM FOR THE SINGLE-PULSE STRUCTURE

In this section, the performance of $(63,k)$ RS coding with different values of k is evaluated so as to determine the optimal RS code rate. We also analyze the performance of the second alternative JTIDS/Link-16 waveform both with and without EED decoding and in AWGN as well as AWGN plus PNI. The analyses on the waveform is based on the single-pulse (with no diversity) structure.

1. Comparison of $(63,k)$ RS Coding in AWGN

The JTIDS/Link-16 waveform's primary limitation is the limited data throughput inherent in its basic architecture [2]. In this chapter, we use (64,47) RS coding instead of the (31,15) RS coding specified for the original JTIDS/Link-16 waveform so as to improve the data rate of the system.

The probability of information bit error versus E_b / N_0 for 64-BOK modulation with $(63,k)$ RS coding in the AWGN environment are shown in Figure 33 and Figure 34. As k increases from 29 to 61, the coding gain increases initially and decreases again as

k continues to increase. From Figure 33 and Figure 34, at $P_b = 10^{-5}$, the performance of 64-BOK with (63,47) RS is the best with $E_b / N_0 = 3.37$ dB. From Figure 33, we see that the required E_b / N_0 for the $(63, k)$ RS codes is reduced as the number of encoded information symbols increases ($k = 29$ to 47). The required E_b / N_0 reaches 3.37 dB for the (63,47) RS code and begins to increase as the number of encoded information symbols increases ($k = 47$ to 61), which is shown in Figure 34.

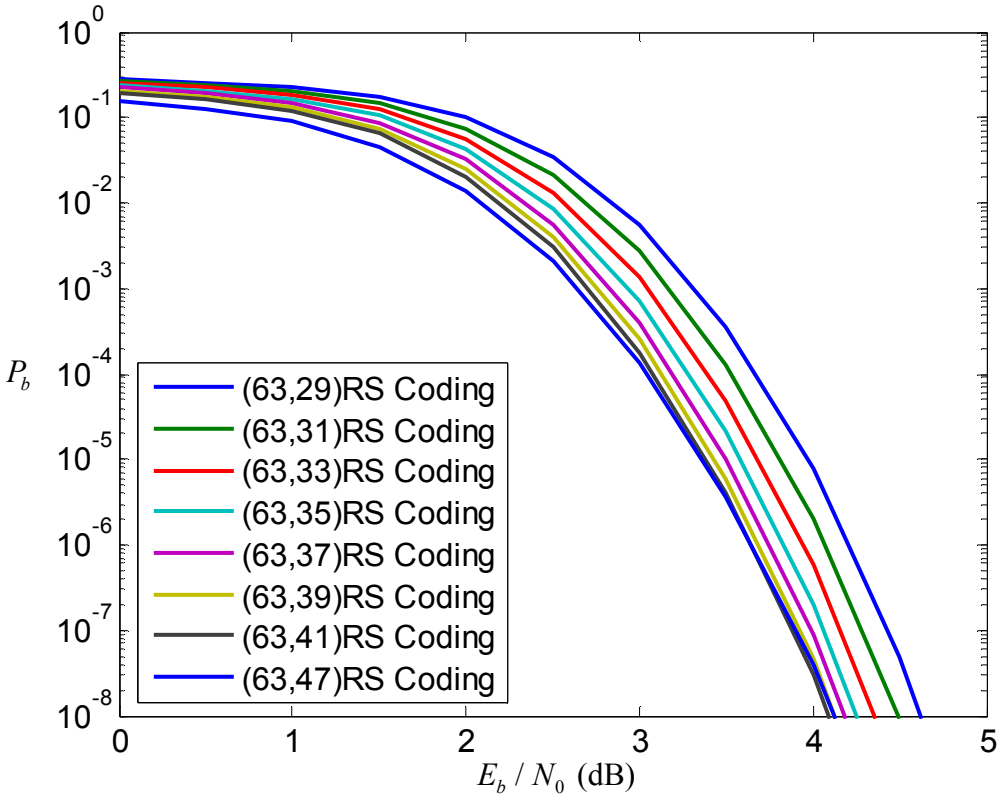

Figure 33. Performance of 64-BOK with $(63, k)$RS coding in AWGN.

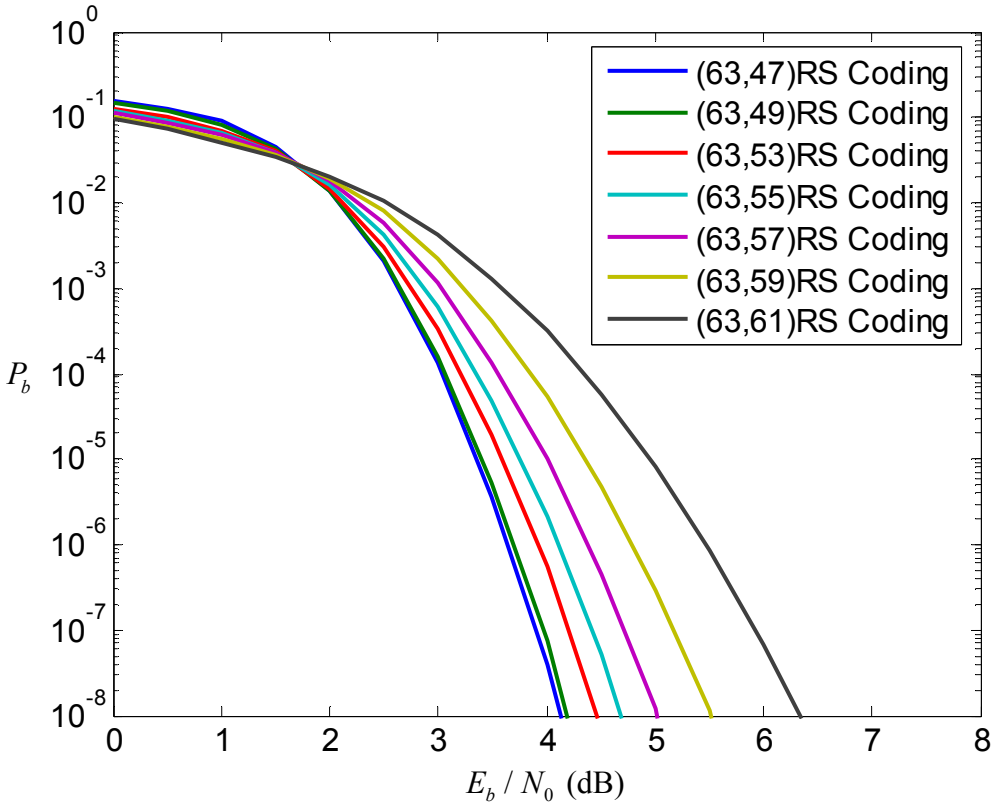

Figure 34. Performance of 64-BOK with $(63,k)$RS coding in AWGN.

A comparison of performance with $(63,k)$ RS coding with k as a parameter is shown in Table 1. From Table 1, the increase in data rate is calculated by comparing the code rate of a $(63,k)$ RS code to the code rate for a (31,15) RS code. We see that as k gets smaller, the number of correctable errors t increases but the data rate decreases. Conversely, increasing k reduces t and increases the data rate. The (63,47) RS code provides the optimal performance and a data rate increase of eighty-five percent with $E_b / N_0 = 3.37$ dB. Note that this choice keeps the number of correctable errors ($t = 8$) per block the same as for the (31,15) RS coding used in the original JTIDS/Link-16 waveform.

Number of code symbols n	**Number of information symbols** k	**Number of correctable symbols** $t=(n-k)/2$	**Data rate increase** $r_{(63,k)}/r_{(31,15)}$	**Percentage of data rate increase** (%)	E_b/N_0 at $P_b=10^{-5}$	**Coding Gain** $(E_b/N_0)_{coded}$ $-(E_b/N_0)_{uncoded}$
63	29	17	1.14	14%	3.97	2.20
63	31	16	1.22	22%	3.80	2.37
63	33	15	1.30	30%	3.69	2.48
63	35	14	1.38	38%	3.58	2.59
63	37	13	1.46	46%	3.50	2.67
63	39	12	1.54	54%	3.43	2.74
63	41	11	1.61	61%	3.37	2.80
63	43	10	1.69	69%	3.37	2.80
63	45	9	1.77	77%	3.37	2.80
63	47	8	1.85	85%	3.37	2.80
63	49	7	1.93	93%	3.41	2.76
63	51	6	2.01	101%	3.49	2.68
63	53	5	2.09	109%	3.60	2.57
63	55	4	2.17	117%	3.76	2.41
63	57	3	2.24	124%	4.00	2.17
63	59	2	2.32	132%	4.34	1.83
63	61	1	2.40	140%	4.94	1.23

Table 1. Comparison performance of $(63,k)$ RS coding.

From the preceding results, (63,47) RS coding is optimal in terms of E_b/N_0 and data rate, while maintaining the same number of correctable symbol errors per block as the (31,15) RS code. Hence, the performance of the second alternative JTIDS/Link-16 waveform uses 64-BOK modulation with (63,47) RS coding provides an overall increase in data rate of 4.44 as compared to the existing JTIDS/Link-16 waveform.

2. Performance in AWGN

The probability of symbol error for *M*BOK is given in (2.5). For the second alternative JTIDS/Link-16 waveform that uses 64-BOK with (63,47) RS coding, the probability of channel symbol error is

$$p_s = 1 - \frac{1}{\sqrt{2\pi}} \int_{-\sqrt{2rE_s/N_0}}^{\infty} e^{\frac{-u^2}{2}} \left[1 - 2Q(u + \sqrt{\frac{2rE_s}{N_0}}) \right]^{\frac{M}{2}-1} du \,. \qquad (4.1)$$

Expressed in terms of bit energy E_b, (4.1) is

$$p_s = 1 - \frac{1}{\sqrt{2\pi}} \int_{-\sqrt{2rmE_b/N_0}}^{\infty} e^{-\frac{u^2}{2}} \left[1 - 2Q\left(u + \sqrt{\frac{2rmE_b}{N_0}} \right) \right]^{\frac{M}{2}-1} du \tag{4.2}$$

or

$$p_s = 1 - \frac{1}{\sqrt{2\pi}} \int_{-\sqrt{2rm\gamma_b}}^{\infty} e^{-\frac{u^2}{2}} \left[1 - 2Q\left(u + \sqrt{2rm\gamma_b} \right) \right]^{\frac{M}{2}-1} du, \tag{4.3}$$

where m is the number of bits per symbol received by *M*BOK demodulator, $r = k/n$ is the code rate of RS encoder, and $\gamma_b = E_b / N_0$.

Substituting (4.3) into (2.14), we obtain the probability of symbol error for 64-BOK with (63,47) RS decoding in the presence of AWGN, repeated here as

$$P_s \approx \frac{1}{n} \sum_{j=t+1}^{n} j \binom{n}{j} {p_s}^j (1 - p_s)^{n-j} . \tag{4.4}$$

The probability of bit error can be approximated using (2.16) and (4.4). Using (2.16), (4.3) and (4.4), we plot the probability of bit error for the second alternative JTIDS/Link-16 waveform, shown in Figure 35, where $r = 47/63$ and $m = 6$. The performance for both coded and uncoded waveforms are presented for comparison purposes, where we (2.5) is used to plot the uncoded waveform with $E_s = mE_b$.

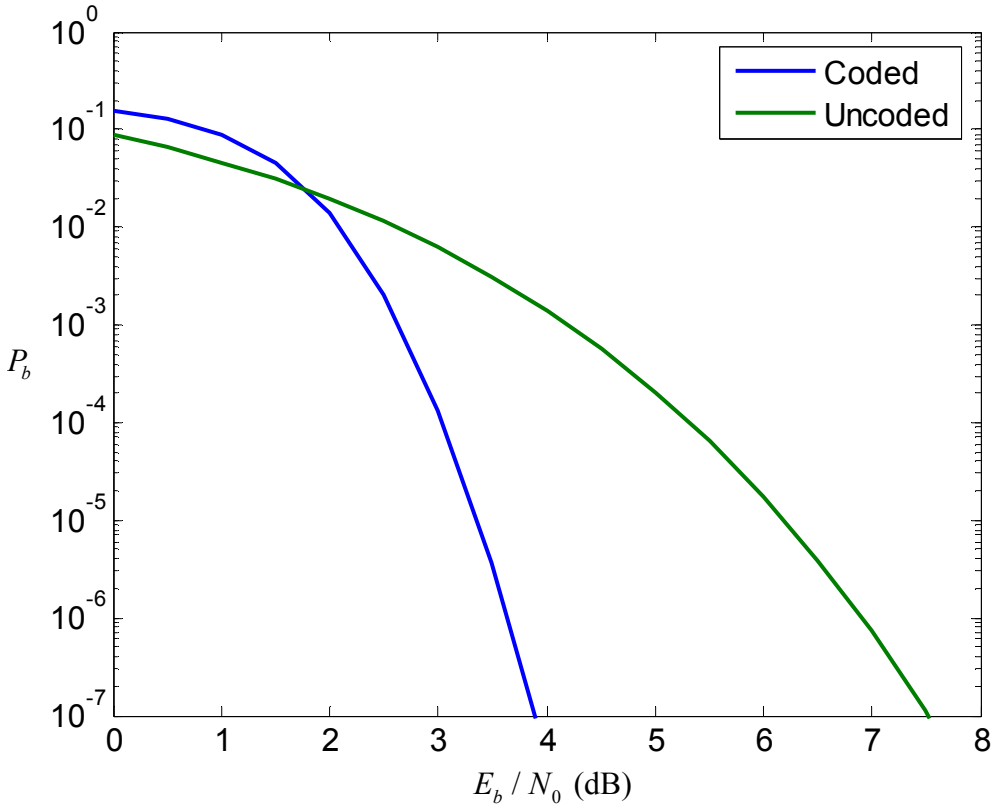

Figure 35. Performance of the second alternative JTIDS/Link-16 waveform in AWGN.

From Figure 35, we see that at $P_b = 10^{-5}$ the coded waveform requires $E_b / N_0 = 3.3$ dB, while the uncoded waveform requires $E_b / N_0 = 6.2$ dB, for a coding gain of 2.9 dB.

3. Performance in AWGN and Pulse-noise Interference

For performance with both AWGN and PNI, using (2.6), (2.8) and (4.3), we obtain the probability of channel symbol error as

$$p_s = \rho\left\{1-\frac{1}{\sqrt{2\pi}}\int_{-\sqrt{\frac{2rm}{\frac{N_I}{\rho E_b}+\frac{N_0}{E_b}}}}^{\infty} e^{\frac{-u^2}{2}}\left(1-2Q(u+\sqrt{\frac{2rm}{\frac{N_I}{\rho E_b}+\frac{N_0}{E_b}}}\right)^{\frac{M}{2}-1} du\right\}$$
$$+(1-\rho)\left\{1-\frac{1}{\sqrt{2\pi}}\int_{-\sqrt{2rmE_b/N_0}}^{\infty} e^{\frac{-u^2}{2}}\left(1-2Q(u+\sqrt{\frac{2rmE_b}{N_0}}\right)^{\frac{M}{2}-1} du\right\} \quad . \qquad (4.5)$$

Replacing E_b / N_I with γ_I and E_b / N_0 with γ_b in (4.5), we get

$$p_s = \rho\left\{1-\frac{1}{\sqrt{2\pi}}\int_{-\sqrt{\frac{2rm}{\frac{1}{\rho\gamma_I}+\frac{1}{\gamma_b}}}}^{\infty} e^{\frac{-u^2}{2}}\left(1-2Q(u+\sqrt{\frac{2rm}{\frac{1}{\rho\gamma_I}+\frac{1}{\gamma_b}}}\right)^{\frac{M}{2}-1} du\right\}$$
$$+(1-\rho)\left\{1-\frac{1}{\sqrt{2\pi}}\int_{-\sqrt{2rm\gamma_b}}^{\infty} e^{\frac{-u^2}{2}}\left[1-2Q(u+\sqrt{2rm\gamma_b}\right]^{\frac{M}{2}-1} du\right\}, \qquad (4.6)$$

and defining $\zeta = 1/\left(\gamma_b^{-1}+\left(\rho\gamma_I\right)^{-1}\right)$, we obtain from (4.6)

$$p_s = \rho\left\{1-\frac{1}{\sqrt{2\pi}}\int_{-\sqrt{2rm\zeta}}^{\infty} e^{\frac{-u^2}{2}}\left[1-2Q(u+\sqrt{2rm\zeta}\right]^{\frac{M}{2}-1} du\right\}$$
$$+(1-\rho)\left\{1-\frac{1}{\sqrt{2\pi}}\int_{-\sqrt{2rm\gamma_b}}^{\infty} e^{\frac{-u^2}{2}}\left[1-2Q(u+\sqrt{2rm\gamma_b}\right]^{\frac{M}{2}-1} du\right\}. \qquad (4.7)$$

The probability of information channel symbol error is obtained from (4.4) and (4.7); substituting the result of (4.4) into (2.16), we obtain the probability of bit error. The performance for both coded and uncoded waveforms in AWGN and PNI for $E_b / N_0 = 9$ dB with $\rho = 1$ and $\rho = 0.2$ are shown in Figure 36 and Figure 37, respectively.

From Figure 36, at $P_b = 10^{-5}$, the required E_b / N_I for the coded waveform is 4.7 dB and for the uncoded waveform is 9.4 dB, which gives a coding gain of 4.7 dB.

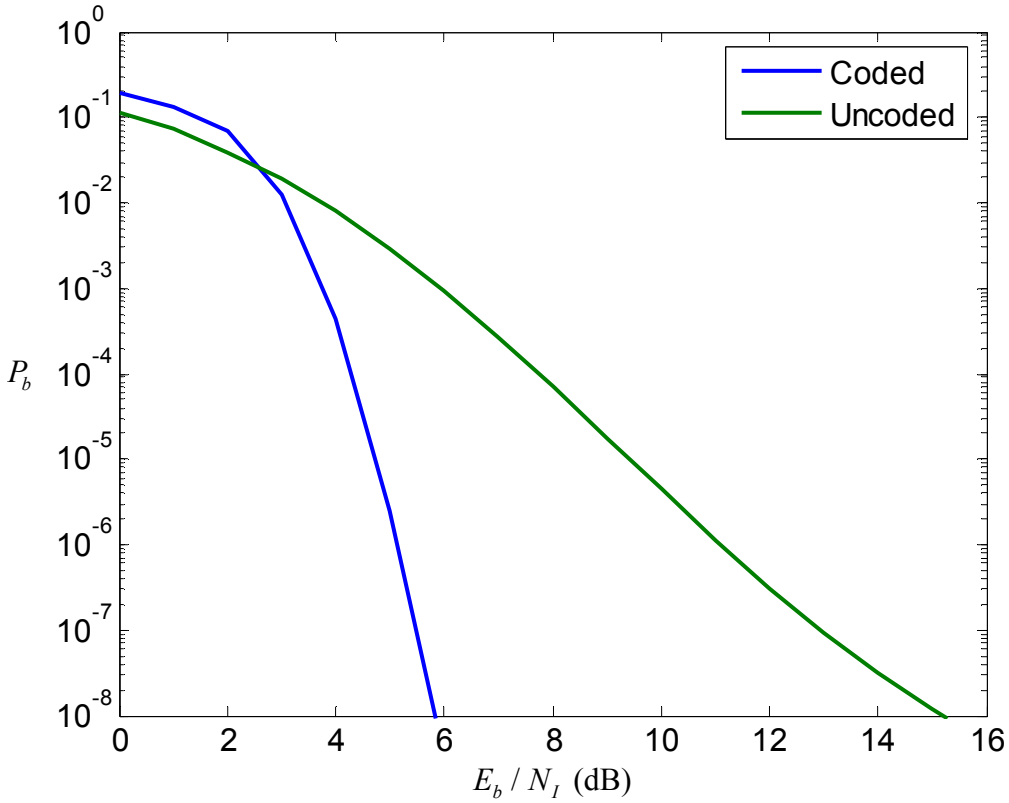

Figure 36. Performance of the second alternative JTIDS/Link-16 waveform for $\rho = 1$ and $E_b / N_0 = 9$ dB.

From Figure 37, at $P_b = 10^{-5}$, the required E_b / N_I for the coded waveform is 9.1 dB and for the uncoded waveform is 15.3 dB, which gives a coding gain of 6.2 dB. From the above results, the coded waveforms perform better than the uncoded waveforms in both AWGN and PNI. Comparing the absolute performance of the coded waveforms from the two figures, we see that $\rho = 1$ performs better than $\rho = 0.2$; although, there is a larger coding gain between the coded and uncoded waveforms when $\rho = 0.2$.

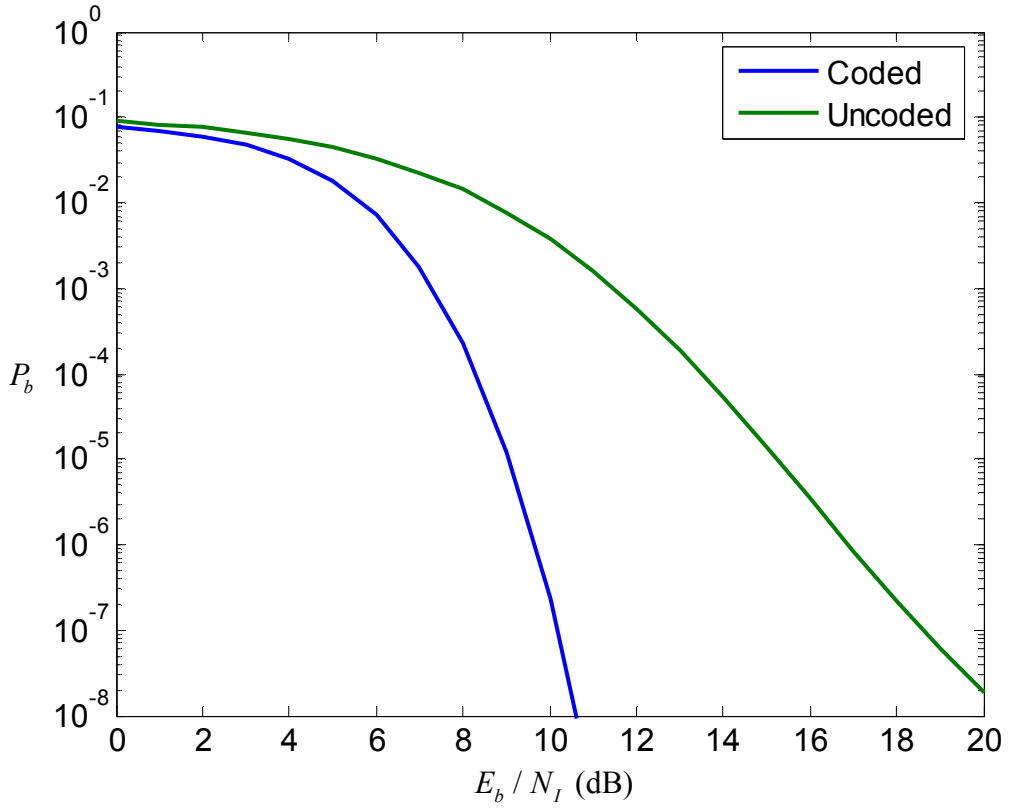

Figure 37. Performance of the second alternative JTIDS/Link-16 waveform for $\rho = 0.2$ and $E_b / N_0 = 9$ dB.

The performance of the second alternative waveform in PNI for $E_b / N_0 = 6$ dB with different values of ρ is shown in Figure 38. When $\rho = 1$, which is equivalent to barrage noise interference, performance is better for $P_b = 10^{-5}$ ($E_b / N_I \approx 6.8$ dB) as compared to that for either $\rho = 0.2$ or 0.1. The degradation due to PNI is about 3.7 dB. From Figure 38, we see that the transition point where $\rho = 1$ gives better performance than either $\rho = 0.2$ or 0.1 occurs for $P_b < 4 \times 10^{-3}$ where $E_b / N_I > 4.8$ dB.

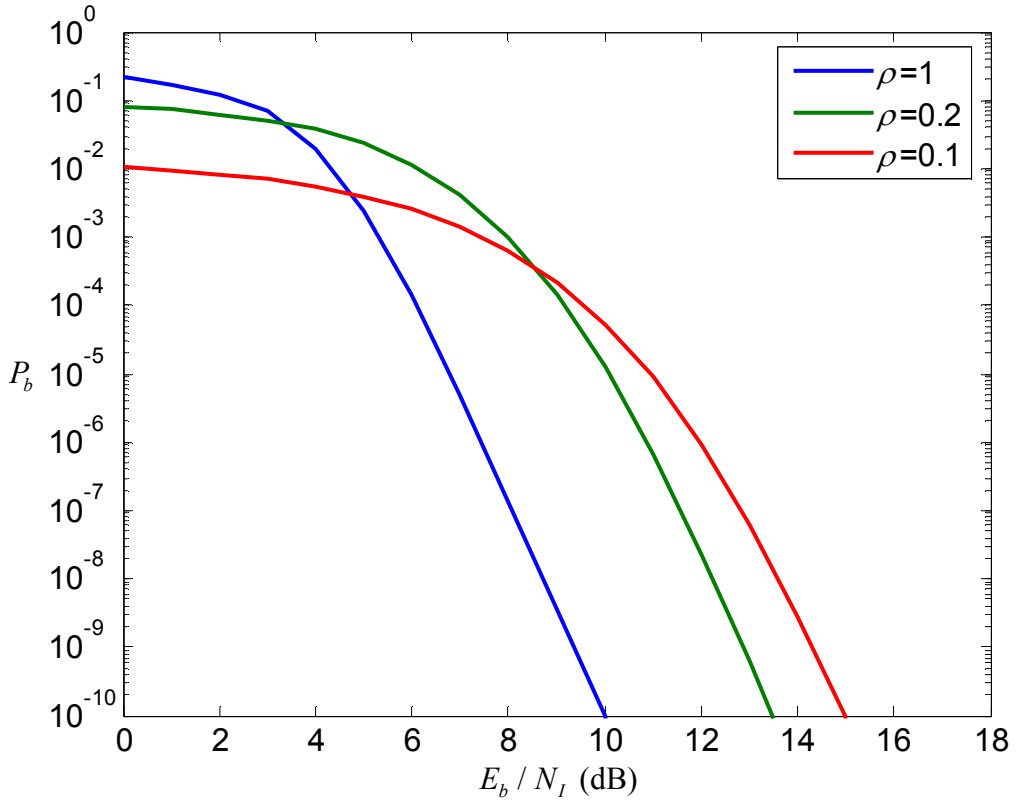

Figure 38. Performance of the second alternative waveform in PNI for $E_b / N_0 = 6$ dB.

The performance of the second alternative waveform in PNI for $E_b / N_0 = 9$ dB with different values of ρ is shown in Figure 39. Comparing Figure 39 to Figure 38, we see an improvement in the overall performance as E_b / N_0 increases. At $P_b = 10^{-5}$, the required E_b / N_I for $\rho = 1$ and $\rho = 0.2$ are 4.7 dB and 9.1 dB respectively; and the degradation due to PNI is about 4.4 dB.

Comparing to the results from Figure 38, where E_b / N_I for $\rho = 1$ and $\rho = 0.2$ are 6.8 dB and 10.1 dB, respectively, we see that smaller values of E_b / N_I are required for the same P_b. Thus, while the increase in E_b / N_0 improves performance in PNI , it also increases relative degradation.

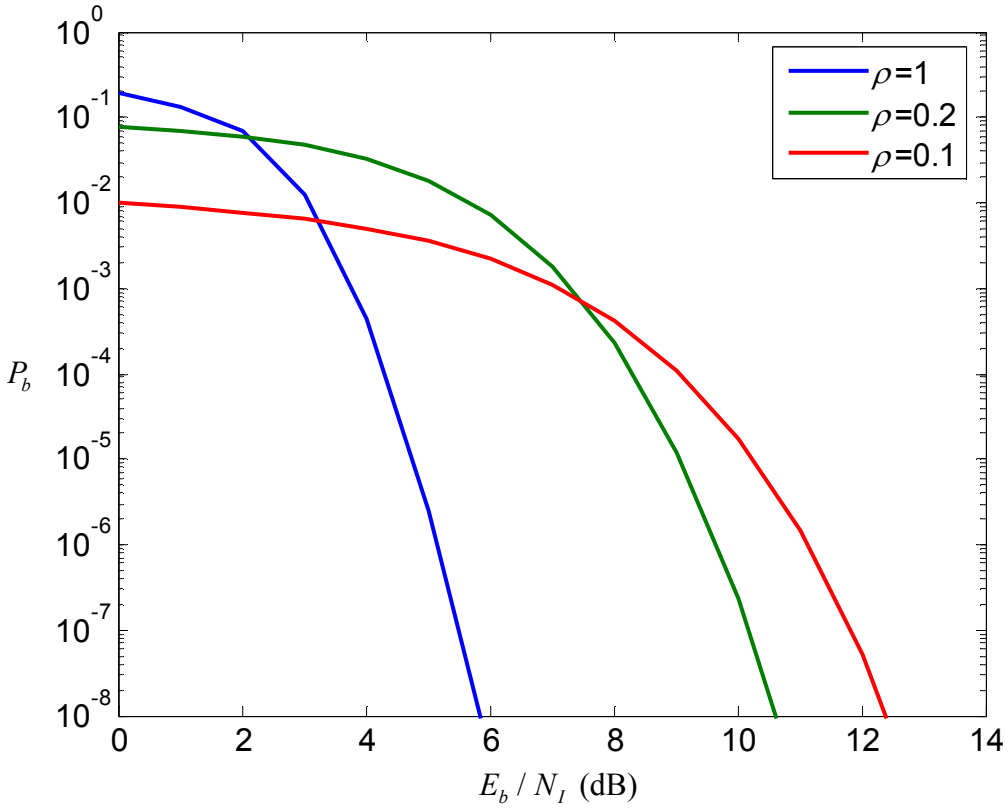

Figure 39. Performance of the second alternative waveform in PNI for $E_b / N_0 = 9$ dB.

4. Performance with Errors-and-Erasures Decoding in AWGN

Referencing Section F of Chapter II, we recall that error-and-erasures decoding (EED) is a simple form of soft decision decoding that is implemented at the receiver to utilize ambiguously received symbols. Hence, the number of possible outputs of the demodulator per symbol is the number of symbols plus one.

The probability of channel erasure and correct symbol detection are given in (3.31) and (3.40), respectively. The equations are repeated here for convenience:

$$p_e = \left[Q\left((1-a)\sqrt{\frac{2rmE_b}{N_0}} \right) - Q\left((1+a)\sqrt{\frac{2rmE_b}{N_0}} \right) \right] \left[1 - 2Q\left(a\sqrt{\frac{2rmE_b}{N_0}} \right) \right]^{\frac{M}{2}-1} \tag{4.8}$$

and

$$p_c = \frac{1}{\sqrt{2\pi}} \int_{-(1-a)\sqrt{\frac{2rmE_b}{N_0}}}^{\infty} e^{-\frac{u^2}{2}} \left[1 - 2Q\left(u + \sqrt{\frac{2rmE_b}{N_0}} \right) \right]^{\frac{M}{2}-1} du \,. \tag{4.9}$$

Substituting (4.8) and (4.9) into (2.21), we obtain the probability of channel symbol error for *M*BOK with EED. The result from (2.21), (4.8) and (4.9) are then used to obtain the probability of block error given by (3.41) and repeated here:

$$P_E = 1 - \left[\sum_{i=0}^{t} \binom{n}{i} {p_s}^i \sum_{j=0}^{d_{\min}-1-2i} \binom{n-i}{j} {p_e}^j {p_c}^{n-i-j} \right]. \tag{4.10}$$

Subsequently, the probability of bit error and symbol error for *M*BOK with (n, k) RS coding and EED in the presence of AWGN are obtained from (2.16) and (2.25), respectively.

The performance of 64-BOK with (63,47) RS coding and EED in AWGN for different values of a is shown in Figure 40, where a varies from 0 (no EED) to 0.9 (with EED). From Figure 40, we notice that the performance degrades rapidly for large values of a ($a \geq 0.8$), but there is not much difference in performance for $a \leq 0.6$. Hence, there is no improvement in performance when EED is used for the second alternative JTIDS/Link-16 waveform in AWGN.

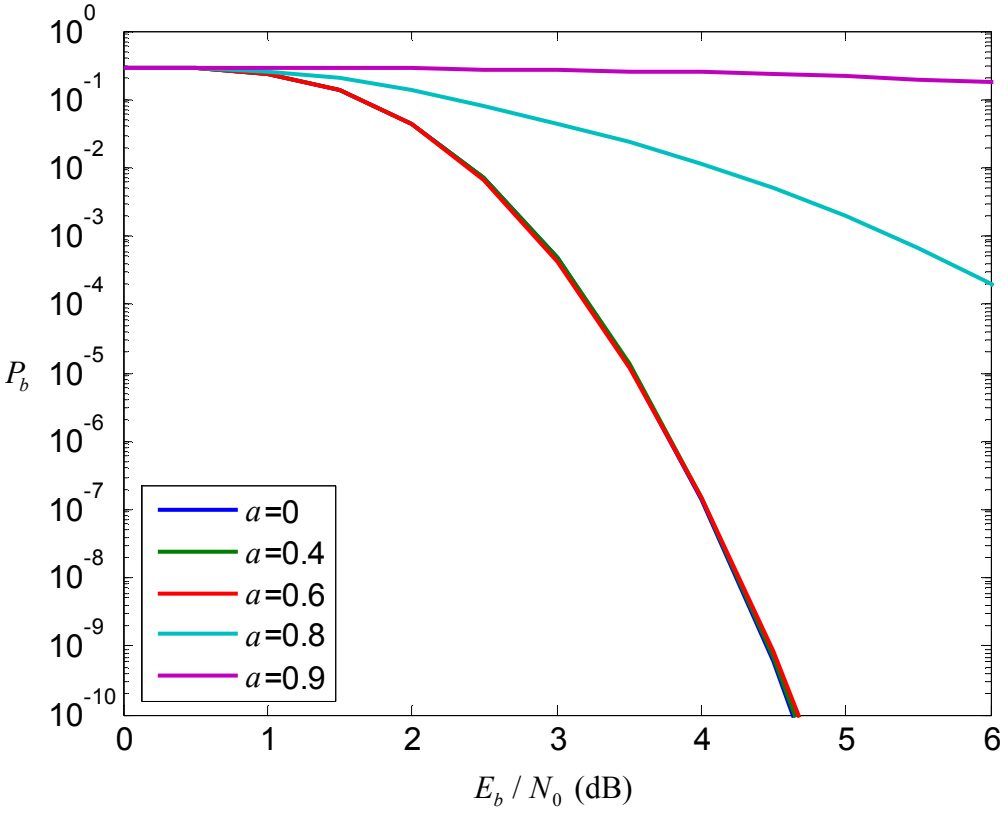

Figure 40. Performance of the second alternative waveform with EED for different values of a in AWGN.

5. Performance with Errors-and-Erasures Decoding in AWGN and Pulse-noise Interference

The probability of channel erasure for the second alternative waveform with EED in the presence of PNI is obtained from (2.6), (2.8) and (4.8) in terms of E_b as

$$p_e = (1-\rho)\left[Q\left((1-a)\sqrt{\frac{2rmE_b}{N_0}}\right) - Q\left((1+a)\sqrt{\frac{2rmE_b}{N_0}}\right)\right]\left[1-2Q\left(a\sqrt{\frac{2rmE_b}{N_0}}\right)\right]^{\frac{M}{2}-1}$$
$$+\rho\left[Q\left((1-a)\sqrt{\frac{2rmE_b}{\frac{1}{\rho}N_I+N_0}}\right) - Q\left((1+a)\sqrt{\frac{2rmE_b}{\frac{1}{\rho}N_I+N_0}}\right)\right]\left[1-2Q\left(a\sqrt{\frac{2rmE_b}{\frac{1}{\rho}N_I+N_0}}\right)\right]^{\frac{M}{2}-1} \quad (4.11)$$

Defining $\gamma_I = E_b / N_I$, $\gamma_b = E_b / N_0$, and defining $\zeta = 1/\left(\gamma_b^{-1} + (\rho\gamma_I)^{-1}\right)$, we obtain from (4.11)

$$p_e = (1-\rho)\left[Q\left((1-a)\right)\sqrt{2rm\gamma_b}\right) - Q\left((1+a)\sqrt{2rm\gamma_b}\right)\right]\left[1-2Q\left(a\sqrt{2rm\gamma_b}\right)\right]^{\frac{M}{2}-1} + \rho\left[Q\left((1-a)\sqrt{2rm\zeta}\right) - Q\left((1+a)\sqrt{2rm\zeta}\right)\right]\left[1-2Q\left(a\sqrt{2rm\zeta}\right)\right]^{\frac{M}{2}-1} \quad (4.12)$$

Similarly, the probability of correct channel detection based on six-bit symbols is obtained from (2.6), (2.8) and (4.9) as

$$p_c = (1-\rho)\left\{\frac{1}{\sqrt{2\pi}}\int_{-(1-a)\sqrt{\frac{2rmE_b}{N_0}}}^{\infty} e^{-\frac{u^2}{2}}\left[1-2Q\left(u+\sqrt{\frac{2rmE_b}{N_0}}\right)\right]^{\frac{M}{2}-1} du\right\} + \rho\left\{\frac{1}{\sqrt{2\pi}}\int_{-(1-a)\sqrt{\frac{2rmE_b}{\frac{1}{\rho}N_I+N_0}}}^{\infty} e^{-\frac{u^2}{2}}\left[1-2Q\left(u+\sqrt{\frac{2rmE_b}{\frac{1}{\rho}N_I+N_0}}\right)\right]^{\frac{M}{2}-1} du\right\}. \quad (4.13)$$

Since $\gamma_I = E_b / N_I$, $\gamma_b = E_b / N_0$, and defining $\zeta = 1/\left(\gamma_b^{-1} + (\rho\gamma_I)^{-1}\right)$, we get from (4.13)

$$p_c = (1-\rho)\left\{\frac{1}{\sqrt{2\pi}}\int_{-(1-a)\sqrt{2rm\gamma_b}}^{\infty} e^{-\frac{u^2}{2}}\left[1-2Q\left(u+\sqrt{2rm\gamma_b}\right)\right]^{\frac{M}{2}-1} du\right\} + \rho\left\{\frac{1}{\sqrt{2\pi}}\int_{-(1-a)\sqrt{2rm\zeta}}^{\infty} e^{-\frac{u^2}{2}}\left[1-2Q\left(u+\sqrt{2rm\zeta}\right)\right]^{\frac{M}{2}-1} du\right\}. \quad (4.14)$$

Subsequently, we obtain the probability of channel symbol error by substituting (4.12) and (4.14) into (2.21). Then we obtain the probability of block error by substituting the results of (2.21), (4.12) and (4.14) into (4.10). Using the result from (4.10), we get the probability of symbol error expressed in (2.25). Using (2.16), we obtain the probability of bit error for the second alternative waveform with EED in both AWGN and PNI.

The performance of the second alternative waveform with EED for different values of a, $\rho = 1$ and $E_b / N_0 = 6$ dB is shown in Figure 41. From Figure 41, there is an insignificant difference in performance for $a \le 0.6$. Performance starts to degrade for $a \ge 0.7$.

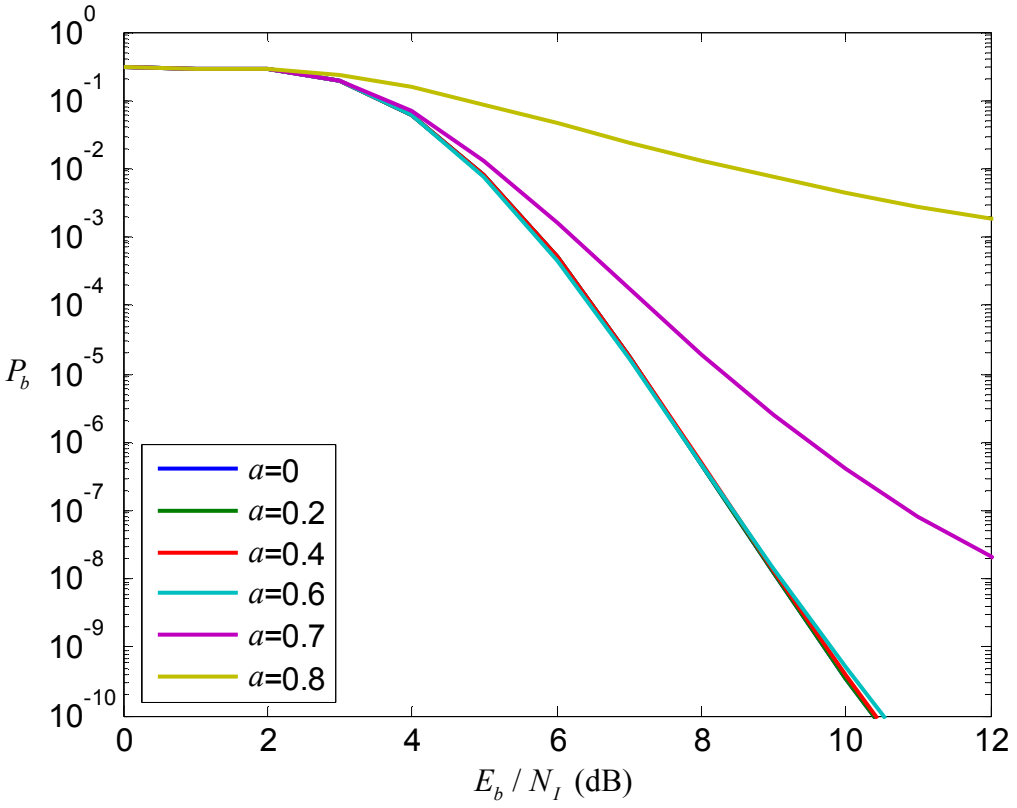

Figure 41. Performance of the second alternative waveform with EED for $\rho = 1$ and $E_b / N_0 = 6$ dB for different values of a in both AWGN and PNI.

The performance of the second alternative waveform with EED in both AWGN and PNI for different values of ρ, $a = 0.6$ and $E_b / N_0 = 6$ dB is shown in Figure 42. At $P_b = 10^{-5}$, the performance degrades for decreasing ρ, and the degradation is limited to about 4.8 dB for the values of ρ plotted.

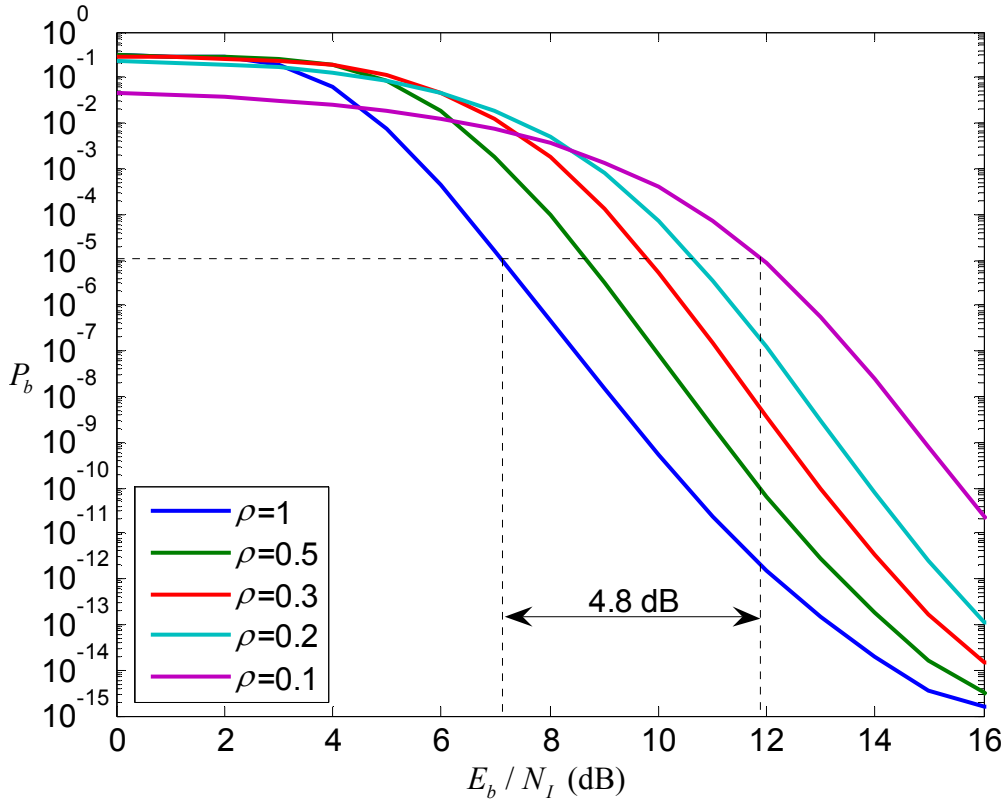

Figure 42. Performance of the second alternative waveform with EED for $E_b / N_0 = 6$ dB and $a = 0.6$ in both AWGN and PNI.

The performance of the second alternative waveform both with and without EED in both AWGN and PNI for $a = 0.6$, $E_b / N_0 = 6$ dB and different values of ρ is shown in Figure 43. At $P_b = 10^{-5}$, we can see that there is a degradation of 0.1 to 1 dB due to EED. The worst performance occurs when $\rho = 0.1$ where the degradation is 1 dB. When $\rho = 1$, the degradation is 0.1 dB.

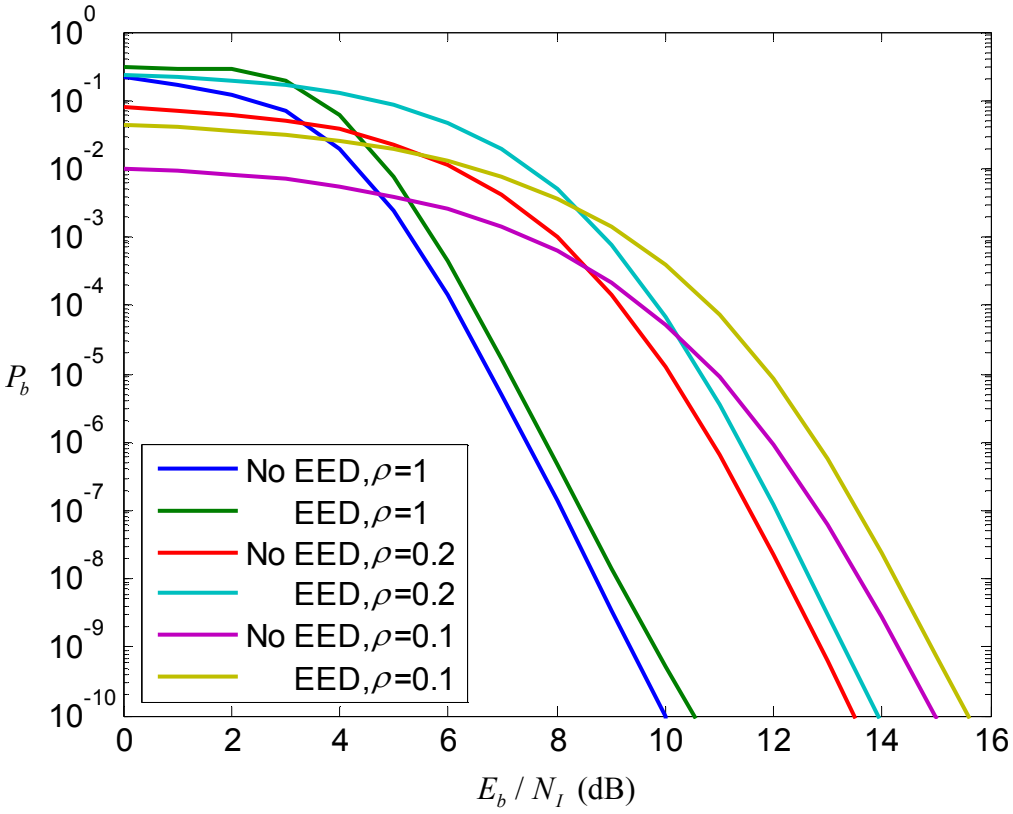

Figure 43. Performance of the second alternative waveform with and without EED for $E_b / N_0 = 6$ dB and $a = 0.6$.

Figure 44 is similar to Figure 43 except $a = 0.4$. Similar results are shown in Figure 44 where there is no improvement in performance for varying ρ due to EED. From the results shown in Figure 43 and Figure 44, we conclude that the use of EED for the second alternative waveform degrades the performance.

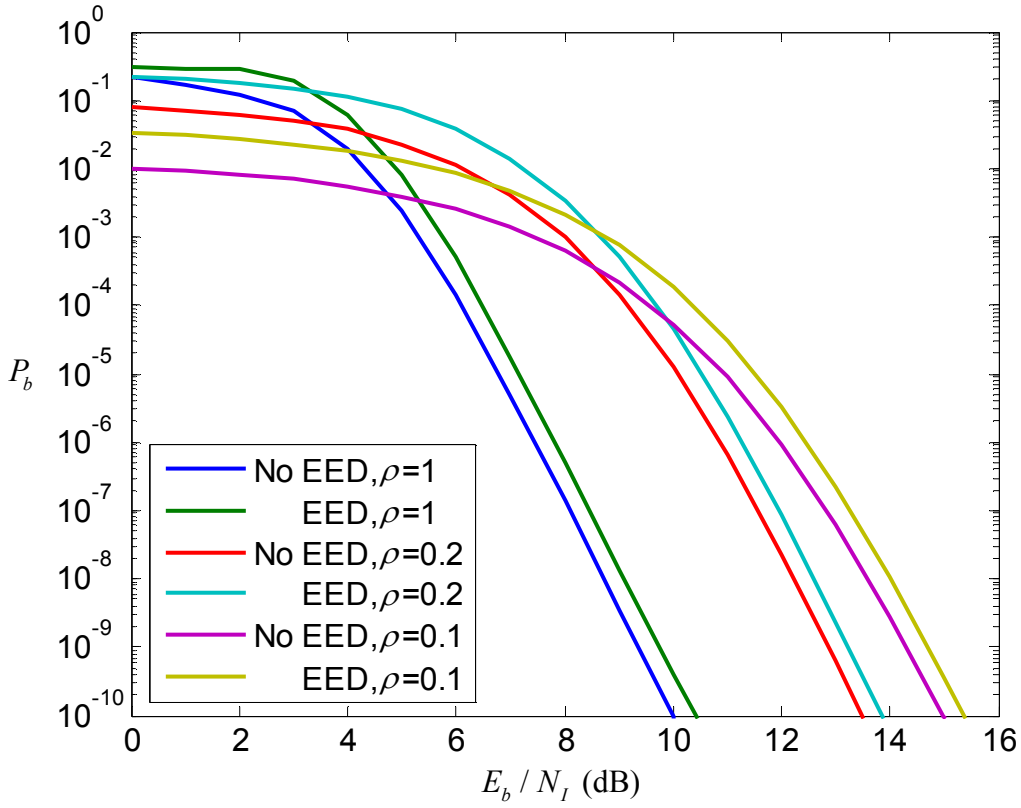

Figure 44. Performance of the second alternative waveform with and without EED for $E_b / N_0 = 6$ dB and $a = 0.4$.

6. Section Summary

In this section, we covered the performance of the second alternative JTIDS/Link-16 waveform for the single-pulse structure (no diversity) both with and without EED and with both AWGN only as well as AWGN plus PNI. We saw that PNI degrades performance, and EED does not improve performance. In the next section, we investigate the performance of the second alternative JTIDS/Link-16 waveform for the double-pulse structure (diversity of two).

B. PERFORMANCE OF THE SECOND ALTERNATIVE WAVEFORM WITH A DIVERSITY OF TWO (DOUBLE-PULSE STRUCTURE)

In this section, we investigate the performance of the second alternative JTIDS/Link-16 waveform for the double-pulse structure (diversity of two). As discussed

earlier, diversity is a widely used method for minimizing the effect of PNI and/or fading when transmitting signals over a channel. It adds the redundancy to the system by transmitting the same symbol twice at different carrier frequencies.

1. Performance in AWGN with a Diversity of Two

We discussed the use of diversity by JTIDS/Link-16 earlier to improve its performance in interference. The double-pulse structure improves the performance of the system while the single-pulse structure allows for higher throughput.

The received energy per bit is L times the average received energy per chip, $E_b = LE_c$. For the double-pulse structure, there is a diversity of two ($L = 2$), and the received energy per bit is the combination of two chip's energy to give twice the energy per symbol received.

The probability of channel symbol error for 64-BOK with (n,k) RS coding with a diversity of two is obtained from (4.2) as

$$p_s = 1 - \frac{1}{\sqrt{2\pi}} \int_{-\sqrt{2LrmE_c/N_0}}^{\infty} e^{-\frac{u^2}{2}} \left[1 - 2Q\left(u + \sqrt{\frac{2LrmE_c}{N_0}} \right) \right]^{\frac{M}{2}-1} du , \qquad (4.15)$$

where E_c is the average energy per chip, $L = 2$ and $m = 6$ bits per symbol. Since $L = 2$, (4.15) can be simplified to

$$p_s = 1 - \frac{1}{\sqrt{2\pi}} \int_{-\sqrt{4rmE_c/N_0}}^{\infty} e^{-\frac{u^2}{2}} \left[1 - 2Q\left(u + \sqrt{\frac{4rmE_c}{N_0}} \right) \right]^{\frac{M}{2}-1} du . \qquad (4.16)$$

Subsequently, the probability of information symbol error and information bit error can be obtained by substituting (4.16) into (4.4) and (4.4) into (2.16).

The performance of 64-BOK with (63,47) RS coding for both the single-pulse and the double-pulse structure in AWGN is shown in Figure 45. At $P_b = 10^{-5}$, the difference in the required E_c / N_0 between the double-pulse and the single-pulse structure is 3 dB in terms of average energy per chip.

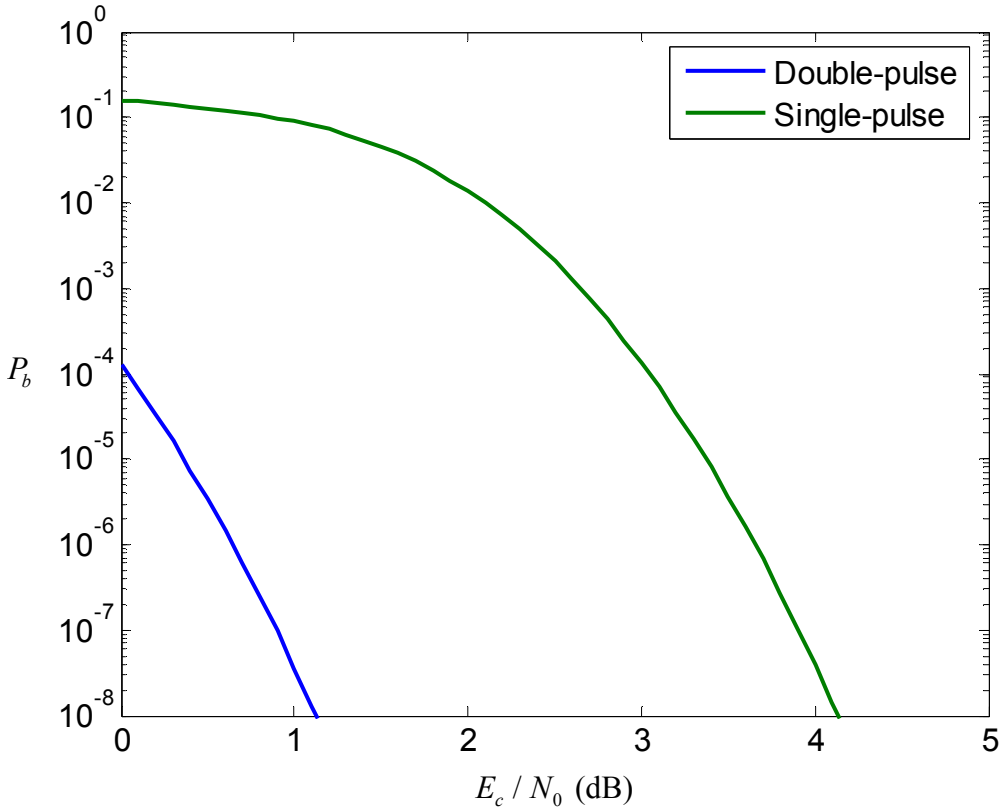

Figure 45. Performance of the second alternative waveform for both the single-pulse and the double-pulse structure in AWGN.

2. Performance in AWGN and PNI with a Diversity of Two

The probability of channel symbol error for *M*BOK with (n,k) RS coding with a diversity of two in AWGN and PNI is shown in (3.56) and is repeated here:

$$p_s = \sum_{i=0}^{2} \binom{2}{i} \rho^i (1-\rho)^{2-i} \, p_s(i), \tag{4.17}$$

where $p_s(i)$ is the conditional probability of channel symbol error given that i symbols experience PNI. The conditional probability of channel symbol error with RS coding is given by (3.65) and (3.66).

Substituting (3.66) into (4.17), we obtain the probability of channel symbol error. The probability of information symbol error and information bit error for *M*BOK with (n,k) RS coding in AWGN and PNI with a diversity of two is obtained by substituting (4.17) into (4.4) and (4.4) into (2.16).

For the 64-BOK with (63,47) RS coding, the performance for different values of ρ with $E_c / N_0 = 1.3$ dB is shown in Figure 46. The E_c / N_0 is chosen to be 1.3 dB since this gives $P_b = 10^{-9}$ at $E_c / N_I = 30$ dB. From Figure 46, we see that varying the ρ does not degrade performance significantly as compared to barrage noise interference ($\rho = 1$). The maximum degradation due to PNI at $P_b = 10^{-5}$ is about 3.2 dB.

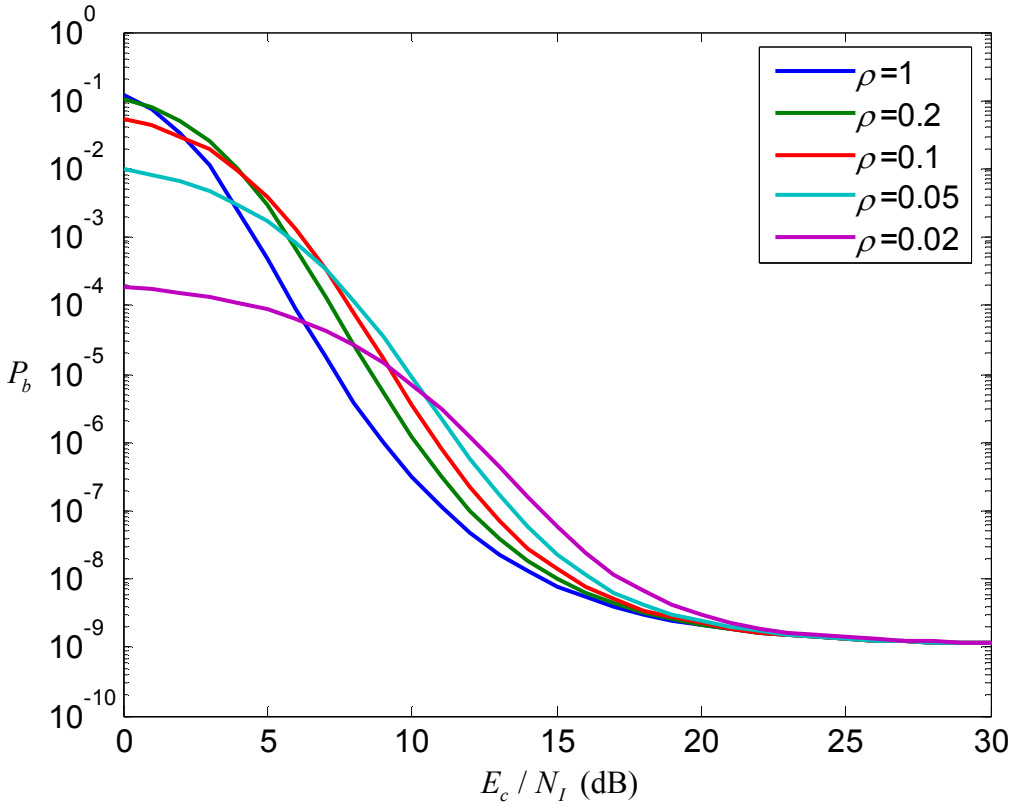

Figure 46. Performance of the second alternative waveform for the double-pulse structure with $E_c / N_0 = 1.3$ dB.

In Figure 47, we compare the performance for receivers both with and without diversity where the probability of bit error approaches 10^{-9} at $E_c / N_I = 30$ dB. For the receiver without diversity, $E_c / N_0 = 4.4$ dB, while with diversity, $E_c / N_0 = 1.3$ dB so that both converge to an asymptotic limit of 10^{-9}. At $P_b = 10^{-5}$, the difference in performance between the waveforms with and without diversity is about 2.8 dB and 3.5 dB for $\rho = 1$ and 0.1, respectively.

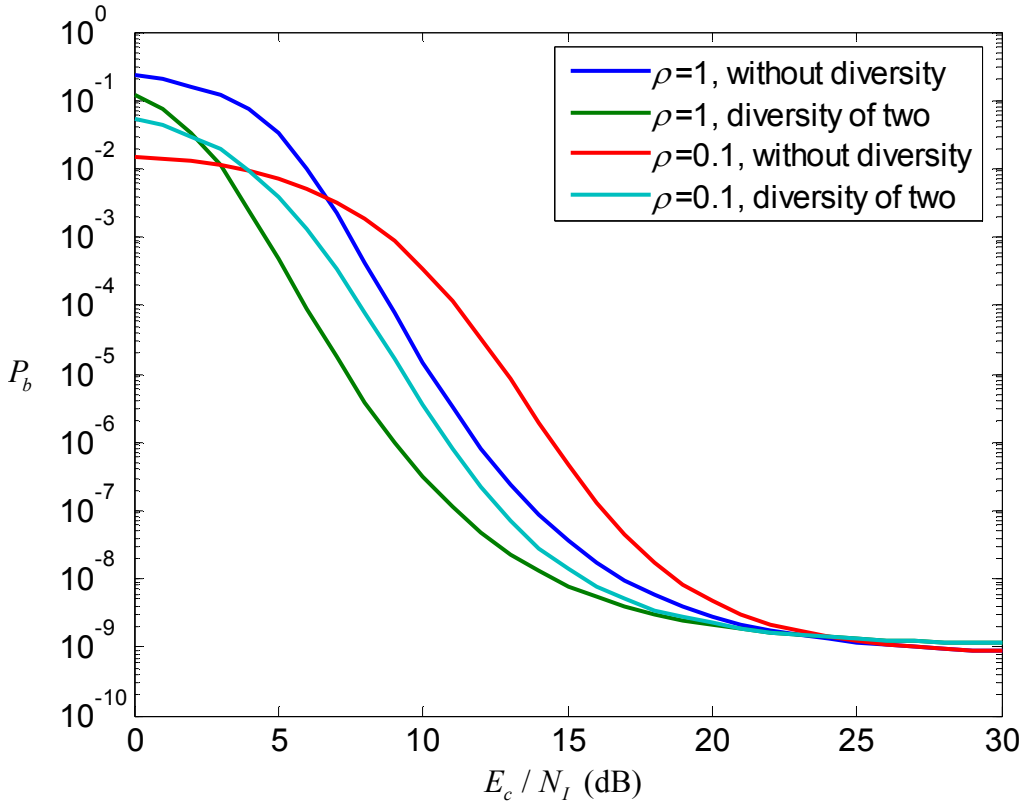

Figure 47. Performance of the second alternative waveform for both the double-pulse structure ($E_c / N_0 = 1.3$ dB) and the single-pulse structure ($E_b / N_0 = 4.4$ dB).

3. Performance in AWGN and PNI with a Diversity of Two and EED

The probability of bit error for *M*BOK with (n, k) RS coding and EED with a diversity of two in AWGN and PNI is obtained by using similar approach as with no diversity. We obtain the probability of correct channel detection and the probability of channel erasure, from which we obtain the probability of channel symbol error.

From Section B-3 of Chapter III, the probability of channel erasure for the double-pulse structure with EED is given by (3.74) and is repeated here:

$$p_e = \sum_{i=0}^{2} \binom{2}{i} \rho^i (1-\rho)^{2-i} \times \left[Q\left((1-a) 2 \sqrt{\frac{2rmE_c}{\frac{i}{\rho} N_I + 2N_0}} \right) - Q\left((1-a) 2 \sqrt{\frac{2rmE_c}{\frac{i}{\rho} N_I + 2N_0}} \right) \right] \times \left[1 - 2Q\left(2a \sqrt{\frac{2rmE_c}{\frac{i}{\rho} N_I + 2N_0}} \right) \right]^{\frac{M}{2}-1} \tag{4.18}$$

The probability of correct channel detection for the double-pulse structure with EED is given by (3.79) and is repeated here:

$$p_c = \sum_{i=0}^{2} \binom{2}{i} \rho^i (1-\rho)^{2-i} \times \frac{1}{\sqrt{2\pi}} \int_{-(1-a)2\sqrt{\frac{2rmE_c}{\frac{iN_I}{\rho}+2N_0}}}^{\infty} e^{-\frac{u^2}{2}} \left[1 - 2Q\left(u + 2 \sqrt{\frac{2rmE_c}{\frac{iN_I}{\rho} + 2N_0}} \right) \right]^{\frac{M}{2}-1} du \tag{4.19}$$

Using (4.18) and (4.19), we obtain the probability of channel symbol error with EED from

$$p_s = 1 - p_e - p_c . \tag{4.20}$$

The probability of block error is obtained by using the results of (4.18), (4.19) and (4.20) in (3.81). The probability of information symbol error and information bit error are obtained by using (4.4) and (2.16), respectively.

For 64-BOK with (63,47) RS coding and EED with a diversity of two in AWGN and PNI, the results for different values of a are shown in Figure 48 and Figure 49, where E_c / N_0 are 1.3 dB and 12 dB, respectively. From Figure 48 and Figure 49, we see that there is not much difference in performance for $0.4 \le a \le 0.6$. However, the performance degrades rapidly when $a > 0.6$. This degradation is expected since, when a

is large, more received symbols are erased and the erasure correction capability of the RS code is overwhelmed. The subsequent analyses use $a = 0.6$ since it provides the best performance with EED.

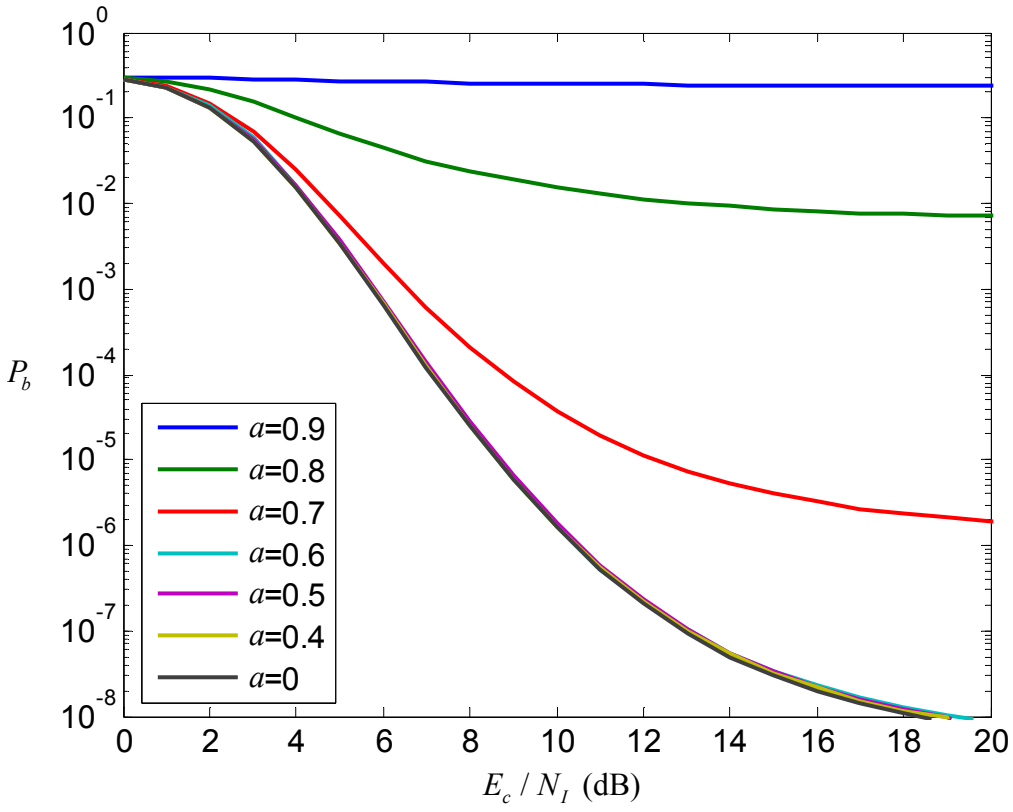

Figure 48. Performance of the second alternative waveform with EED for the double-pulse structure with $\rho = 0.5$ and $E_c / N_0 = 1.3$ dB for different values of a.

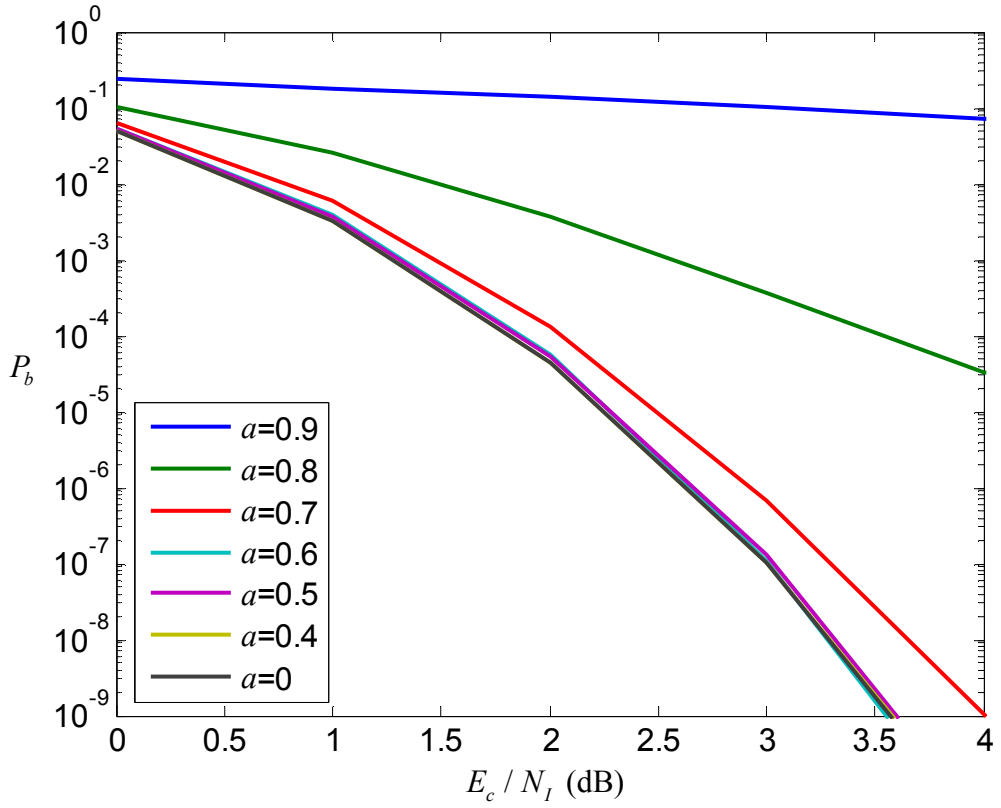

Figure 49. Performance of the second alternative waveform with EED for the double-pulse structure with $\rho = 0.5$ and $E_c / N_0 = 12$ dB for different values of a.

The performance of 64-BOK with (63,47) RS coding and EED with a diversity of two for $a = 0.6$ for different values of ρ is shown in Figure 50 and Figure 51. At $P_b = 10^{-5}$, and $E_c / N_0 = 1.3$ dB, there is a difference of 2.2 dB in E_c / N_I between the best and the worst performance. The best performance is when $\rho = 1$ at $E_c / N_I = 8.2$ dB and the worst performance is when $\rho = 0.1$ at $E_c / N_I = 10.4$ dB.

Similarly, from Figure 51, we can see that the difference in performance increases as E_c / N_0 increases to 12 dB. At $P_b = 10^{-5}$, the best performance is when $\rho = 1$ at $E_c / N_I = 0.8$ dB, the worst performance is when $\rho = 0.1$ at $E_c / N_I = 5.8$ dB, which is a difference of 5 dB.

From results shown in Figure 50 and Figure 51, we see that there is an improvement in the absolute performance for the larger E_b / N_0, but there is also a significant increase in the relative performance gap between $\rho = 1$ and $\rho = 0.1$.

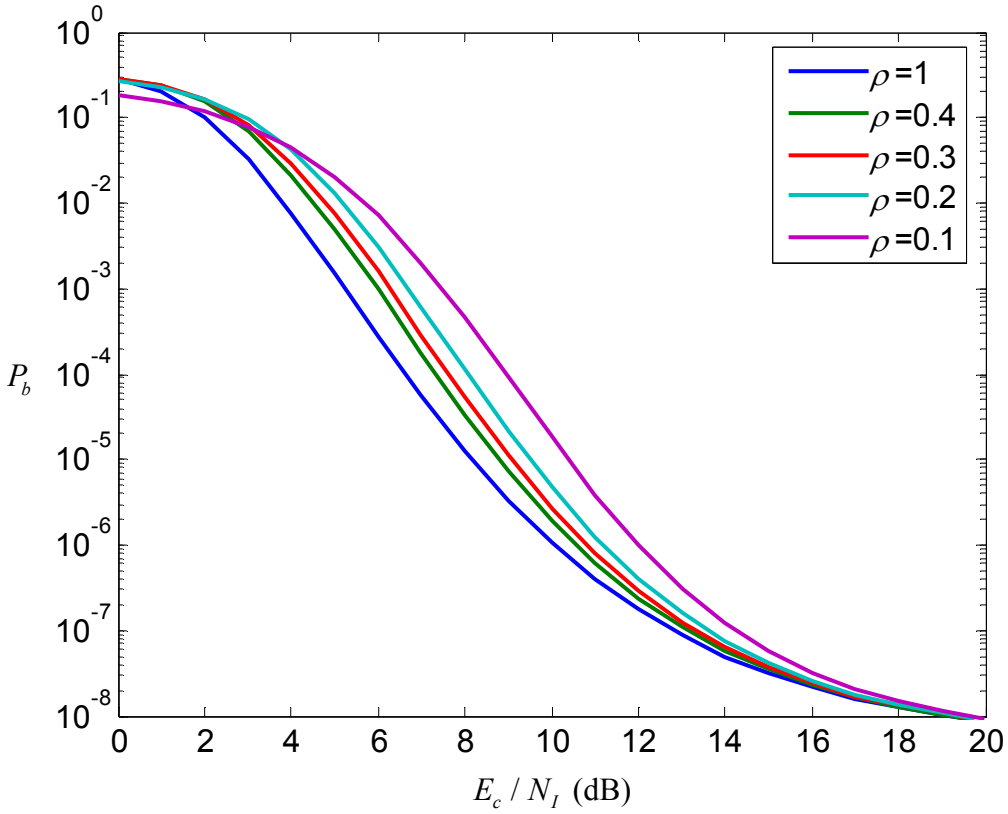

Figure 50. Performance of the second alternative waveform with EED for the double-pulse structure with $a = 0.6$ and $E_c / N_0 = 1.3$ dB for different values of ρ.

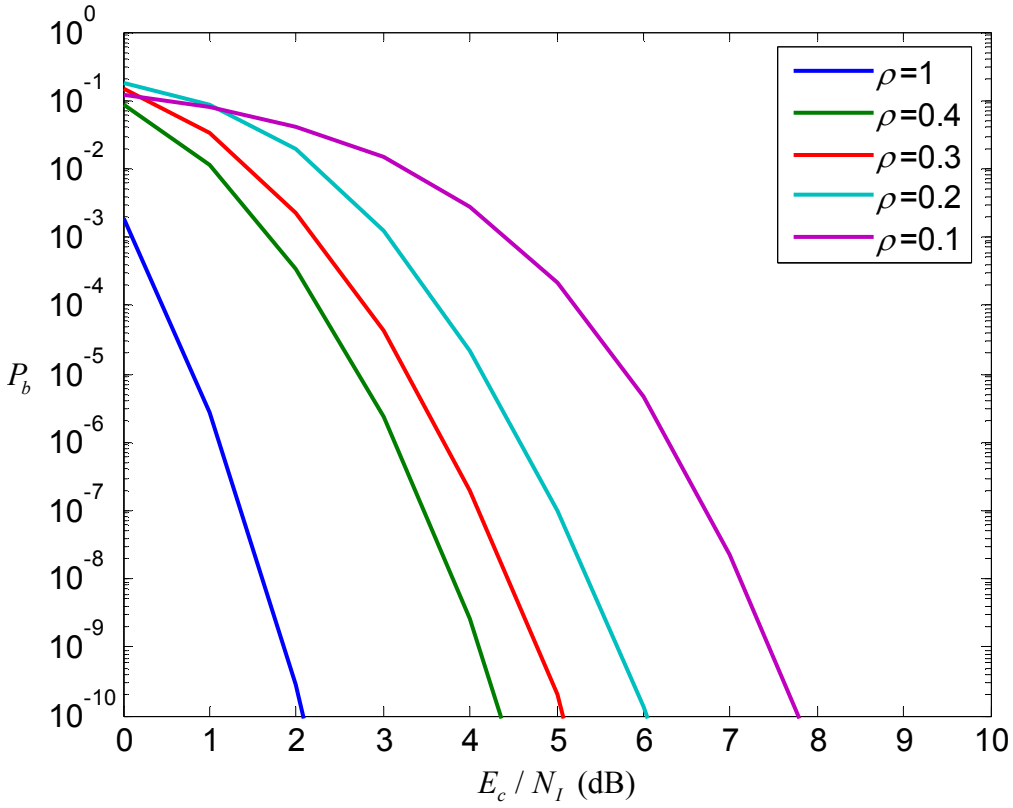

Figure 51. Performance of the second alternative waveform with EED for the double-pulse structure with $a = 0.6$ and $E_c / N_0 = 12$ dB for different values of ρ.

The performance for 64-BOK with (63,47) RS coding and EED, both with and without diversity, for the case of an asymptotic convergence to near 10^{-8} is shown in Figure 52. As expected from the results, at $P_b = 10^{-5}$, we see that there is about 3 dB difference in performance between the single-pulse and double-pulse structure. The 3 dB improvement is due to the advantage of using the double-pulse structure.

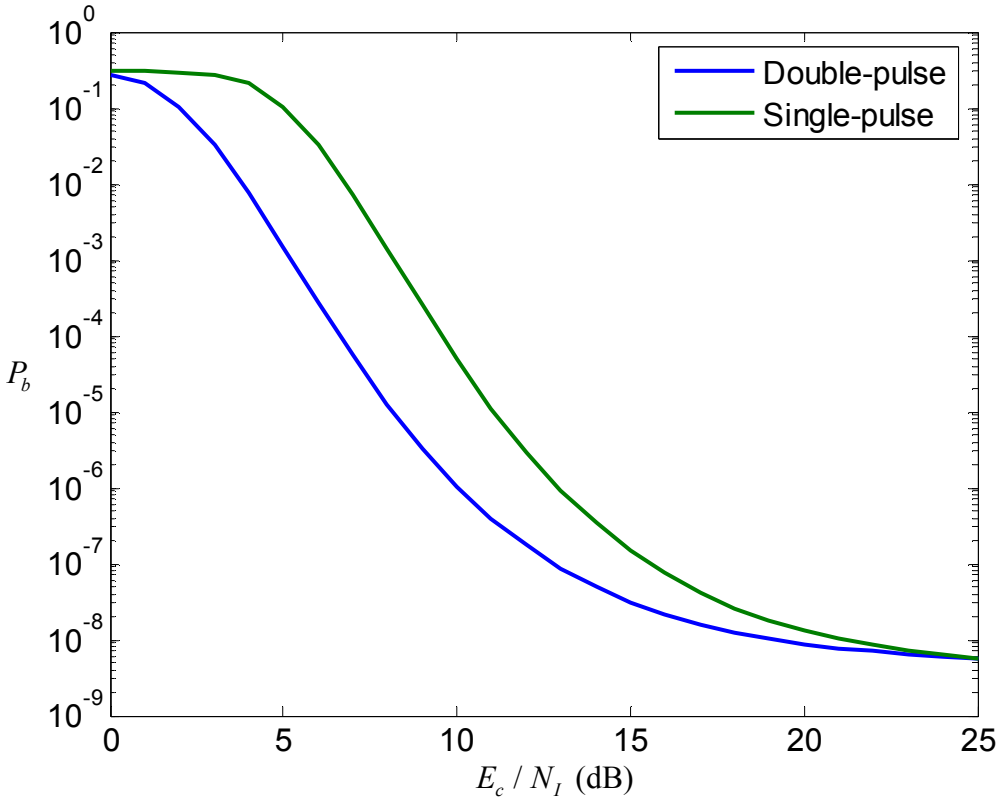

Figure 52. Performance of the second alternative waveform with EED, $a = 0.6$, $\rho = 1$ for both the double-pulse structure ($E_c / N_0 = 1.3$ dB) and single-pulse structure ($E_b / N_0 = 4.4$ dB).

The performance of 64-BOK with (63,47) RS coding both with and without EED for $E_c / N_0 = 1.3$ for different values of ρ is shown in Figure 53. From Figure 53, at $P_b = 10^{-5}$, the difference in performance when comparing both with and without EED is about 1 dB.

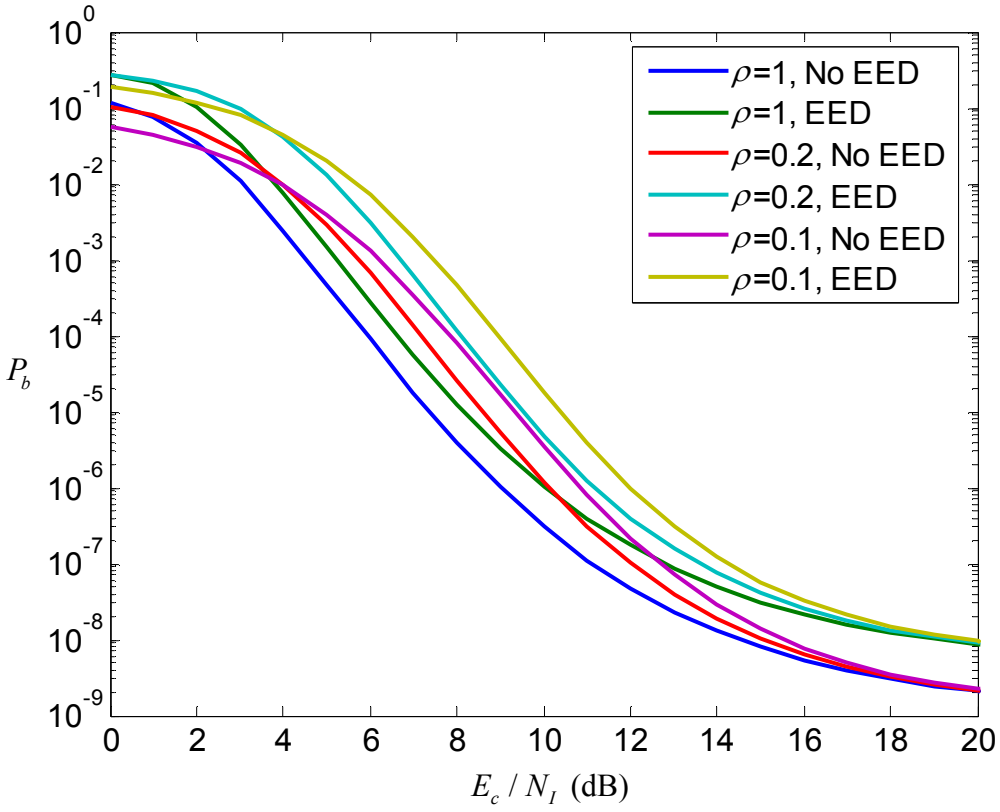

Figure 53. Performance of the second alternative waveform with and without EED for $E_c / N_0 = 1.3$ dB and $a = 0.6$ for different values of ρ.

The effect of increasing E_c / N_0 to 12 dB is shown in Figure 54. From Figure 54, we observe that there is a small difference of about 0.3 dB when comparing performance with EED to that without EED. This comparison shows that there is no benefit to EED for the double-pulse structure, which was also the case for the single-pulse structure.

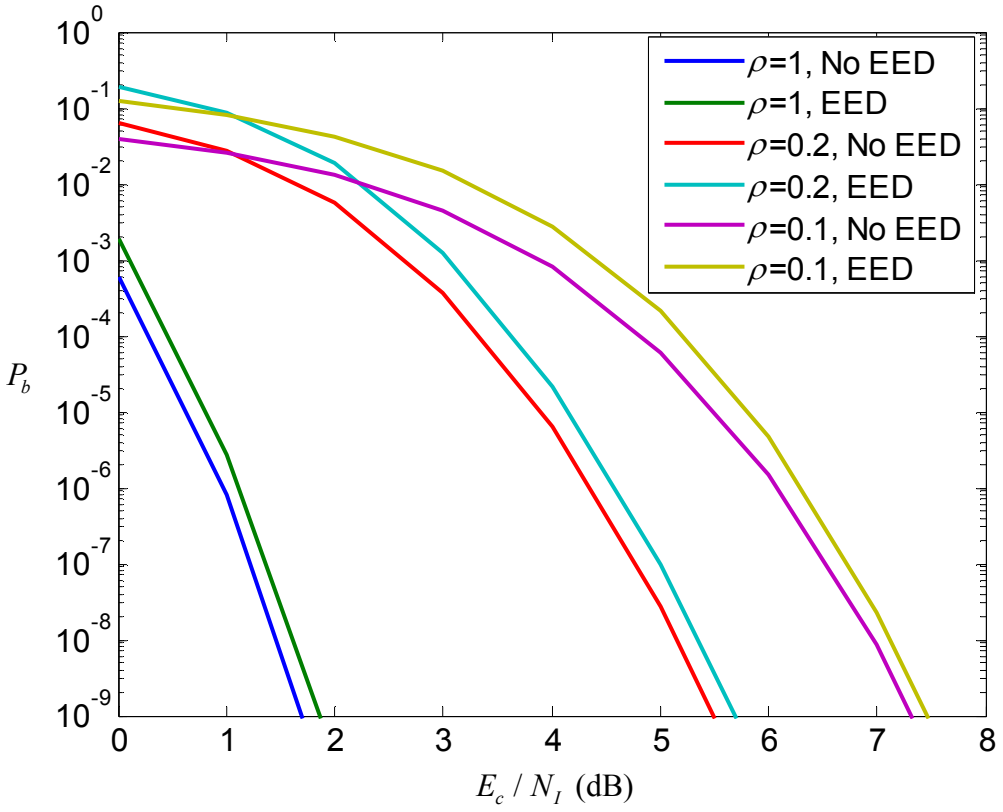

Figure 54. Performance of the second alternative waveform with and without EED for $E_c / N_0 = 12$ dB and $a = 0.6$ for different values of ρ.

4. Performance with Perfect-side Information in AWGN and PNI

PSI modulation is now considered for a system with a diversity of two where each diversity reception is received independently. When only one diversity reception is affected by PNI, the decoding decision is based on the diversity reception that is free from PNI. The probability of channel symbol error with a diversity of two is given in (3.86).

The conditional probability of channel symbol error when there is no PNI present in either diversity reception is given by (3.87) and is repeated here:

$$p_s(0) = 1 - \frac{1}{\sqrt{2\pi}} \int_{-\sqrt{\frac{4rmE_c}{N_0}}}^{\infty} e^{-\frac{u^2}{2}} \left[1 - 2Q\left(u + \sqrt{\frac{4rmE_c}{N_0}}\right) \right]^{\frac{M}{2}-1} du . \qquad (4.21)$$

The conditional probability of channel symbol error when only one of the diversity receptions suffers from PNI and is discarded is given by (3.88) and is repeated here:

$$p_s(1) = 1 - \frac{1}{\sqrt{2\pi}} \int_{-\sqrt{\frac{2rmE_c}{N_0}}}^{\infty} e^{-\frac{u^2}{2}} \left[1 - 2Q(u + \sqrt{\frac{2rmE_c}{N_0}} \right]^{\frac{M}{2}-1} du \,. \tag{4.22}$$

Finally, the conditional probability of channel symbol error when both diversity receptions suffer from PNI is given by (3.89) and is repeated here:

$$p_s(2) = 1 - \frac{1}{\sqrt{2\pi}} \int_{-2\sqrt{\frac{2rm}{\frac{2}{\rho}\gamma_I^{-1} + 2\gamma_c^{-1}}}}^{\infty} e^{-\frac{u^2}{2}} \left[1 - 2Q\left(u + 2\sqrt{\frac{2rm}{\frac{2}{\rho}\gamma_I^{-1} + 2\gamma_c^{-1}}} \right) \right]^{\frac{M}{2}-1} du \,. \tag{4.23}$$

The performance of 64-BOK with (63,47) RS coding with and without PSI is shown in Figure 55. From Figure 55 with $E_c / N_0 = 1.3$ dB, there is no difference in performance when $\rho = 1$ whether PSI is used or not. This makes sense since the channel is experiencing barrage noise interference. At $P_b = 10^{-5}$ and $\rho = 0.2$, the E_c / N_I required for the waveforms with and without PSI are 2.5 dB and 8.6 dB, respectively. Hence, there is a gain of 6.1 dB when PSI is used, which is a significant improvement in performance.

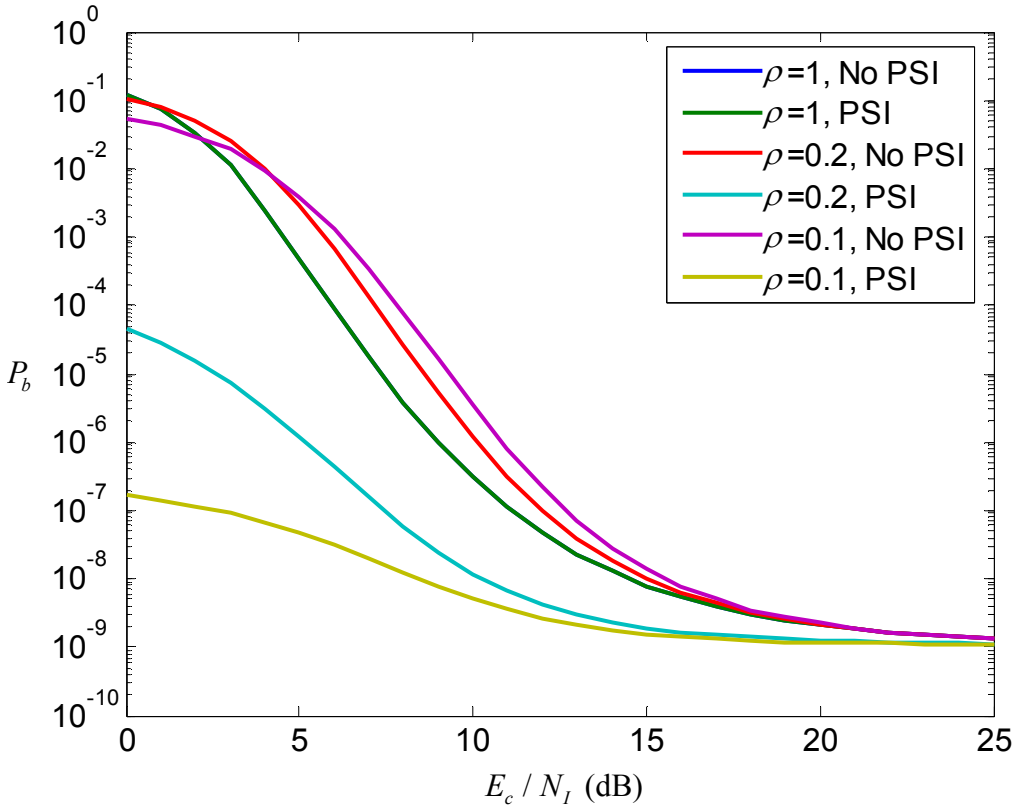

Figure 55. Performance of the second alternative waveform with and without PSI for different ρ with $E_c / N_0 = 1.3$ dB.

The performance when $E_c / N_0 = 12$ dB is shown in Figure 56. From Figure 56, we see identical results for $\rho = 1$. At $P_b = 10^{-6}$ and $\rho = 0.2$, the E_c / N_I required for the waveform with and without PSI are 1.2 dB and 4.3 dB, respectively. Hence, there is a gain of 3.1 dB when PSI is used. Thus, PSI forces a jammer to adapt a barrage noise jamming strategy.

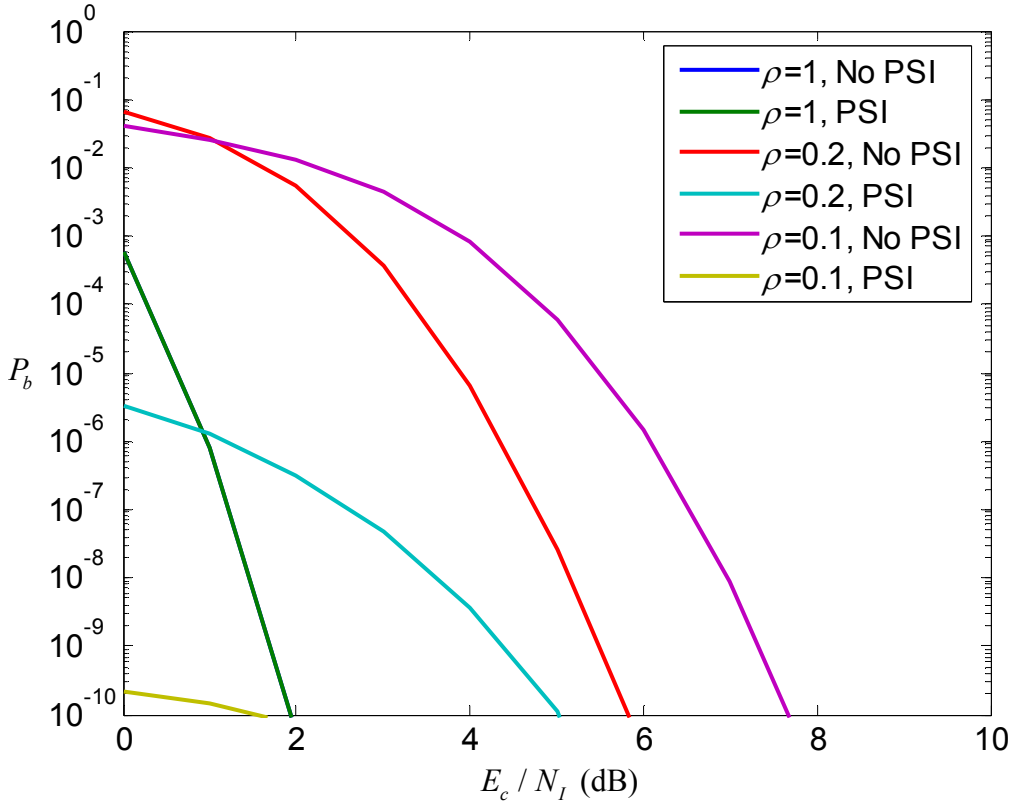

Figure 56. Performance of the second alternative waveform with and without PSI for different ρ with $E_c / N_0 = 12$ dB.

5. Section Summary

In this section, the performance of the second alternative JTIDS/Link-16 waveform with a diversity of two (double-pulse structure), with and without EED for both AWGN as well as AWGN plus PNI was examined. The performance of the waveform is generally better when $\rho = 1$ (barrage noise interference) than $\rho < 1$. We saw that EED decoding does not improve the performance of the receiver. The performance of the waveform with PSI was also analyzed, and the results showed a significant improvement in performance for a channel with AWGN plus PNI. In Section C, we compared the performance of 64-BOK with (63,47) RS coding to the performance of the original JTIDS/Link-16 waveform for both the single-pulse and the double-pulse structures for both AWGN and as well as AWGN plus PNI.

C. COMPARISON OF SECOND ALTERNATIVE JTIDS/LINK-16 WAVEFORM WITH JTIDS/LINK-16 WAVEFORMS FOR BOTH AWGN AND AWGN PLUS PNI

In Section C, we compare the performance of the second alternative JTIDS/Link-16 waveform to the original JTIDS/Link-16 waveform. The analyses are based on the single-pulse and the double-pulse structures. Detailed analysis of the original JTIDS/Link-16 waveform can be found in [7]. Results from [7] are used to obtain the performance of the original JTIDS/Link-16 waveform for comparison with the second alternative JTIDS/Link-16 waveform.

1. Comparison of 64-BOK with (63,47) RS Coding to the JTIDS/Link-16 Waveform for AWGN, Single-pulse Structure

The performance of the second alternative compared to the original JTIDS/LINK-16 waveform for the single-pulse structure in AWGN is shown in Figure 57. At $P_b = 10^{-3}$, $E_b / N_0 = 6.1$ dB and $E_b / N_0 = 2.7$ dB for the JTIDS/Link-16 waveform and the second alternative JTIDS/Link-16 waveform, respectively. There is a gain of 3.4 dB for the second alternative JTIDS/Link-16 waveform over the JTIDS/Link-16 waveform in AWGN. Similarly, at $P_b = 10^{-5}$, there is a gain of 3.6 dB for the second alternative JTIDS/Link-16 waveform over the JTIDS/Link-16 waveform, with $E_b / N_0 = 3.4$ dB and $E_b / N_0 = 7.0$ dB for the second alternative JTIDS/Link-16 waveform and the JTIDS/Link-16 waveform, respectively.

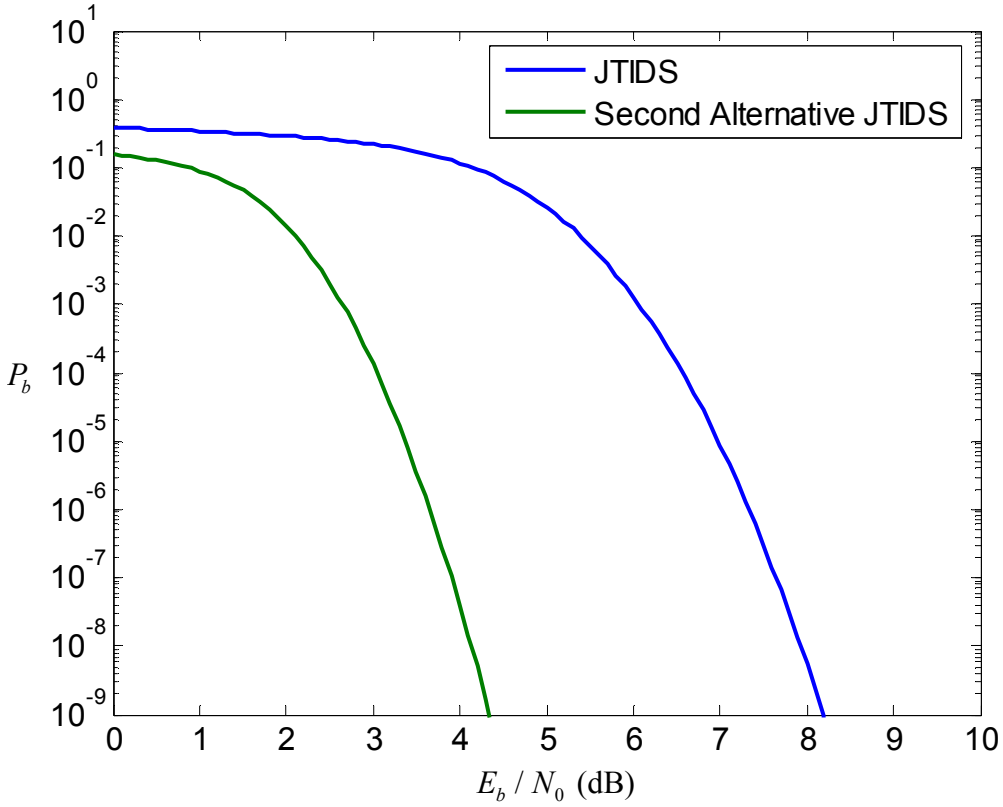

Figure 57. Performance of the second alternative JTIDS/Link-16 waveform and the JTIDS waveform for the single-pulse structure.

2. Comparison of 64-BOK with (63,47) RS Coding to the JTIDS/Link-16 Waveform for AWGN and PNI, Single-pulse Structure

The performance for both the second alternative JTIDS/Link-16 waveform and the JTIDS/Link-16 waveform in both AWGN and PNI for different values of ρ is shown in Figure 58. We consider the case where the performance of the two waveforms both converge to $P_b = 10^{-7}$. The E_b / N_0 required for the second alternative waveform is 3.9 dB, while the E_b / N_0 required for the JTIDS/Link-16 waveform is 7.7 dB.

At $P_b = 10^{-5}$ and $\rho = 1$, the E_b / N_I required for both the alternative JTIDS/Link-16 waveform and the JTIDS/Link-16 waveform are 12.6 dB and 15 dB, respectively, for a difference of 2.4 dB. For $\rho = 0.2$, the difference in E_b / N_I between the alternative JTIDS/Link-16 waveform ($E_b / N_I = 14$ dB) and the JTIDS/Link-16 waveform

($E_b / N_I = 16$ dB) is 2 dB. Similarly, for $\rho = 0.1$, the difference in E_b / N_I between the alternative JTIDS/Link-16 waveform ($E_b / N_I = 14.5$ dB) and the JTIDS/Link-16 waveform ($E_b / N_I = 16$ dB) is 1.5 dB.

Comparing the results between the two waveforms, we see that the second alternative JTIDS/Link-16 waveform performs better than the JTIDS/Link-16 waveform by about 1.5 to 2.4 dB at $P_b = 10^{-5}$. Clearly, the JTIDS/Link-16 waveform will have substantially inferior performance if the two waveforms are compared on an equal E_b / N_0 basis. This is shown in Figure 59 where $E_b / N_0 = 7.7$ dB for both waveforms.

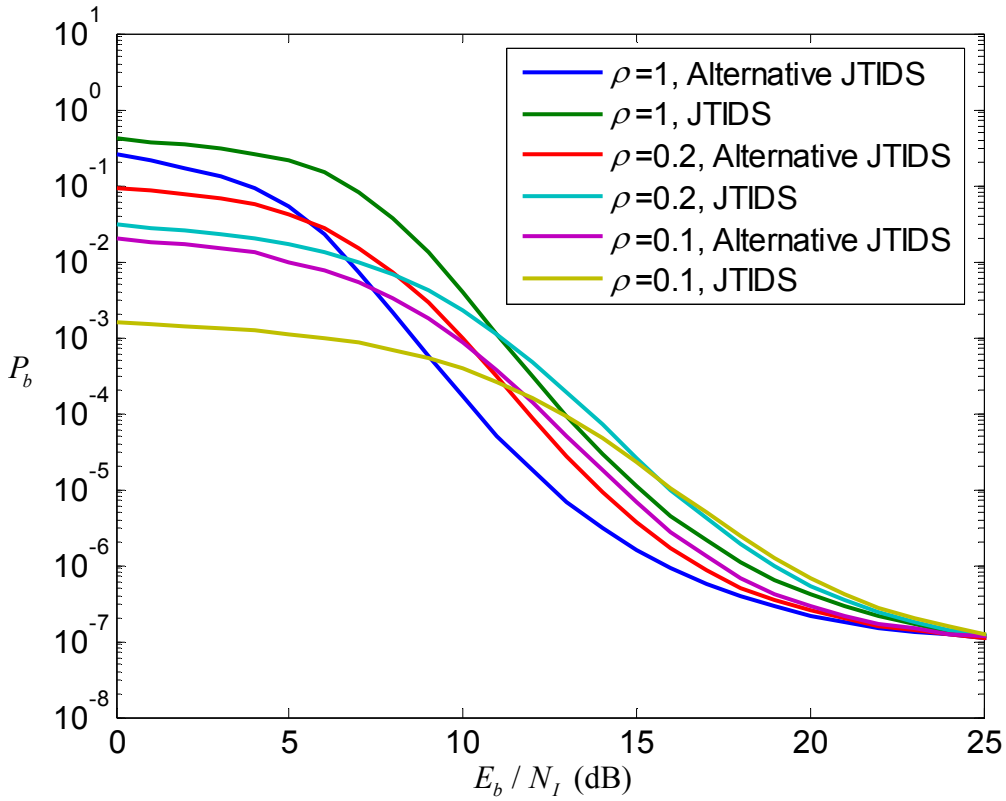

Figure 58. Performance of the second alternative JTIDS/Link-16 waveform ($E_b / N_0 = 3.9$ dB) and the JTIDS waveform ($E_b / N_0 = 7.7$ dB) for the single-pulse structure.

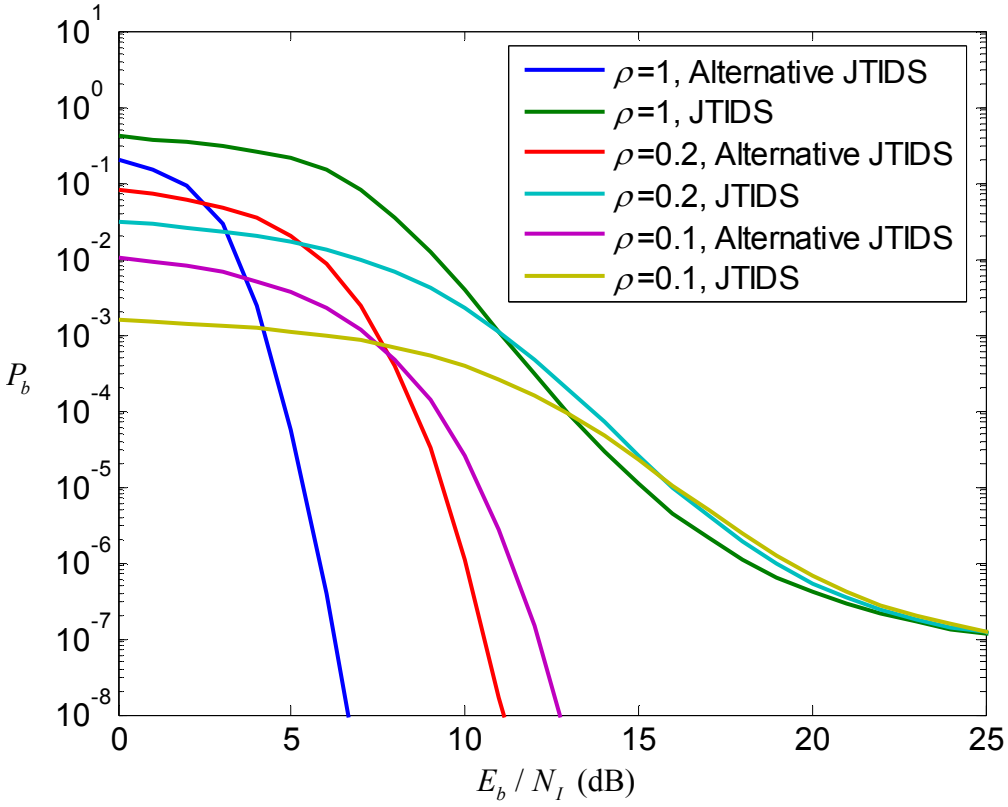

Figure 59. Performance of the second alternative JTIDS/Link-16 waveform and the JTIDS waveform, both with $E_b / N_0 = 7.7$ dB, for the single-pulse structure.

3. Comparison of 64-BOK with (63,47) RS Coding to the JTIDS/Link-16 Waveform for AWGN, Double-pulse Structure

The performance of the second alternative JTIDS/Link-16 waveform and the original JTIDS/Link-16 waveform in AWGN for the double-pulse structure is shown in Figure 60. At $P_b = 10^{-5}$, $E_c / N_0 = 4$ dB and $E_c / N_0 = 0.4$ dB for the JTIDS/Link-16 waveform and the 64-BOK waveform, respectively, for a 3.6 dB gain for the second alternative JTIDS/Link-16 waveform over the JTIDS/Link-16 waveform. This is about the same advantage as was found for the single-pulse structure in Figure 57. Comparing Figure 60 with Figure 57, there is a 0.4 dB advantage for the single-pulse structure 64-BOK waveform ($E_b / N_0 = 4.3$ dB) as compared to the double-pulse JTIDS/Link-16 waveform.

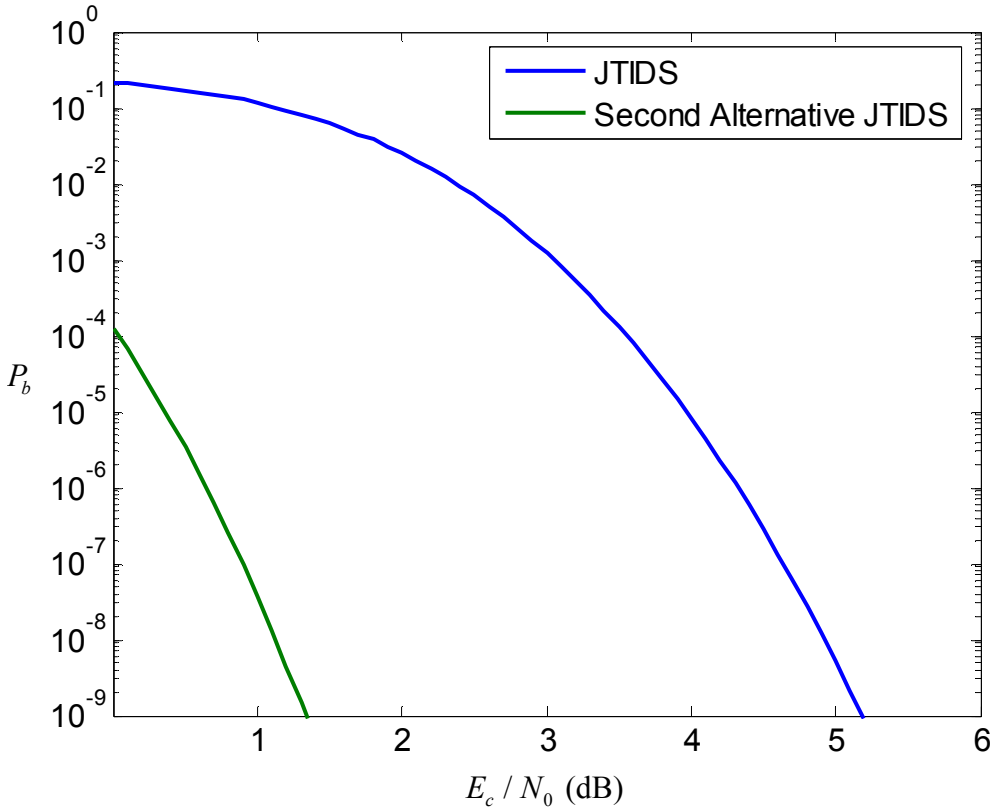

Figure 60. Performance of the second alternative JTIDS/Link-16 waveform and the JTIDS waveform for the double-pulse structure.

4. Comparison of 64-BOK with (63,47) RS Coding to the JTIDS/Link-16 Waveform for AWGN and PNI, Double-pulse Structure

The performance for both the second alternative JTIDS/Link-16 and the JTIDS/Link-16 waveform for the double-pulse structure in both AWGN and PNI for different values of ρ is shown in Figure 61. We consider the case where the performance plots of the two waveforms converge to $P_b = 10^{-9}$, and the required E_c / N_0 for the second alternative waveform and the JTIDS/Link-16 waveform are 1.4 dB and 5.2 dB, respectively, for a difference of 3.8 dB gain.

At $P_b = 10^{-5}$ and $\rho = 1$, the E_c / N_I required for the alternative JTIDS/Link-16 waveform and the JTIDS/Link-16 waveform are 7.2 dB and 10 dB, respectively, for a difference of 2.8 dB. For $\rho = 0.2$, there is minor difference of 0.3 dB when comparing

the required E_c / N_I for the alternative JTIDS/Link-16 waveform ($E_c / N_I = 8.5$ dB) and the JTIDS/Link-16 waveform ($E_c / N_I = 8.2$ dB). The JTIDS/Link-16 waveform performs better than the second alternative waveform when $E_c / N_I < 9$ dB.

For $\rho = 0.1$ and at $P_b = 10^{-6}$, the JTIDS/Link-16 waveform performs much better than the second alternative waveform when $E_c / N_I < 12.5$ dB. The difference in E_c / N_I for the alternative JTIDS/Link-16 waveform ($E_c / N_I = 10.7$ dB) and the JTIDS/Link-16 waveform ($E_c / N_I = 7.9$ dB) is 2.8 dB.

Comparing the performance of the two waveforms, we see that the second alternative JTIDS/Link-16 waveform performs better than the JTIDS/Link-16 waveform by about 2.8 dB at $P_b = 10^{-5}$ when $\rho = 0.1$. The second alternative JTIDS/Link-16 waveform is outperformed by the JTIDS/Link-16 waveform when $\rho = 0.1$ and $\rho = 0.2$ for $E_c / N_I < 9$ dB and $E_c / N_I < 12.5$ dB, respectively. However, the second alternative JTIDS/Link-16 waveform will outperform the JTIDS/Link-16 waveform if the two waveforms are compared based on an equal E_c / N_0 basis. This can be seen in Figure 62, where $E_c / N_0 = 5.2$ dB for both waveforms.

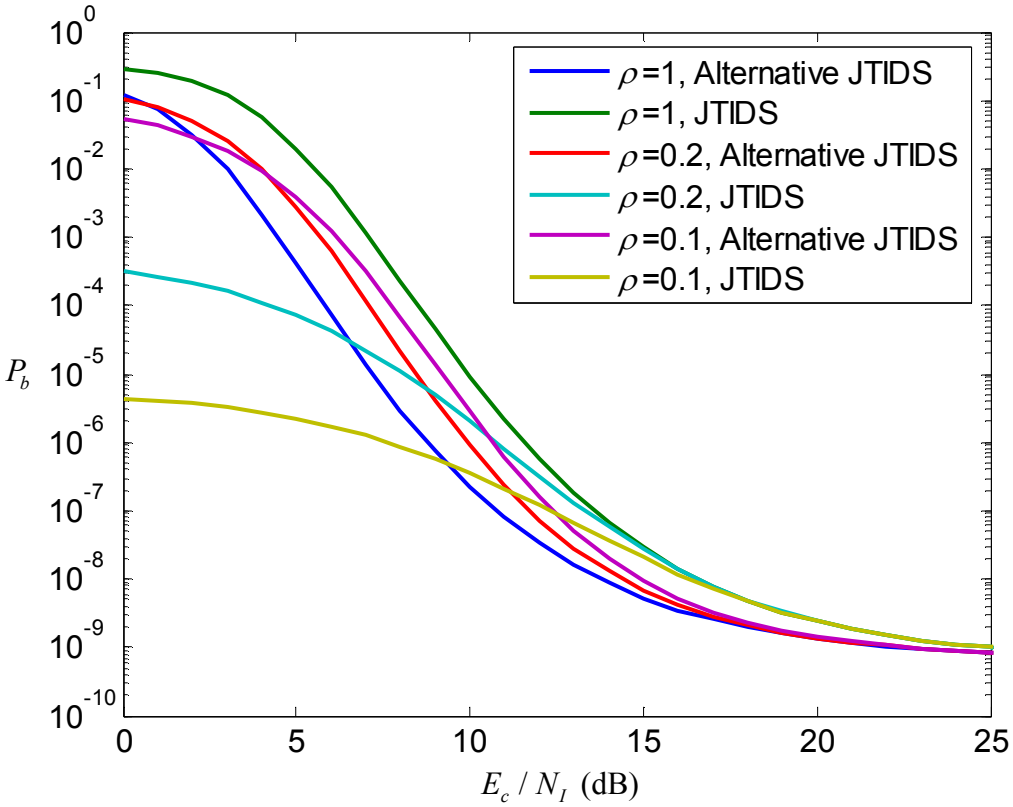

Figure 61. Performance of the second alternative JTIDS/Link-16 waveform ($E_c / N_0 = 1.4$ dB) and the JTIDS waveform ($E_c / N_0 = 5.2$ dB) for the double-pulse structure.

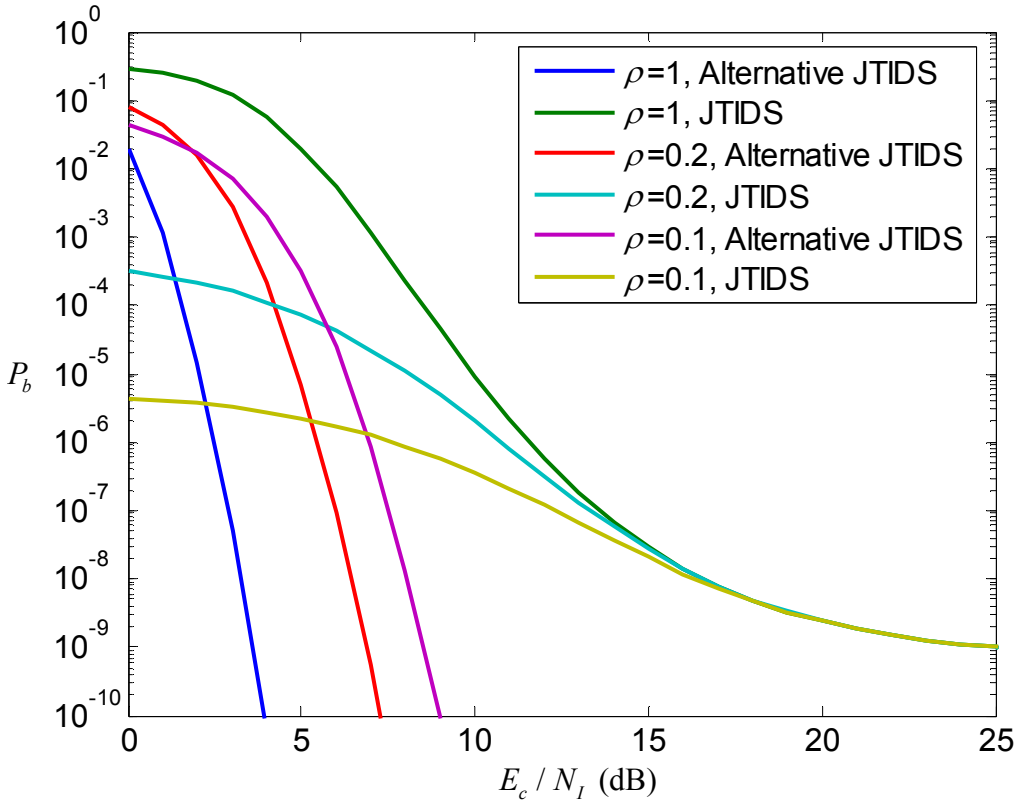

Figure 62. Performance of the second alternative JTIDS/Link-16 waveform and the JTIDS waveform, both with $E_c / N_0 = 5.2$ dB, for the double-pulse structure.

5. Section Summary

In this section, the performance of the second alternative JTIDS/Link-16 waveform was compared to that of the original JTIDS/Link-16 waveform for a channel with both AWGN as well as AWGN plus PNI with both the single-pulse and the double-pulse structure. The results show that the second alternative JTIDS/Link-16 waveform outperforms the original JTIDS/Link-16 waveform for both the single-pulse and the double-pulse structure.

D. CHAPTER SUMMARY

The performance of the second alternative JTIDS/Link-16 waveform, 64-BOK with (63, 47) RS coding were covered in this chapter. The performance of the second alternative JTIDS/Link-16 waveform was compared to that of the original JTIDS/Link-16

waveform in both AWGN as well as AWGN plus PNI for both single-pulse and double-pulse structures. The results show significant improvement for the alternative waveform as compared to the original JTIDS/Link-16 waveform when compared based on equal E_b / N_0 basis. In addition to requiring less signal power than the original JTIDS/Link-16 waveform, the second alternative JTIDS/Link-16 waveform yields an overall increase in data rate of 4.44 as compared to the original JTIDS/Link-16 waveform.

In the next chapter, we summarize the findings of this thesis.

V. CONCLUSIONS AND FUTURE RESEARCH AREAS

A. CONCLUSIONS

Two alternative JTIDS/Link-16 waveforms were presented in this thesis. The first alternative JTIDS/Link-16 waveform uses 64-BOK with (31,15) RS coding, and the second alternative JTIDS/Link-16 waveform uses 64-BOK with (63,47) RS coding. The performance of the two proposed waveforms for both errors-and-erasure and errors-only decoding, with and without diversity, both in AWGN as well as AWGN plus PNI was analyzed. The efficacy of PSI was also considered. The performance of the alternative JTIDS/Link-16 waveforms was compared to that for the existing JTIDS/Link-16 waveform.

From the results obtained, both alternative waveforms perform better than the original JTIDS waveform in AWGN for both single-pulse and double-pulse structures. For a channel with AWGN plus PNI, the waveforms were analyzed for the case when P_b for both waveforms asymptotically approach the same P_b for large E_b / N_I. The two alternative waveforms outperform the JTIDS/Link-16 in barrage noise interference when $\rho = 1$. When the channel experiences PNI for the single-pulse structure, the alternative waveforms outperforms the JTIDS/Link-16 waveform. For double-pulse structure and $\rho < 1$, the two alternative waveforms do not always outperform the JTIDS/Link-16 waveform. However, we have to consider that the JTIDS/Link-16 waveform requires a larger E_c / N_0 to achieve the same asymptotic P_b for large E_b / N_I, and the alternative waveforms outperform the JTIDS/Link-16 waveform when both waveforms are compared with the same E_c / N_0.

Lastly, we also found no benefit to EED for either alternative waveform. There is virtually no improvement in performance as compared to errors-only-decoding. We also found that PSI provides a significant improvement in performance in an AWGN plus PNI environment.

The primary advantages of the two proposed alternative waveforms are the improvement in data rate and the reduction in required signal power required to achieve the same probability of information bit error as compared to the existing JTIDS/Link-16 waveform. The first alternative JTIDS/Link-16 waveform that utilizes 64-BOK with (31,15) RS coding supports a data rate that is greater than the original JTIDS/Link-16 waveform by a factor of 2.4 while requiring less signal power to achieve the same probability of information bit error. The second alternative waveform that utilizes 64-BOK with (63,47) RS coding supports a data rate that is greater than the original JTIDS/Link-16 waveform by a factor of 4.44 while requiring less signal power to achieve the same probability of information bit error. When only AWGN is present and for the same probability of information bit error, the E_b / N_0 required for the first and second alternative JTIDS/Link-16 waveforms is less than that required by the original JTIDS/Link-16 waveform by 2.7 dB and 3.8 dB, respectively. The above results are achieved with no increase in the required signal bandwidth.

B. FUTURE RESEARCH AREAS

In this thesis, we have analyzed two alternative JTIDS/Link-16 waveforms, where the first alternative waveform utilizes complex 64-BOK modulation with (31,15) RS coding, and the second alternative waveform utilizes complex 64-BOK modulation with (63,47) RS coding. The two alternative waveforms provide a significant improvement to the data rate as compared to the existing JTIDS/Link-16 waveform. A possible future research area is to utilize differential encoding for the data transmission and non-coherent detection at the receiver that provides unambiguous signal detection. In addition, the performance of the waveform may be improved by using concatenated coding as proposed in [9].

LIST OF REFERENCES

[1] Northrop Grumman Corporation, Information Technology Communication & Information Systems Division, *Understanding Link-16: A Guidebook for New Users*, NCTSI, San Diego, CA, Sept 2001 (Prepared, 1994, First Revision, 1998; Second Revision, 1998; Third Revision, 2001).

[2] Dr. Carlo Kopp, "Network Centric Warfare Fundamentals – Part 3" [Online]. Available: http://www.ausairpower.net/NCW-101-3.pdf.

[3] John Asenstorfer, Thomas Cox and Darren Wiksh, *Tactical Data Link systems and the Australian Defense Force (ADF) – Technology Developments and Interoperability Issues*, DSTO-TR-1470, pp 8-10, Feb. 2004.

[4] Michael B. Pursley, Thomas C. Royster and Michael Y. Tan, "High-Rate Direct-Sequence Spread Spectrum" *Proc. IEEE MILCOM*, vol. 2, pp. 1101-1106, Oct. 2003.

[5] Michael B. Pursley and Thomas C. Royster, "High-Rate Direct-Sequence Spread Spectrum With Error-Control Coding," *IEEE Transactions on Communicaitons*, vol. 54, pp. 1693-1702, Sept. 2006.

[6] Hua Wang, Jingming Kuang, Zheng Wang, Hui Xu, "Transmission Performance Analysis of JTIDS", *Proc. IEEE MILCOM*, vol. 4, pp. 2264-2268, Oct. 2005.

[7] Chi-Han Kao, "Performance Analysis of JTIDS/Link-16-type Waveform Subject to Narrowband Waveform over Slow, Flat Nakagami Fading Channels," *Proc. IEEE MILCOM*, Nov. 2008.

[8] B. Sklar, *Digital Communications: Fundamental and Applications*, 2nd Edition, Prentice Hall, Upper Saddle River, NJ, 2001.

[9] Kok Kiang Cham, "Performance Analysis of an Alternative Link-16/JTIDS Waveform Transmitted over a Channel with Pulse-Noise Interference," Naval Postgraduate School, Monterey, CA, Mar. 2008.

[10] Clark Robertson, Notes for EC4550 Digital Communications, Naval Postgraduate School, Monterey, CA, 2007.

[11] Clark Robertson, Notes for EC4550 Sequential and Parallel Diversity, Naval Postgraduate School, Monterey, CA, 2007.

[12] Clark Robertson, Notes for Frequency-Hopped Spread Spectrum, Naval Postgraduate School, Monterey, CA, 2007.

[13] Clark Robertson, Notes for EC4580 Error Correction Coding; Discrete Memory Channel, Naval Postgraduate School, Monterey, CA, 2008.

[14] Georgios Zouros and Clark Robertson, "Performance Analysis of BPSK with Errors and Erasures Decoding to Mitigate the Effects of Pulse-Noise Interference," *Proc. IEEE MILCOM*, Oct. 2006.

[15] John G. Proakis and Masoud Salehi, *Digital Communications,* Fifth Edition, Mc Graw Hill, New York, NY 10020, 2008.

INITIAL DISTRIBUTION LIST

1. Defense Technical Information Center
   Ft. Belvoir, Virginia

2. Dudley Knox Library
   Naval Postgraduate School
   Monterey, California

3. Professor Jeffery B. Knorr, Chairman
   Department of Electrical and Computer Engineering
   Naval Postgraduate School
   Monterey, California

4. Professor R. Clark Robertson
   Department of Electrical and Computer Engineering
   Naval Postgraduate School
   Monterey, California

5. Professor Roberto Cristi
   Department of Electrical and Computer Engineering
   Naval Postgraduate School
   Monterey, California

6. Seah Peng Hwee
   Defence Science and Technology Agency
   Singapore

7. Yeo Tat Soon
   Temasek Defence Systems Institute
   National University of Singapore
   Singapore

8. Tan Lai Poh
   Temasek Defence Systems Institute
   National University of Singapore
   Singapore

9. Kee Cheng Hoe
   Defence Science and Technology Agency
   Singapore